DESIGN OF A POWERED ANKLE ORTHOSIS FOR REHABILITATION

A thesis proposal presented to the faculty of the Graduate School of
Western Carolina University in partial fulfillment of the
requirements for the degree of Master of Science in Technology

By
Theodore Herbert Waltz

Advisor:
Dr. Martin L. Tanaka
School of Engineering and Technology

Committee:

Dr. Gregory Sawicki,
Joint Department of Biomedical Engineering,

Dr. Wesley Stone,
School of Engineering and Technology

September 2016

Table of Contents

LIST OF FIGURES

ABSTRACT

DESIGN OF A POWERED ANKLE ORTHOSIS FOR REHABILITATION

Theodore Herbert Waltz, M.S.T.

Western Carolina University (September 2016)

Thesis Director: Dr. Martin L. Tanaka

This research describes the design, development, and testing of a powered ankle orthosis (PAO), designed to provide exoskeletal assistance with plantar flexion for a user unable to properly complete this portion of normal gait. A PAO is a powered assistive device with a large variety of potential applications, such as rehabilitation and enhancement of human performance. The PAO is an exoskeletal orthosis that is easily removable and simple to operate for any user. The PAO is worn using a simple fitted orthosis mold and no surgery is required. The PAO is strapped onto the user's foot and shank and is generally used to provide additional force to the ball of the user's foot during push-off.

Roughly 90% of the gait cycle is spent with negligible ankle energy output. A device designed to store energy over a larger portion of the gait cycle would be able to take advantage of the ankle's idle time to prepare for push-off. The main power source for this PAO is an electric motor which was selected because of its large power density and clean operation. In order to reduce the size of the motor needed to drive the system, a spring is compressed during gait to store the energy needed for push-off. This enables the PAO to use a small electric motor to meet the peak power demand during gait. The device is powered by transferring energy from an electric motor to compress a spring via a transmission. At push-off, the energy release

mechanism quickly releases the spring's energy. The PAO pulls the heel upward, causing the toe to be pushed down; thus creating artificial plantar flexion.

After creating a conceptual design, the next phase was to fabricate and assemble the components using the College of Engineering and Technology's subtractive prototyping lab (machine shop) for testing. Once the components were built, the PAO system was assembled and tested on a benchtop testing frame using high-speed video footage. Results from these tests include displacement, velocity, acceleration, torque, and force created during the operation of the powered ankle orthosis. Through this research, it was determined that a PAO powered by a small DC motor is able to produce enough force to be a viable option for gait rehabilitation. The analysis also provided a basic understanding of the dynamics of a PAO releasing energy from a spring. Additionally, the effect of the component properties was examined to understand how the PAO system can be configured to each individual user, as well as the effect the user's foot size has on the performance of the PAO.

CHAPTER 1: INTRODUCTION

1.1 Physically Handicapped Among the Population

According to the United States Census Bureau, in 2010, there were approximately 41.5 million people over the age of 15 who were physically disabled in the U.S (Brault, 2012). This equates to about 1 out of 6 people (17.2%). Roughly 30.6 million of the physical disabilities were associated with ambulatory difficulties, such as walking. Difficulty walking is commonly associated with a gait abnormality, such as foot drop, a limp, or plantar flexion failure (Brault, 2012). These gait abnormalities often result in limited mobility, such as inability to walk over prolonged distances or on inclined planes. However, through proper rehabilitation methods, many types of gait abnormalities can be improved using assistive devices (Gordon & Ferris, 2007).

For centuries passive devices, such as canes and orthotic braces, have been used to assist people with walking abnormalities. In more severe cases, when a cane or brace is insufficient, one of the only remaining options is a wheel chair. At this point, the user begins to develop a complete dependence on the wheel chair. In order to bridge the gap between the low-assistance canes and the total-assistance of the wheel chair, new assistive devices are needed to expand the spectrum of rehabilitatable patient conditions. Powered assisted orthoses are wonderful candidates for bridging this gap.

1.2 Existing Powered Assistive Devices

Orthoses, as defined by the American National Standards Institute (ANSI), are externally applied devices used to modify the structural and functional characteristics of the neuromuscular

and skeletal system (1, 2007). These include passive devices such as wheelchairs, canes and orthotic braces. Some of these device, such as canes or crutches, can be tiring to use, making them difficult to use for long durations. Furthermore, these devices are not well suited for assisting users in normal gait with varying levels of assistance. Some people may only require minor assistance while others may need more. In addition, another problem with canes is that, a person walking with a cane may learn an adapted gait that relies on the passive device. This may lead to dependency on the device or orthopaedic problems resulting from gait asymmetry.

Passive orthotic devices help to guide movement and rely on the user to provide the energy. Passive orthoses can assist with gait, but sometimes the energy that the person is able to provide is not enough. Powered orthoses have the advantage of using energy from an external power source in addition to the user's energy to accomplish tasks. A powered orthosis can be used for a variety of functions: movement restriction, movement assistance and movement guidance are just a few of the common uses for orthoses (Yan, Cempini, Oddo, & Vitiello, 2014). When one of these devices are given an alternate source of power, such as a motor, pneumatics or hydraulics, the device becomes a powered assistive device. Powered orthoses, also referred to as powered exoskeletons, exoframes or exosuits, are an advancing field in technology for human assistance and enhancement (Krebs, Dipietro, & Levy-Tzedek, 2008). Measuring heart and metabolic rates, powered orthoses have shown positive results for use in rehabilitation and assistance. These systems have even allowed nonambulatory patients to walk again (Asselin, et al., 2015).

The first practical powered exoskeleton design was developed in 1965 with GE's Hardiman I (General Electric, 1969). However, the design never achieved a final product and it was decades before functional prototypes begin to appear. Powered orthosis prototypes have

been quickly gaining attention since the early 2000s, but have been limited by their power sources. Early models were restricted to designated facilities using a tethered power supply to operate the orthosis (Shorter, Xia, Hsiao-Wecksler, Durfee, & Kogler, 2013). In 2009, Dr. Homayoon Kazerooni of University of California at Berkley and his team announced the Human Universal Load Carrier, or HULC. The HULC exoskeletal system is designed to assist soldiers with carrying up to 90.7 kg (200 lb_m) in environments with lowered oxygen levels, such as the mountains of Afghanistan (Kazerooni, 2009). With further research and development of these systems, the exoskeletons can be fitted for a multitude of tasks, both in military and industrial applications. The HULC is a hydraulic system powered by a battery with up to eight hours of walking time. However, the HULC's primary objective is to enhance the performance of an already healthy user.

In 2011, a full body powered exoskeleton, called HAL-5, was released in Japan to hospitals for use by people with disabilities and elderly patients. The HAL-5 device is one of the first commercially available exosuits. It marks a milestone in powered orthotic devices and has shown the value of such devices. The device is targeted towards patients who have limited mobility. This was seen as an imminent necessity due to a unique phenomenon in Japan where the combination of the world's longest life expectancy and the lowest fertility rates (Ministry of Internal Affairs and Communication, 2014) have created a large Japanese elderly population with a small younger working generation that struggles to provide sufficient care. Alternatively, the system can be modified for use as a long-term rehabilitative device (Keizai, 2013). Currently, a newer lower body variation of the HAL-5 exoskeleton is being tested, which may be less cumbersome and better suited for patient rehabilitation (Cyberdyne, 2015).

There are several other exoskeletal systems being developed for users with permanent nerve damage or disabilities. Many of these devices assist with a specific assistive function of the user's limbs; e.g. assistance with standing up from being seated or carrying weight. (Yan, Cempini, Oddo, & Vitiello, 2014). While there are several powered assistive devices for a variety of functions, when a powered device is needed for assistance with a specific ability such as plantar flexion, there are very few commercial devices for the task. Further, these assistive devices have limitations, making each suitable under only certain circumstances, such as in-clinic only use (Kogler, Loth, Durfeee, Hsiao-Wecksler, & Shorter, 2011).

With the advancement of the exoskeletal technology comes the development and refinement of different driving mechanisms. Improvements over previous systems can be made to increase efficiency and/or response time. In addition, the development of new powered orthoses will allow for smaller and better suited assistive devices for those with more specific rehabilitative needs. Currently, many powered ankle orthoses are primarily driven by a fluid, such as hydraulic or pneumatic (Ferris, Czerniecki, & Hannaford, 2006). This is because, during normal gait, the ankle produces a peak power of about two watts per kilogram-meter, (Figure 1.1). This would be 175 watts for an 85 kg (187 lb_m) person (Winter, 2009). An electric servo motor capable of producing enough power to produce this power would be bulky and impractical. However, roughly 90% of the gait cycle is spent with negligible energy output. A device designed to store potential energy, rather than work on an impulse, would be able to take advantage of the ankle's idle time to prepare for push-off.

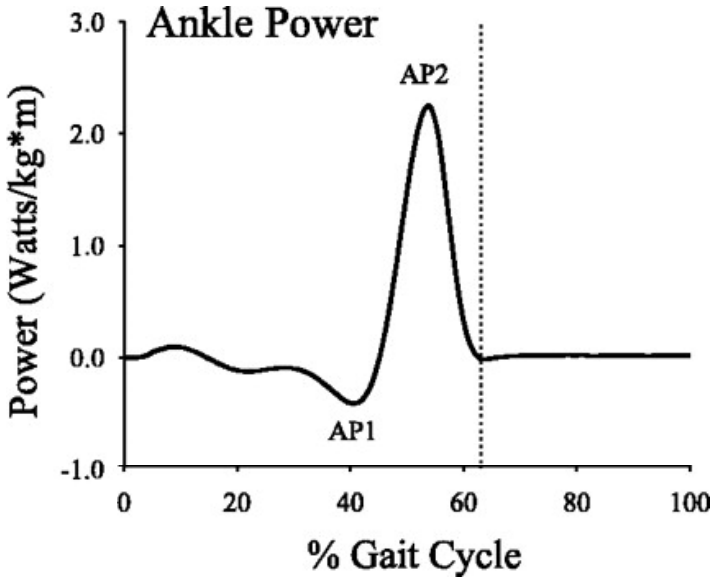

Figure 1.1: Ankle power output over gait cycle (Winter, 2009)

1.3 Electric Motor Powered Ankle Orthosis

With any assistive device, there is a level of intrusiveness that the device places on the user. For the purposes of this research, the intrusiveness of these devices was broken down into three levels; Figure 1.2 displays a chart depicting a scale of intrusiveness. Level I devices include the previously mentioned devices such as canes, wheel chairs and strap on braces. These devices generally provide a low level of assistance, only providing support to the user. The Level II devices include powered orthoses and exoskeletons. This level of device provides high level of assistance by contributing energy to the user. These devices do not require surgery and can be easily attached and removed. This level is relatively new and not only expands the group which can be rehabilitate, but may potentially expedite the rehabilitation process. The level III devices are the most intrusive, often requiring surgical implementation, such as a pacemaker, deep brain stimulator or prostheses to replace an entire limb.

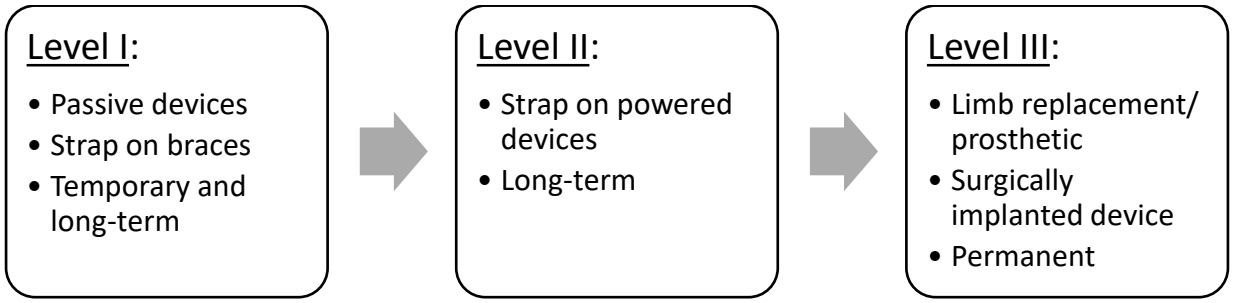

Figure 1.2: Scale of device intrusiveness

At this time, the availability of small portable (non-tethered) powered orthoses is very limited. Externally powered, or tethered, systems can be problematic because they confine the use area of the orthosis to labs and specially designed clinics. An untethered system such as the one studied in this research would allow its user to wear the PAO in most everyday environments. Similar untethered systems are being tested at several research facilities across the country. These systems are primarily fluid-powered (pneumatic or hydraulic) (Kogler, Loth, Durfeee, Hsiao-Wecksler, & Shorter, 2011). These systems show promising results of assisting plantar flexion in impaired walkers with an untethered PAO (Kogler, Loth, Durfeee, Hsiao-Wecksler, & Shorter, 2011). The PAO designs used for some of the recent research was powered pneumatically, which may not be suitable for many users. Pneumatic systems require either an attached air compressor or a compressed air reservoir, which are both bulky by nature. While the air tank can be easily carried about the user's body, the tank can be dangerous to mount to unstable patients and difficult to fill. Pneumatic systems also require frequent maintenance to ensure seal integrity.

The goal of this research was to develop an ankle orthosis falling under level II on the scale of intrusiveness. The ankle orthosis includes a small electric motor which builds energy

throughout the gait cycle and releases the energy to assist with plantar flexion. This would increase the motor operation time from one tenth of a second to about one second, reducing the peak power requirement by an order of magnitude. By taking advantage of idle time in the gait cycle, the size of the motor could be decreased.

An electric system also provides additional benefits that are not necessarily performance based. A purely electric powered system would be cleaner, quieter and without the potential for fluid leaking. In the future, the battery powering the system could be charged via a charging dock, located next to a bed or under a work desk. A PAO design like this makes for a device that can be easily integrated into a patient's everyday life.

By using springs to store potential energy, the PAO becomes more adaptable. The main spring can be swapped with softer or stiffer springs depending on the user's weight and the level of assistance needed by the user. A patient needing a high level of assistance would use a stiffer spring at the beginning of rehabilitation. As the patient's rehabilitation progresses and requires less assistance, a softer spring could be used, providing less force at push-off.

CHAPTER 2: LITERATURE REVIEW

2.1 Normal Gait (Anatomy and Muscle Function)

When people walk, they complete a process known as the gait cycle, shown in Figure 2.1 (Rose & Gamble, 1994). The gait cycle begins with the heel strike, the moment the heel of the foot touches the ground. Impact energy is absorbed by the soft tissues around the heel as the foot continues to make contact with the ground. Impact energy is absorbed by the muscles and tendons used to slow the foot during impact, while also helping to maintain stability. This is an important step since the absorbed energy is stored in the tendons loaded in tension. After heel strike, the body's weight is shifted forward to progress the leg through single-limb stance, loading the tendons further. At the end of the single-limb stance phase, the leg reaches the push-off stage, which is the main point of interest for this research. At this point, the foot needs to produce enough force to push the body upward and forward. The stored tendon energy is released, and muscles are recruited to push the ball of the foot downward. The torque generated for plantar flexion during the push-off stage of gate and the highest joint energy output during gait. This push-off force provides the necessary propulsion to carry the walker forward. (Shorter, Xia, Hsiao-Wecksler, Durfee, & Kogler, 2013). During this time, the opposite leg is transitioning through the gait cycle as well.

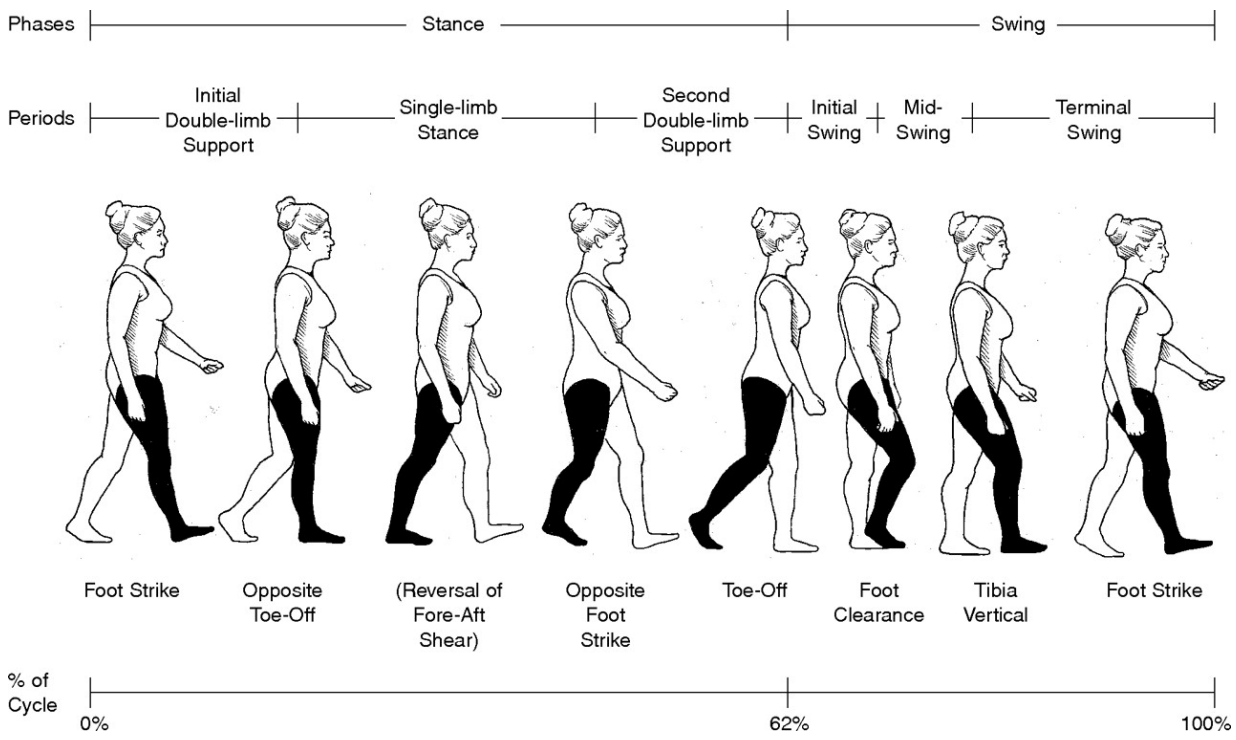

Figure 2.1: The steps undergone during the gait cycle (Adapted with permission from Sutherland DH, Kaufman KR, Moitoza JR: Kinematics of normal human walking, in Rose J, Gamble JG [eds]: Human Walking, ed 2. Baltimore, MD: Williams and Wilkins, 1994, pp 23-44.)

During normal gait, the ankle undergoes two crucial types of joint movement. The first type is called dorsiflexion, which is the movement of picking up the front of the foot. This action is controlled by the tibialis anterior muscles in the leg and prevents tripping during normal gait (Kreighbaum & Barthels, 1990). When damage occurs to these muscles, the ability to dorsiflex is impaired, resulting in a condition called Foot Drop. The second type of muscle movement is plantar flexion, the action of pushing the ball of the foot downwards. This motion is controlled mainly by the Gastrocnemius and soleus muscles and, with the help of stored energy in the Achilles tendon (Sawicki, Lewis, & Ferris, 2009), creates propulsion during the push-off portion of the gait cycle. The propulsion must carry enough momentum to complete a full stride; otherwise, a limp occurs during gait. Plantar flexion in the ankle accounts for roughly 70% of the

hip, knee and ankle joint work output during normal gait, making it a crucial ability (Kuo, Donelan, & Ruina, 2005). The inability to push off could be caused by several factors, e.g. injury, disease, stroke or movement disorders. The difference between the two motions is illustrated in Figure 2.2.

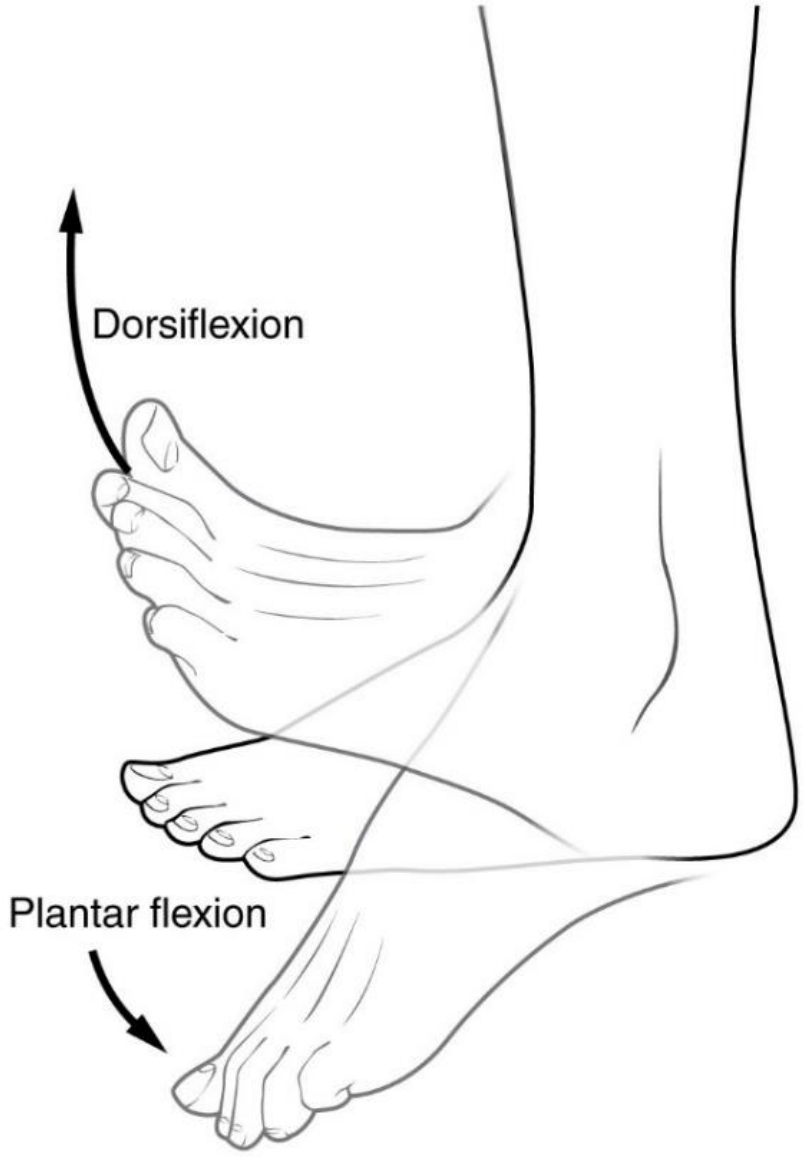

Figure 2.2: Illustrating the difference between planter and dorsiflexion (By Connexions (http://cnx.org) [CC-BY-3.0], via Wikimedia Commons)

2.2 Diseases Disabilities and Injuries Leading to Abnormal Gait

One patient population this device would be targeted for are people suffering from multiple sclerosis (MS). MS is an inflammatory disease that affects the protective layers that insulate nerve cells in the brain and spinal cord leaving them to be easily damaged (Compston & Coles, 2008). Once the damage has occurred, the brain may not be able to communicate with the associated muscles in the body. If, for example, the gastrocnemius and/or soleus muscles that attach to the Achilles tendon were affected, the individual may have difficulty or a complete inability to planter flex (Kreighbaum & Barthels, 1990). This would, in turn, cause difficulty in walking. Other diseases that can affect planter flexion and gait include Huntington's disease, polio, and Parkinson's disease.

Individuals with muscular dystrophy (MD) are another patient population that this research may be able to assist. Muscular dystrophy refers to a group diseases characterized by progressive degeneration of the skeletal muscles. This includes muscle weakness, defects in muscle proteins caused by genetic mutations, and the death of muscle cells and tissue (The Muscular Dystrophy Association, 2016). Since all muscles in the body are affected by MD, common symptoms include frequent falls, a waddling gait and an inability to walk altogether. There is no cure for these diseases, but treatment such as physical therapy, medication, surgery and orthopedic devices can help alleviate symptoms (U.S. National Library of Medicine, 2016).

Beyond disease and disability, plantar flexion difficulty can be caused by physical trauma (Dietz, 2013). One group in particular that receives large numbers of limb injuries are soldiers. Between October 1, 2001 and June 1, 2006; 3,854 soldiers received injuries to lower extremities requiring battlefield evacuation (Stansbury, Lalliss, Branstetter, Bagg, & Holcomb, 2008).

Improvised explosive devices, or IEDs, are a major cause of many of these injuries. For many of these soldiers, months or even years of physical therapy and specialized equipment are required.

Among the population as a whole, damage to the spinal cord can cause numbness and degraded control of the nervous system in parts of the body. Likewise, physical injury of the Achilles tendon may impair the muscles used during plantar flexion. These injuries can occur from a variety of incidents including automobile accidents, falls or impacts from heavy objects. Even after some of these injuries are addressed surgically, physical therapy is often needed for months following this injury in order to improve recovery.

Stroke victims are also associated with plantar flexion difficulty. A stroke can be described as a "brain attack" and can affect anyone at any time. A stroke is caused when blood flow is cut off to an area of the brain, causing brain cells to become oxygen deprived and die. Common areas affected by strokes control memory and muscle control. More than 2/3 of stroke survivors suffer some type of disability and strokes are the leading cause of disability in the U.S. (National Stroke Association, 2016). A common consequence of strokes is hemiparesis, a weakness, numbness, or paralysis of either the left or right side of the body. The weakness or numbness often causes difficulty in controlling the required muscle groups to complete gait. Treatment for stroke usually includes physical and/or speech therapy along with utilization of low-intrusion assistive devices.

2.3 Electric Motors

In order to build the powered ankle orthosis, specifications for crucial components, such as the motor, needed to be defined. The process of the electric DC motor selection required an understanding and comparison of available motors. First, the pros and cons of servomotors and stepper DC motors were examined. A stepper motor consists of many poles surrounding the

motor shaft in precise intervals. As an electrical drive pulse is sent to the motor and the motor shaft moves to the next pole. With the large number of poles and precise increments between them, a stepper motor is ideal for uses that require precision. Stepper motors also have the added benefit of not requiring positional feedback for the motor. Further, stepper motors provide more torque than similarly sized servo motors at low speeds. However, stepper motors have a significant loss of torque at higher speeds (Burris, 2016).

Servomotors were the next electric DC motor type considered. Servomotors consist of usually two or four poles which are energized accordingly to push/pull the motor shaft into rotation. Servomotors are not as precise as stepper motors by themselves, but can be equipped with position encoders when knowledge of angular position is needed. A major advantage to servomotors is their ability to operate at high RPM while maintaining most of their torque. For this reason, a servomotor was chosen to be used to drive the PAO (Burris, 2016).

2.4 Springs

In order to use a smaller electric servomotor operating over time to drive the PAO, a method to store potential energy was necessary. Springs are an excellent device to store energy due to their high reliability and consistent performance over time. Springs are commonly available in a large variety of configurations to suit almost any task. Common springs, such as coil springs, are a relatively inexpensive component that can be easily swapped.

When determining the proper spring for a project, the first characteristic to consider is the spring size (diameter and length). Size is an important first consideration because it is important to find a spring that fits properly. Too large of a spring would not fit in the device; too small would be loose and would not take complete advantage of the operating space inside the PAO.

The next specification to consider is the load capacity of the spring. The load capacity of a spring is simply the maximum load the spring is rated to hold without deforming (Oberg, Jones, Horton, & Ryffel, 2008). It is important to use a spring which does not exceed the load capacity under operation. This will allow the spring to operate for its full lifespan.

Finally, the spring rate must be considered. The spring rate defines the amount of force a spring imposes when being compressed. The spring rate is based on several spring properties, such as spring material, spring thickness and spring pitch (Oberg, Jones, Horton, & Ryffel, 2008). A spring made with thick high-carbon steel wound tightly will make a stiffer spring with a higher spring rate than a thin brass spring wound loosely. The availability of springs with varying combinations of these properties enables customization of the PAO's performance characteristics.

2.5 Threads and Threaded Transmission

Screws are a common mechanical method of converting rotational motion into linear motion. The conversion is done using threading, helical ridges wrapped around an axis. Threads must correspond with another threaded object to operate smoothly, e.g. a bolt and nut. The two most common types of threads are coarse and fine threads. The most easily distinguishable difference between these two thread types is the pitch which is the distance between the threads. A coarse thread has a larger pitch than a fine thread, meaning less threads per inch (TPI). Fine threads have the advantage of stronger shear, tensile, and pull-out strength due to greater surface area. However, coarse threads have the advantage of larger threads, which have better resistance to wear (Oberg, Jones, Horton, & Ryffel, 2008).

For situations requiring abnormally high load, there are also Acme threads. Acme threads are a common form of trapezoidal thread used for applications such as vises and leadscrews

(Bhandari, 2007). The main disadvantages of Acme screws are a larger pitch when compared to coarse and fine threaded rods of the same diameter. Also, Acme rods are not as commonly available and lack the variety of coarse and fine threaded rods. Still, acme threads have strong potential for a transmission in a PAO system.

When using a threaded shaft for power transmission, the thread's lead plays an important role in the selection process. A thread's lead is the linear distance travelled with one revolution of the screw. Lead and pitch are commonly the same value, except when the thread has more than one start. This means that the lead is directly related to the mechanical advantage associated with the threaded shaft; a smaller lead will mean a larger mechanical advantage.

Lead also effects the efficiency of a threaded shaft transmission. When the lead of a thread is increased, the lead angle of the thread is increased as well. Imagine the threads being "steeper" to cover the distance of a greater lead in one revolution. As the lead angle increases, so will the efficiency (Vahid-Araghi & Golnaraghi, 2011). The friction coefficient between the two mating threads remains constant at varying leads. This means that a threaded shaft transmission with a lower lead will have greater mechanical advantage, but a lower efficiency. A balance must be found to optimize performance from the transmission.

CHAPTER 3: DESIGNS & CONSTRUCTION

A crucial component of this research was the design and fabrication of a proof-of-concept powered ankle orthosis prototype. First, an initial prototype was designed, built and evaluated. Using information gained from testing the initial design, a final proof-of-concept design was developed. This chapter covers the development of each design, the flaws of the initial design, and the steps taken to address them which ultimately lead to the final proof-of-concept design.

3.1 System Design

The central idea driving this research was to design a PAO system that can replace a large, heavy, and bulky motor with a small electric motor. A system which runs continuously, storing energy and releasing energy at a specific time requires a specialized system of components. A PAO that could store energy and release 400 N (90 lb_f) of force during push-off was the long-term goal.

The PAO design consists of five main functional components. The first component is the electric motor used to provide power to the system. The next component is the threaded rod, which acts as a transmission for the system by converting rotational motion output from the electric motor into linear movement of the clutch block. The energy storage mechanism (ESM) is a significant component group for the system. The ESM consists of the clutch block, threaded inserts and a steel coil spring for energy storage. The fourth component for the system is the shell which stores the internal mechanisms. The final main component is the orthosis which allows the system to be mounted to a user. The orthosis was substituted for a benchtop fixture for this research to assist with early observation and preliminary testing. All of these components were

integrated into one system to design; a PAO that could be used to test the feasibility of a small motor orthosis.

3.2 Design Approach

The powered ankle orthosis was designed to test the device's feasibility as a rehabilitative device, with the goal for the device to assist a person to replicate normal gait as closely as possible. During normal gait, the average person requires roughly one and a third seconds to complete a gait cycle, from push-off to the next ipsilateral push-off (von Schroeder, Coutts, Lyden, Billings Jr., & Nickel, 1995). Within the same time frame, the PAO system must be able to store energy, release the energy and be ready to begin storing energy again. Because of this small window, it was crucial to maximize the amount of time available to store the necessary energy for the system. In order to maximize the storage time, a clutch-type system was designed and fabricated for the energy release mechanism. A clutch is appealing because it allows the motor to disengage from the transmission, allowing the remainder of the system to reset more quickly and reengage quickly. Without the clutch, the system would have to reverse every action taken in order to prepare for the next cycle.

3.2.1 Motor Specifications

At the preliminary CAD stage of the PAO, a Dewalt DCD950 cordless drill was chosen to drive the device. This was opposed to a standard/stock electric servomotor, for several reasons. To start, the cordless drill uses a readily available motor and gives a good example of the capabilities of a smaller DC motor. Another huge advantage of using a drill is that it is a relatively finished product. In other words, the drill does not require modifications to be used for the bench model, only a simple adapter for the chuck and threaded rod. Lastly, the adjustable chuck is an additional benefit for performing easy adjustments during testing.

In the highest speed settings on the Dewalt DCD950 drill, the motor operates at approximately 2000 RPM and capable of 450 unit watts out (UWO). Unit watts out is an indication of the drills power at varying speeds, as opposed to the more common max torque and max speed values. To understand if 450 UWO was enough power to compress the spring and power the PAO, the necessary torque to compress the spring needed to be calculated.

The first step in determining the required torque for spring compression was to calculate the maximum force placed on the system by the spring. Due to the nature of foot geometry, the distance from the fulcrum to the ball of the foot is greater than the distance to the heel. For any amount of desired force at the ball of the foot, a larger force is required when the PAO is attached to the heel. The mechanical advantage can be calculated using the ratio of the lengths

$$R = \frac{L_{Heel}}{L_{Ball}} \tag{1}$$

Where L_{heel} is the distance between the foot fulcrum and L_{ball} is the length between the fulcrum and the ball of the foot. For the dummy foot, the mechanical advantage is less than 1 with R=0.654. As a result, the spring force needs to be about 153% of the desired push-off force.

By calculating the maximum necessary force, the minimum torque needed from the motor to compress the spring can now be found. This is calculated using the equation (Oberg, Jones, Horton, & Ryffel, 2008)

$$\tau_{max} = \frac{F_{max} * D_p}{2}\left(\frac{L + \pi * \mu * D_p}{\pi * D_p - \mu * L}\right) \tag{2}$$

With equation 2, the peak torque will occurs at the maximum load. Since the goal force is 400 N (90 lb_f) for push-off force, using the previously mentioned ratio, maximum force (F_{max}) of 612 N

(138 lb_f) on the PAO is calculated. This is the force valueused to find the max torque. The next step is to use the pitch diameter (D_p) for a 3/8"-16 threaded rod. This value has a range based on thread tolerance, determined by the thread's class of fit. For these calculations, a value of 8.46 mm (.3331 in) was used because it is the median value of the tolerance range. The thread lead is found by simply dividing the number of threads over one inch for the threaded rod. The thread lead (L) for the 3/8"-16 thread is 1.59 mm (.0625 in). The next value in equation 2 is the friction coefficient (μ) of .18 for dry steel on steel (Oberg, Jones, Horton, & Ryffel, 2008). Including the friction coefficient into the equation is needed to predict a more accurate value by taking into account the threads efficiency. When these values are placed into equation 2, the equation appears as

$$\tau_{max} = \frac{612\ N * 8.46\ mm}{2}\left(\frac{1.59\ m + \pi * .18 * 8.46\ mm}{\pi * 8.46mm - .18 * 1.59\ mm}\right) = 628\ Nmm = .63\ Nm \quad (3)$$

Using the calculated data, the PAO motor needs 0.63 N-m (5.6 in·lb_f) of torque to compress the spring.

Another aspect of the motor that was taken into consideration was the motor displacement. The amount of angular displacement is related to the spring rate of the main spring used in the system. To easily find the necessary angular displacement, the linear spring displacement (x) is calculated by rearranging the equation for spring force, shown below

$$F = kx \ \rightarrow x = \frac{F}{k} \quad (4)$$

If the maximum force value from the max torque calculation for force was used, the required linear displacement to compress a spring with a spring rate (k) of 10.49 N/mm (60 lb/in) can be determined. This calculation is shown below

(5)

$$x = \frac{612\ N}{10.49 \frac{N}{mm}} = 58.34\ mm$$

This linear spring displacement shows that the spring needs to be compressed 58.3 mm (2.3 in) to generate the desired 612 N force. The next step in finding angular displacement is calculating the necessary revolutions required to travel 58.3 mm (2.3 in) along a 3/8”-16 threaded rod. The number of revolutions is calculated using the equation

$$Revolutions = \frac{x}{L} \tag{6}$$

When this equation is used with the previously calculated linear displacement (x) value and the lead value from the max torque calculation, the equation appears as

$$Revolutions = \frac{58.34\ mm}{1.59\ mm} = 36.7 \tag{7}$$

What this equation shows is that using the same 3/8”-16 threaded rod and 10.49 N/mm (60 lb/in) spring, the main spring will require 36.7 revolutions to compress the spring to 612 N (138 lb_f) of force.

3.2.2 Solenoid Requirements

Originally, the PAO system was held in place and released by a small tubular pull-type solenoid. However, the force from the compressed spring was creating too much friction to allow the solenoid to operate properly. To find a solution, the frictional forces must be calculated. Using the formula below, the frictional forces can be found for various materials using their friction coefficients.

$$F_f = \mu * N$$

(8)

Where F_f is the total frictional force, μ is the friction coefficient for the used material and N is the normal forces acting on the moving object. The friction coefficient for steel against aluminum is .61 (Oberg, Jones, Horton, & Ryffel, 2008). This means that if the PAO was under the max spring load of 612 N (138 lb_f), the frictional force against the pin would be roughly 373 N (84 lb_f). This is a difficult issue to get around, since the only way to reduce the friction would be to use different materials or the load angle. A further complication is that the shaft of the pin is also required to be ferrous (magnetic).

After performing calculations for the friction of various materials, the necessary solenoid strength for the PAO was determined, as well as a method to reduce the friction. The solenoid used is a low-profile tubular pull solenoid. This solenoid has a pull force of approximately 378.1 N (85 lb_f) at a 3.81 mm (.15 in) stroke (Magnetic Sensor Sytems, 2005). A graph of the solenoids pull strength over distance is seen in Figure 3.1.

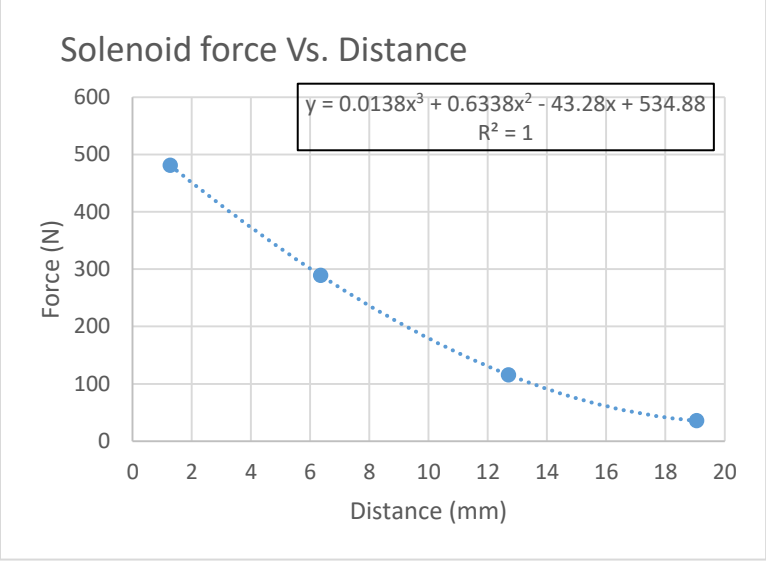

Figure 3.1: Graph of solenoid strength at varying stroke lengths

While the solenoid is a larger size than desired, it allows for purpose-flexibility as well as design redundancy during the testing of the proof-of-concept design. Furthermore, to reduce friction, a brass tip was fashioned for the solenoid pin. The brass tip reduces the friction coefficient from .61 to roughly .30 (Nuruzzaman & Chawdhury, 2012). In turn, this decreases the friction force against the pin to roughly 183.6 N (41 lb_f). An option to reduce the required solenoid size further would be to use a Teflon coating; with a friction coefficient of .041, a system using the same spring would only have approximately 25.1 N (5.6 lb_f) of friction. A concern with a Teflon coating would be the coatings resistance to wear and deformation under load.

3.2.3 Spring Requirements

The main spring for the PAO is a very crucial part that is easy to overlook. Springs are a valuable mechanical method for storing potential energy. Springs do not require electricity or wiring, they are lighter than motors and very reliable. Furthermore, by using a spring to store energy, many of the user's gait parameters can be changed by simply swapping out the main spring. This is done by considering both the spring's load capacity and spring rate.

The spring needs to be designated to handle the necessary maximum output force during the propulsion stage of gait. For user's who are large or in the beginning stages of rehabilitation, which may require more assistance, a spring with a higher load capacity and spring rate would be used. As the user progresses during rehabilitation, smaller load capacity springs can be used to help reduce dependency on the device.

The spring rate effects the PAO performance much like the pitch of the threaded rod. The spring rate effects the amount of energy stored over a length of compression. This translates to a spring with a higher spring rate storing sufficient energy to operate the PAO more quickly, but

requires more work from the motor. For the proof-of-concept model of the PAO, the design uses a spring with about half the needed load capacity and spring rate. This was to allow adequate system testing with a reduced risk of part failure of a crucial component. This is because a system using only enough force to prove the concept will place less stress and strain on the components while still providing valuable results.

3.3 Development Tools

Several development tools were used to create detailed designs for each component of the system. The development tools include 3D CAD (Computer Aided Design) software for individual component modeling and virtual part assembly, and computer aided manufacturing (CAM) software used to develop cutting tool paths based on the 3D CAD models.

3.3.1 CAD Software

Pro Engineer (Pro/E) Wildfire 5.0/Creo Elements is a computer aided design (CAD) software by PTC used to create virtual models of parts in a 3D representation. Pro/E uses a parametric modeling style that creates parts that are driven by dimensions and allows design constraints to help maintain design intent. This is an important feature in 3D part modeling because when creating and editing models, existing model dimensions can be modified and the changes automatically propagate through the associated features. Part models can be made using 2D sketches and extruded or rotated to bring the part into virtual 3D space. Once the part models are completed, an assembly model can be created by merging several parts and setting locational relationships between each part. Furthermore, the assembly can be animated with simulations of servo motors, cams, springs, etc. to observe how parts will interact in device operation. An animated assembly, allows users to inspect a model's operation and part dimensions to look for potential failures. This includes parts that will not fit during assembly or parts which interact or

jam with another part in a way that defeats design intent. Finding a failure at this stage saves the cost and time consumed creating a tangible part.

3.3.2 CAM Software and Manufacturing Equipment

Machining is the process of creating a part by removing material with equipment such as mills or lathes. These machines can make precision cuts in material with either manual operation or Computer Numeric Control (CNC) programming. To assist with complicated cuts, a Computer-Aided Manufacturing (CAM) software such as OneCNC is used to generate the CNC programming code. With CAM software, geometry can be created within the software; for more complex shapes, geometry can be imported from a CAD software, such as Pro/E or Creo. The geometry can then be used to create tool paths for the machine to follow. Because of this, it is essential that all part models are created correctly and designed with the machining process in mind.

The prototype CAD models for the powered ankle orthosis required several custom pieces to be manufactured or modified. Much of this fabrication work took place in the College of Engineering and Technology machine shop at Western Carolina University. The machine shop has four vertical CNC milling centers, three CNC lathes and a CNC CO_2 cutting laser. Also in the machine shop, there are several band saws, power tools and hand tools; all of this equipment was necessary for the fabrication of the custom components used in the PAO.

3.4 Initial Design

The first PAO design concept, shown in Figure 3.2, used an electric motor to store energy over time until needed for push-off. A cross sectional view of the conceptual design is shown in Figure 3.3. The system used a clamshell housing with grooves cut into the housing at a continuous pitch. Inside the housing was a mechanism which used retractable threads to engage

with the housing. A solenoid mounted at the end of the mechanism with a pin moving through the center controlled when the pins were engaged or retracted. When the pin was extended, the threads were engaged with the threads in the housing. When the solenoid was activated and the pin was pulled back, the threads were able to retract, disengaging the system from the housing threads. For this system, the electric motor spins the housing while the mechanism inside would remain stationary (relative to rotation), causing the housing to thread the center mechanism downward. As the center mechanism moves downward, it compresses a spring to store energy for push-off. When the user is ready for push off, the solenoid is activated, retracting the pin and allowing the threads to disengage from the housing. Next, the spring would release the stored energy upward, pulling the attached heel with it. When the mechanism reached the top of the housing, the solenoid would release the pin, reengaging the threads with the housing and preparing the system for the next cycle.

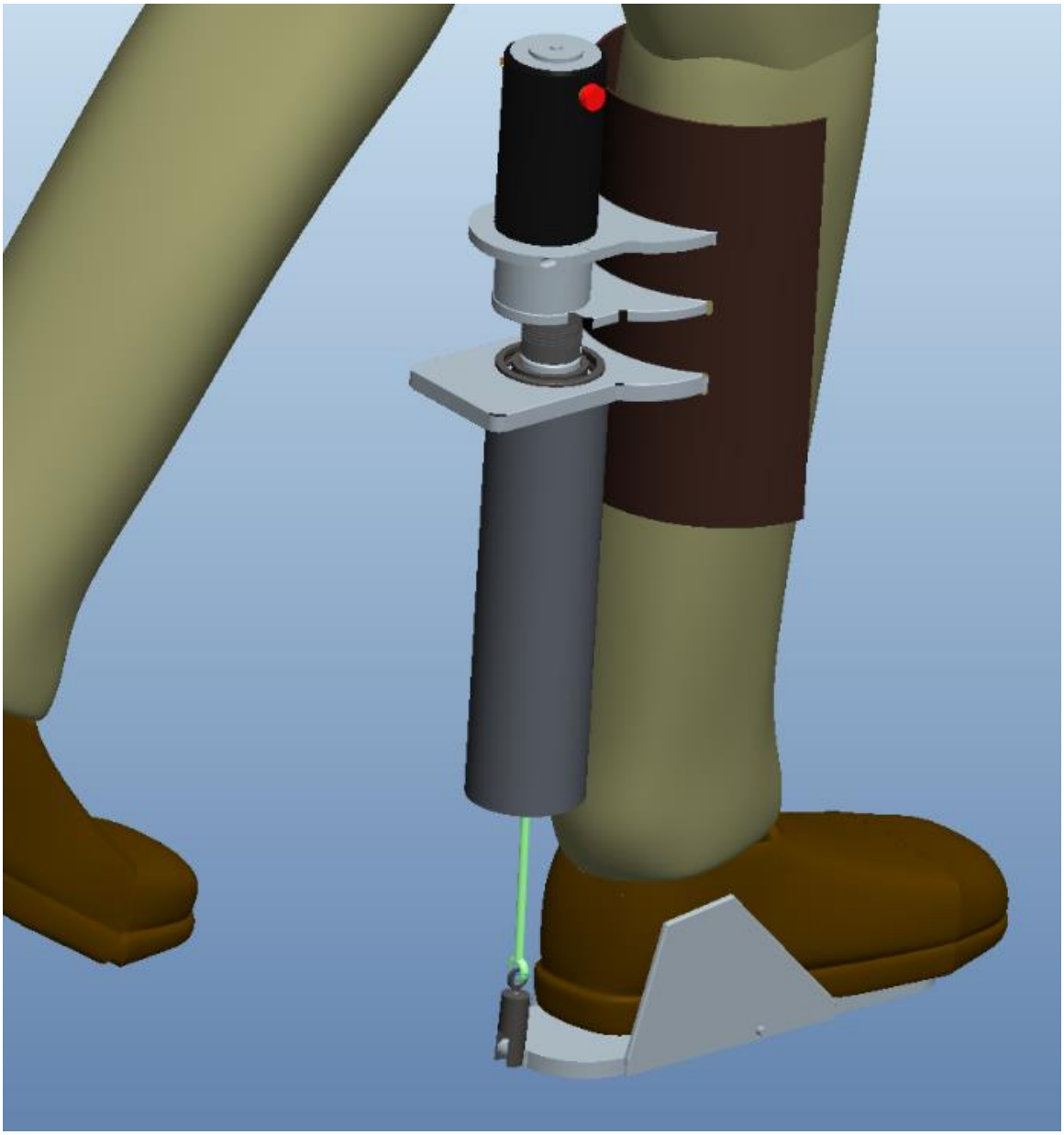

Figure 3.2: A CAD representation of the initial design being worn.

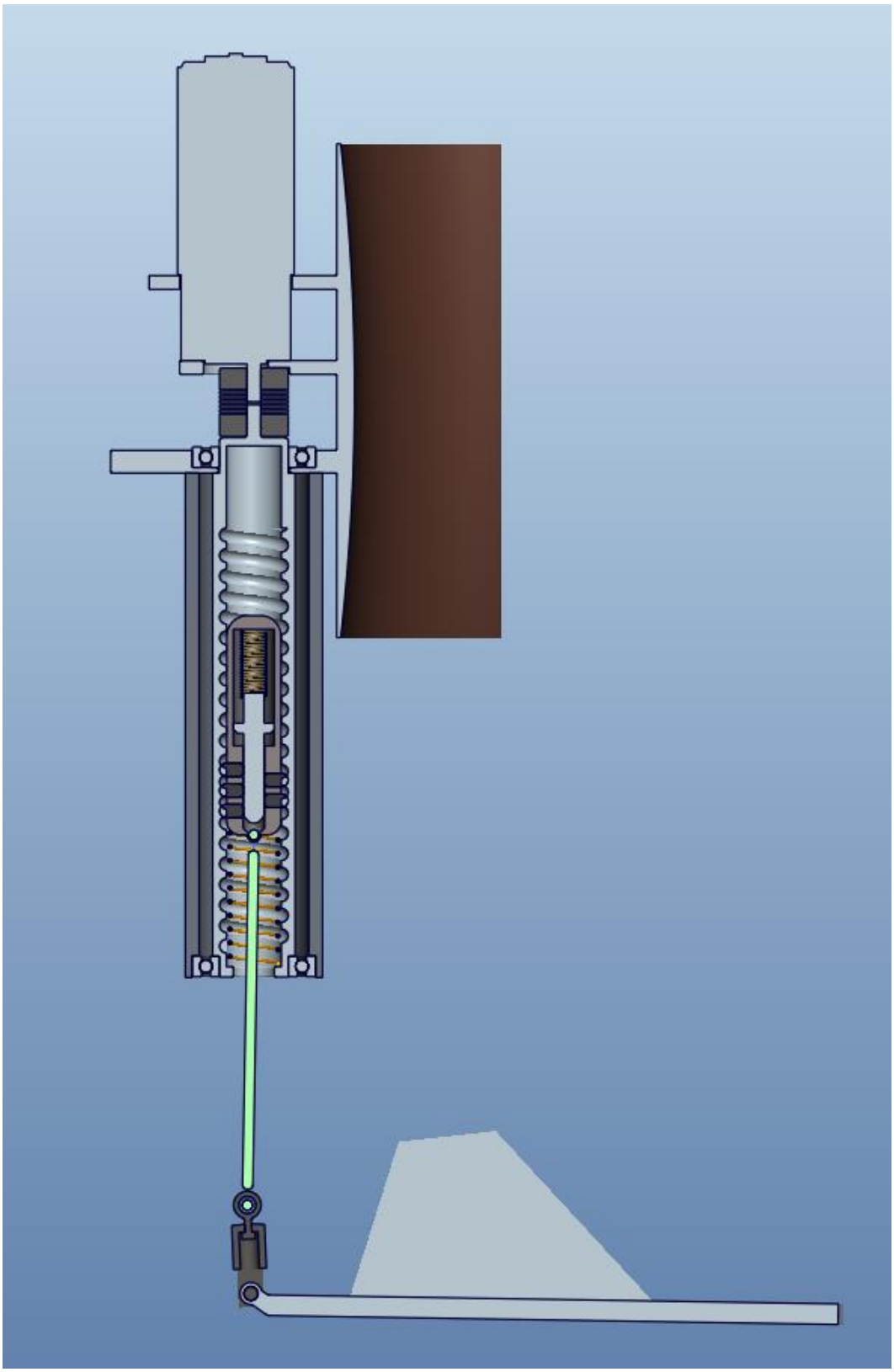

Figure 3.3: Cross-section of initial design

This initial design occupied much of the beginning of this PAO research. Several components were manufactured and tested, including a proof of concept test piece shown in Figure 3.4. However, the concept was dismissed after observing that there were too many uncontrollable variables and design flaws. Due to the complex nature of the design, many of the flaws were not realized until proof-of-concept models had been tested. Some of these issues were due to the lack of direct control of the retractable threads. Since the threads could reengage with the housing at any time, the system had considerable potential for jamming. Furthermore, the release mechanism did not have any rotational constraints, so it was able to spin freely with the housing, if that was the motion with least resistance. Another concern was for user safety, the larger housing's rotating mass seemed undesirable in case a component should break during use or any body part were to come into contact with the rotating housing.

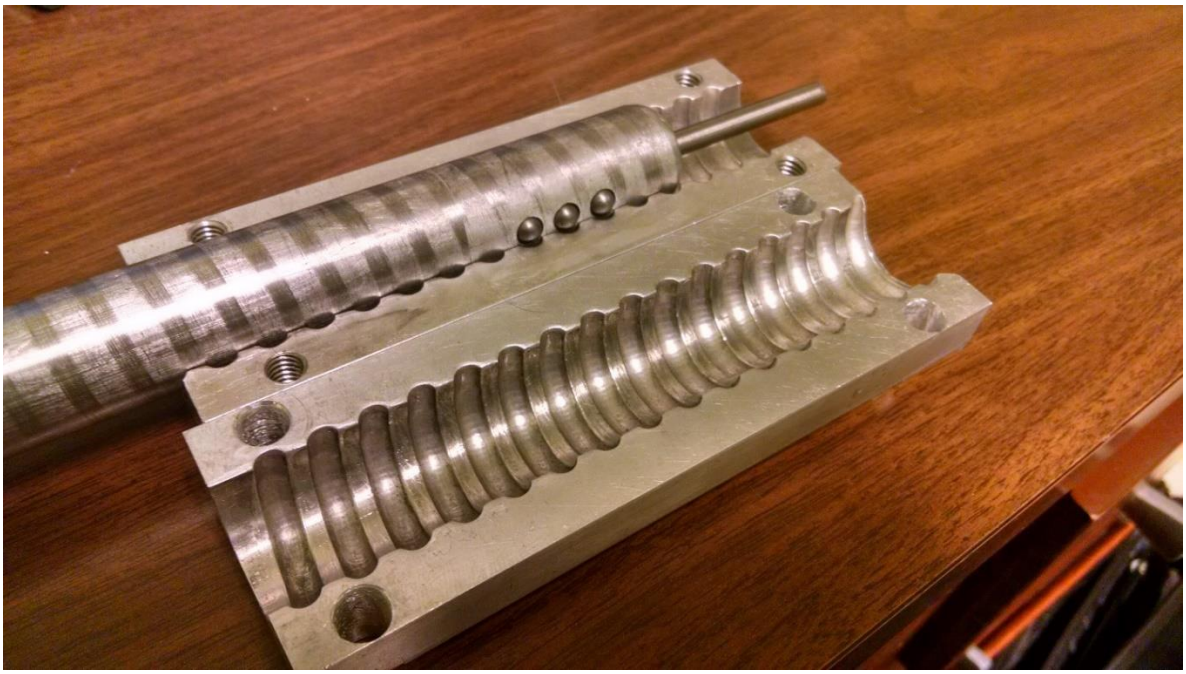

Figure 3.4: Machined test pieces of the initial design.

This first conceptual design provided valuable feedback on the PAO design process. Shortcomings of the initial design were addressed with a new concept. The new design was to have dynamic parts contained within the housing as much as possible. The design also had to prevent the energy release mechanism from rotating with the motor's transmission. Furthermore, the clutch for the transmission needed to have better control to prevent the system from jamming. This new design evolved into the final design described in section 3.5.

3.5 PAO Final Design and Operation

The final design for the powered ankle orthosis is as a bench top device used to evaluate the performance of the system (Figure 3.5). The system includes the motor, drive screw, energy storing spring, solenoid, housings, a simulated foot, and a weight. Although the system was not attached to the body as a wearable orthosis, verification of the function of the mechanical system is a necessary step in the overall device design. Figure 3.6 shows the conceptual PAO design in an isometric and normal cross-sectional view. These views provide a more comprehensive understanding of the PAO's operation.

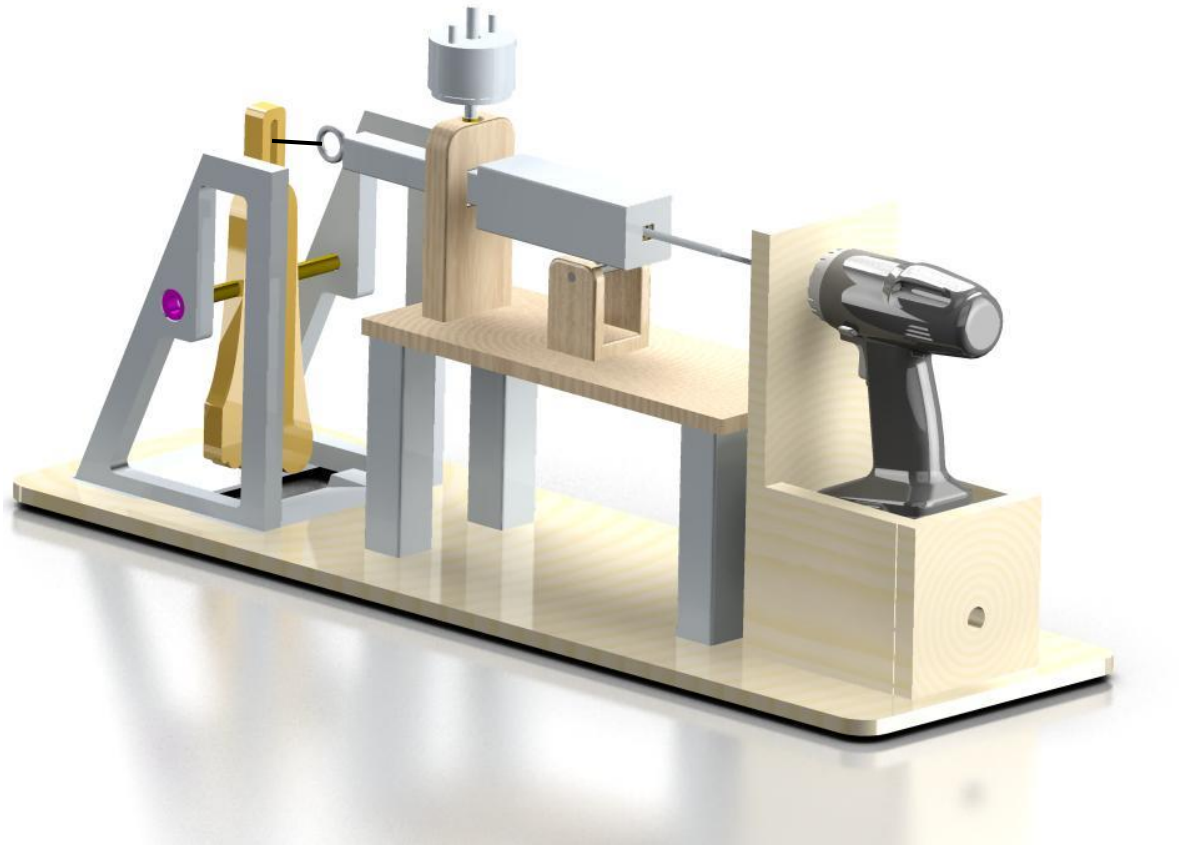

Figure 3.5: CAD rendering of final proof of concept design

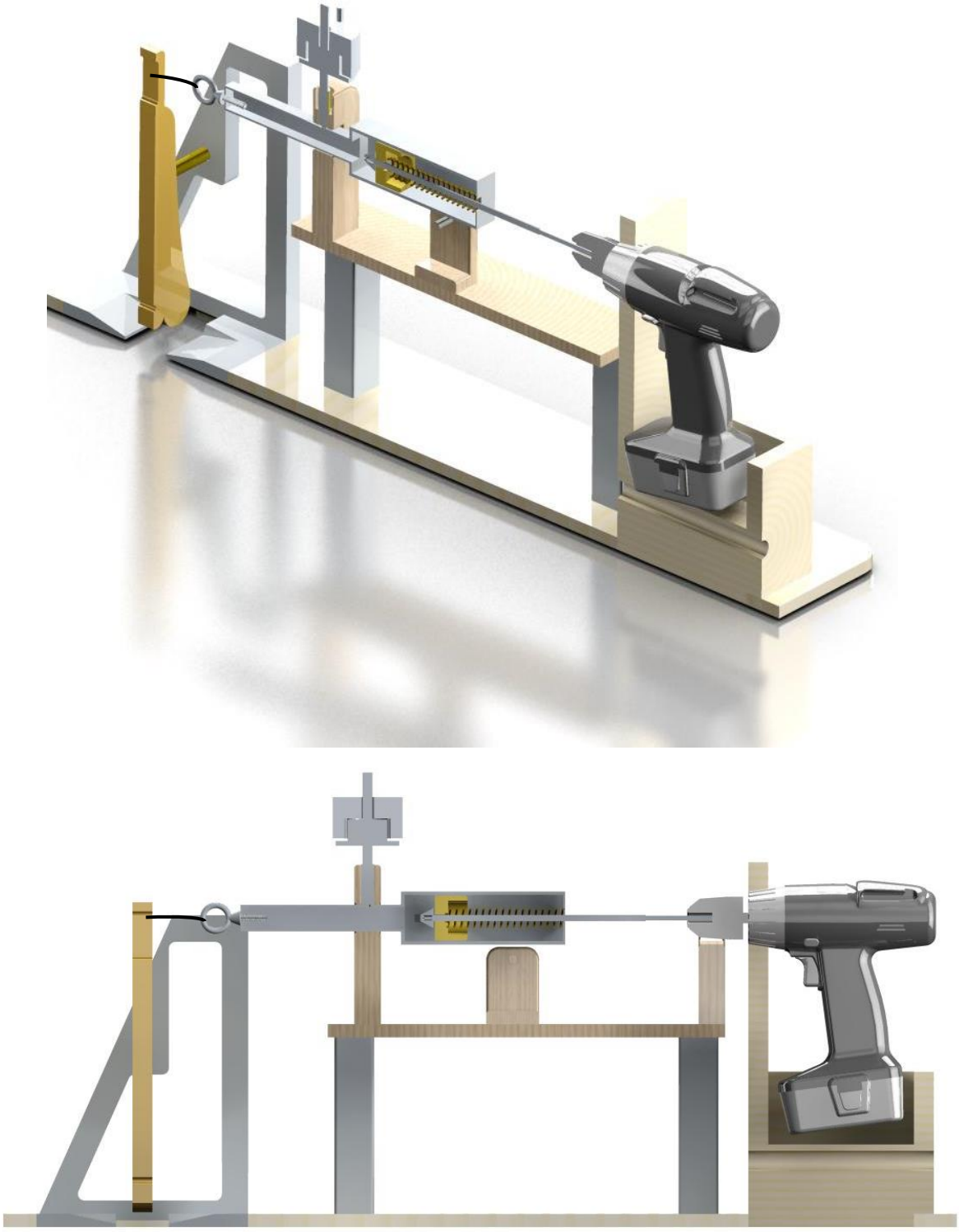

Figure 3.6: Isometric (top) and normal (bottom) cross sectional views of Proof of Concept design

As mentioned previously, the PAO is driven using an electric servomotor; a cordless drill was used for the final design. The drill's power density provides a valuable balance of speed, torque, and control; with the convenience of swappable batteries and being commercially available.

Operation of the device may be divided into three stages. The first stage is the storage of energy in the spring. Figure 3.7 begins with the PAO shell secured in place by the solenoid pin and the spring fully extended. This represents the PAO in a starting state, ready to begin storing energy. The electric motor is connected to the threaded rod, working as a transmission to transfer the motor's power. The pinch threads of the energy-storage mechanism are engaged with threaded rod.

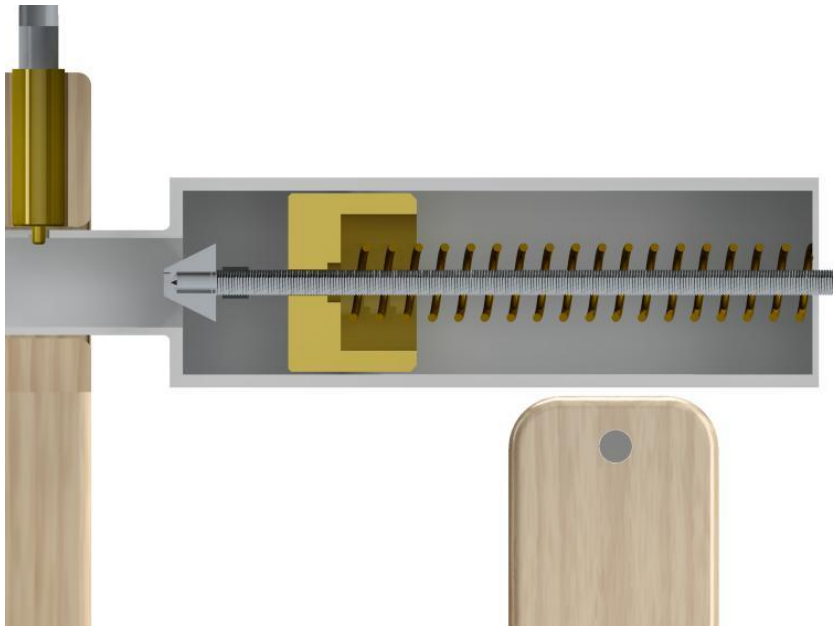

Figure 3.7: Close-up on PAO internal mechanism, ready to store energy.

When the electric motor is powered, the rotation is transferred directly through the threaded rod. The threaded rod is engaged with the remainder of the PAO via the threaded clutch

block in the energy-storage mechanism, or ESM. With the ESM mounted on the threaded rod, the ESM pinch thread inserts translate the rotational motion into linear motion. The block travels along the threaded rod while contained inside the PAO shell, which also holds the main spring in place. As the block moves along the threaded rod, the spring is compressed between the block and the opposite end of the shell. This is depicted in Figure 3.8

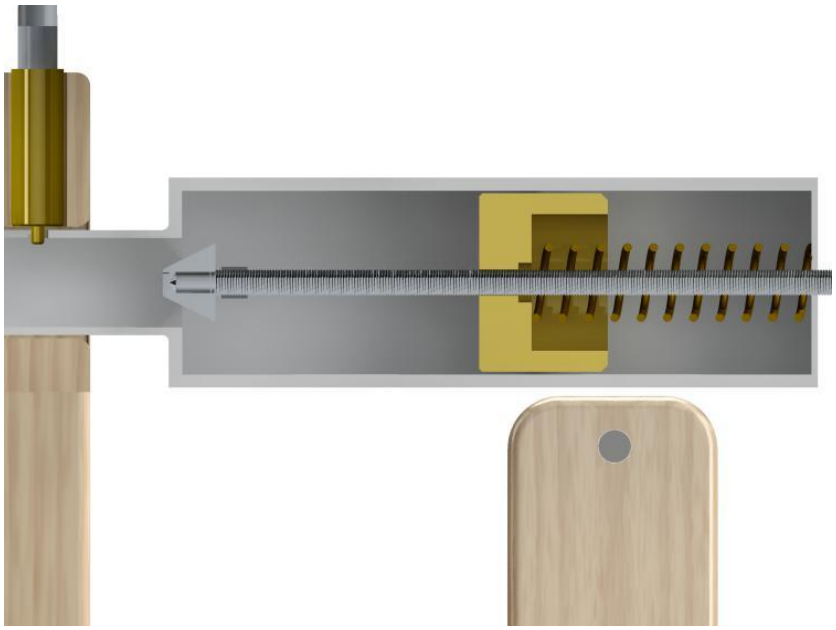

Figure 3.8: Close-up on PAO internal mechanism, ESM compressing the main spring

However, the shell must be held in place during the spring compression; otherwise, the shell would slide along the rod with the spring and block. The shell is held in place by a solenoid pin further along the shell. The pin secures the shell in place while the block compresses the spring. Now, the spring has been compressed and the foot is ready for push-off. At this point, the first stage of the PAO's cycle is completed.

Once the user is ready for push-off, the solenoid is energized, pulling the solenoid pin, as shown in Figure 3.9. At this point, while the pinch threads secure the ESM linearly, the stored

energy in the spring is released and propels the PAO shell around the ESM along the threaded rod, as shown in Figure 3.10. Along with the shell, an elastic band attached to the heel mount is also pulled upward. As the heel is pulled up, push-off is created as the ball of the foot is forced downward, simultaneously. At the toe-end of the dummy foot, a 5 kg (11 lb_m) mass is attached and ran along the bottom of the test rig. This weight is to simulate dorsi-flexion, which is necessary to reset the PAO for the next step in gait. Once the spring's energy has been released and the shell reaches the full forward position, the grooves in the shell cause the pinch threads in the ESM to disengage from the threaded rod. At this point the ESM is free to move relative to the shell.

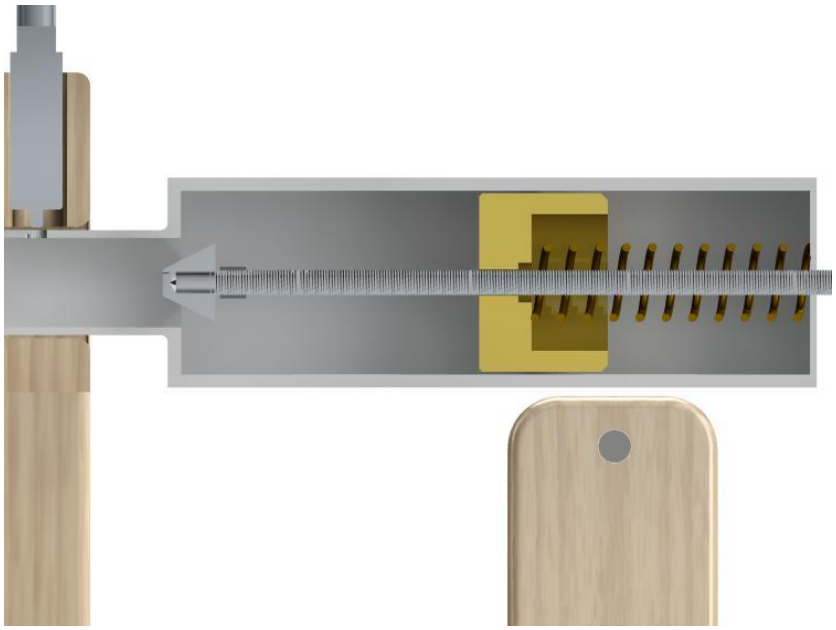

Figure 3.9: Close-up on PAO internal mechanism, solenoid pin releases the shell

Figure 3.10: Close-up on PAO internal mechanism, shell is thrusted upward

With the block, transmission, and motor disconnected from the rest of the system, the weight at the front of the foot pulls the shell back towards its original position. As the shell moves back (Figure 3.11), the solenoid pin descends down the ramp leading into the hole to secure the shell. The retaining nut at the end of the rod forces the ESM to reengage with the

transmission. With all of this complete, the PAO is then ready to start the cycle again to assist with the next step in gait.

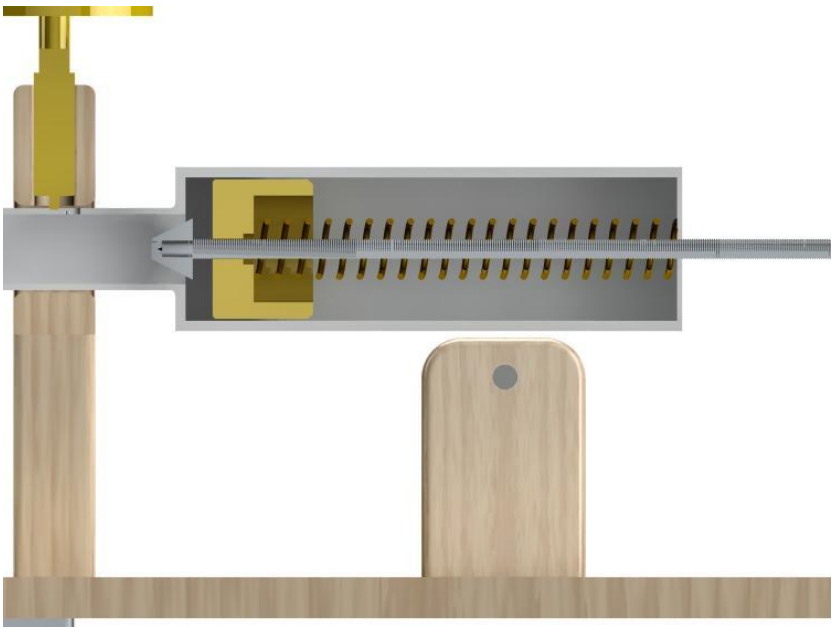

Figure 3.11: Close-up on PAO internal mechanism, shell is nearing reset point

3.5.1 Component 1: PAO Shell

The shell of the PAO houses the ESM mechanism and protects the user from dynamic parts. Without this protection, exposed parts could potentially pinch, cut or strike the PAO user or anyone nearby. The shell is made from 50.8 mm (2 in) aluminum square stock for the wider section and 25.4 mm (1 in) square stock for the narrower section. The squared profile keeps the ESM block from rotating freely around the threaded rod's axis, allowing the system to store energy more effectively than cylindrical stock. The main section of the shell, shown in Figure 3.12, has a window cut across the top to allow for easy monitoring of spring compression. The PAO also contains two parallel notches cut near the end of this section. The notches are a critical

feature to allow for the clutch system in the block to disengage from the transmission and reset the system.

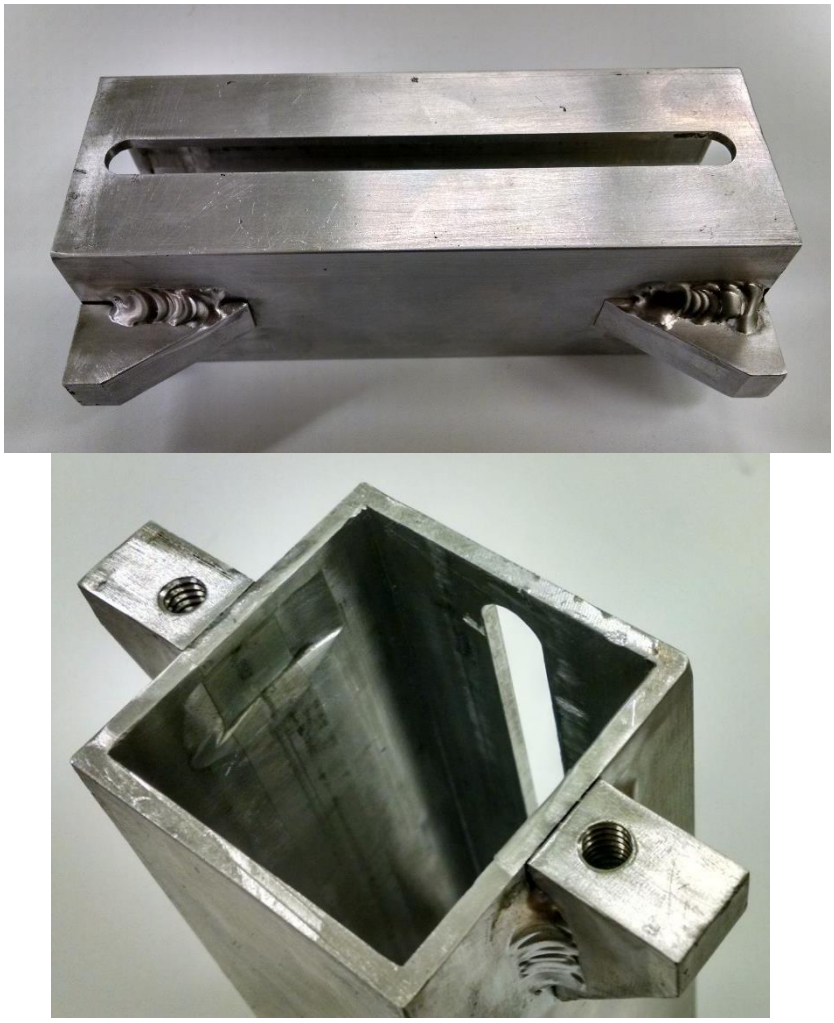

Figure 3.12: Larger PAO section overview (top) and close-in image of the grooves (bottom)

In the narrower section of the shaft, there is a 3/16” hole. This is for the solenoid pin to catch and hold the housing containing the spring in place until the user is ready for push-off. A ramped cut leading to the hole was added to allow more time for the pin to catch the shell and hold it in place without bouncing over the hole. Both the notches to disengage the clutch and

ramped cut are shown in Figure 3.13. This section of the shell is also hollowed to allow the threaded rod to pass through when the system releases the spring's energy. At the end of the narrow section, a custom fixture holds the elastic cord which connects to the testing "dummy" foot. The caps at each end of the main section can be removed for swapping out threaded rods, springs, and any required maintenance on the PAO. The caps are bolted into the triangular mounts which are welded to the shell.

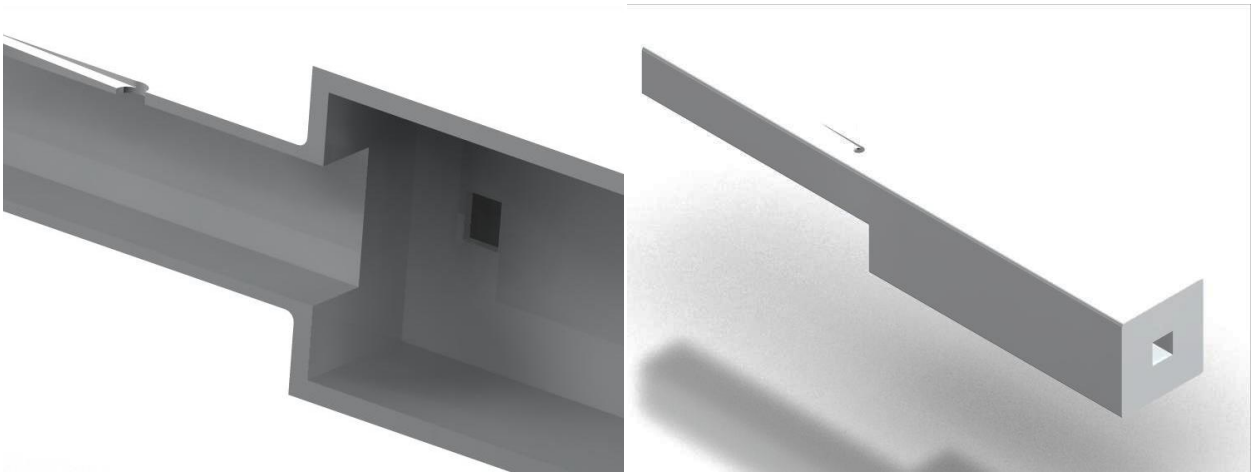

Figure 3.13: Cross section (left) and complete (right) view of PAO Shell

3.5.2 Component 2: Clutch Mechanism

The clutch mechanism is a key component in the PAO design. Figure 3.14 is a test version of the ESM with ¼"-20 threaded inserts.

Figure 3.14: An experimental ESM

The ESM is used to store energy and also serves as a clutch to disengage and reengage with the transmission. The ESM can be imagined as a quick-disconnect nut. The mechanism was machined from a brass cube with a bow-tie like shape machine cut in the center. The cuts are to allow room for the “pinch thread” inserts to slide in and out. These “pinch thread” inserts engage with the threaded rod through the center when pressed in. There are also two holes drilled through either side of the block which guide the post of the pinch threads. This can be seen more easily in the cross-section seen in Figure 3.15.

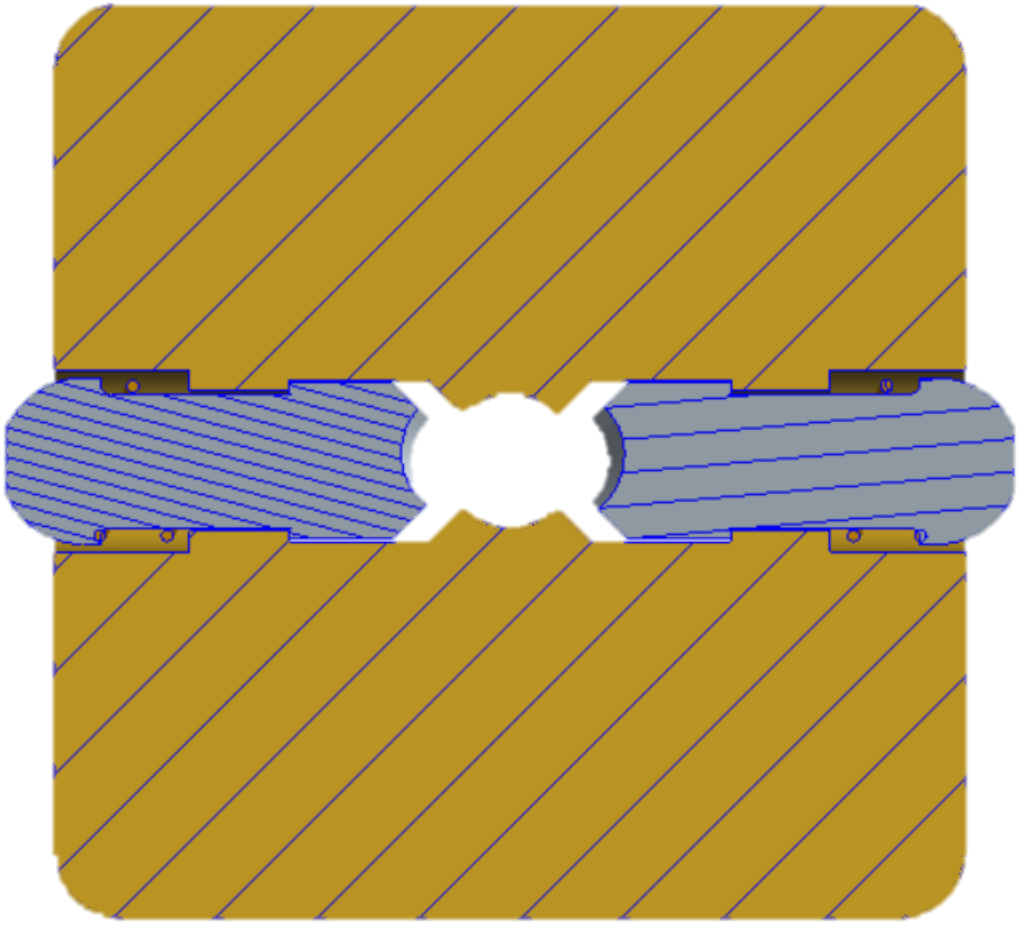

Figure 3.15: Cross section of ESM

When the inserts are pressed in by the surrounding walls of the PAO shell, the inserts are forced against the drive screw. The ESM is engaged with the threaded rod and moves linearly as the motor turns. As the mechanism moves down the threaded rod, it compresses the spring, storing energy for push-off.

After the energy of the spring is released, resulting in the PAO shell moving forward, the pinch thread inserts line up with the notches cut in the PAO shell. With the interior wall of the shell no longer holding the inserts in place, the pinch thread inserts pop back out of the

mechanism, forced by springs. The mechanism's ability to engage and disengage with the transmission is vital in the design for the PAO to operate more quickly. When the pinch threads disengage from the threaded rod, the block can move along the length of the threaded rod while bypassing the threads. This action saves the time needed to move the block via rotating the rod almost entirely. In Figure 3.16, the top image shows the ESM with the pinch thread inserts released by the notches in the shell. With the inserts in the out position, the ESM is disengaged from the threaded rod. In the bottom picture, the inserts are being held in by the walls of the shell. This holds the inserts firmly against the thread rod. Figure 3.17 shows the CAD model of a pinch thread and a milled interchangeable thread insert

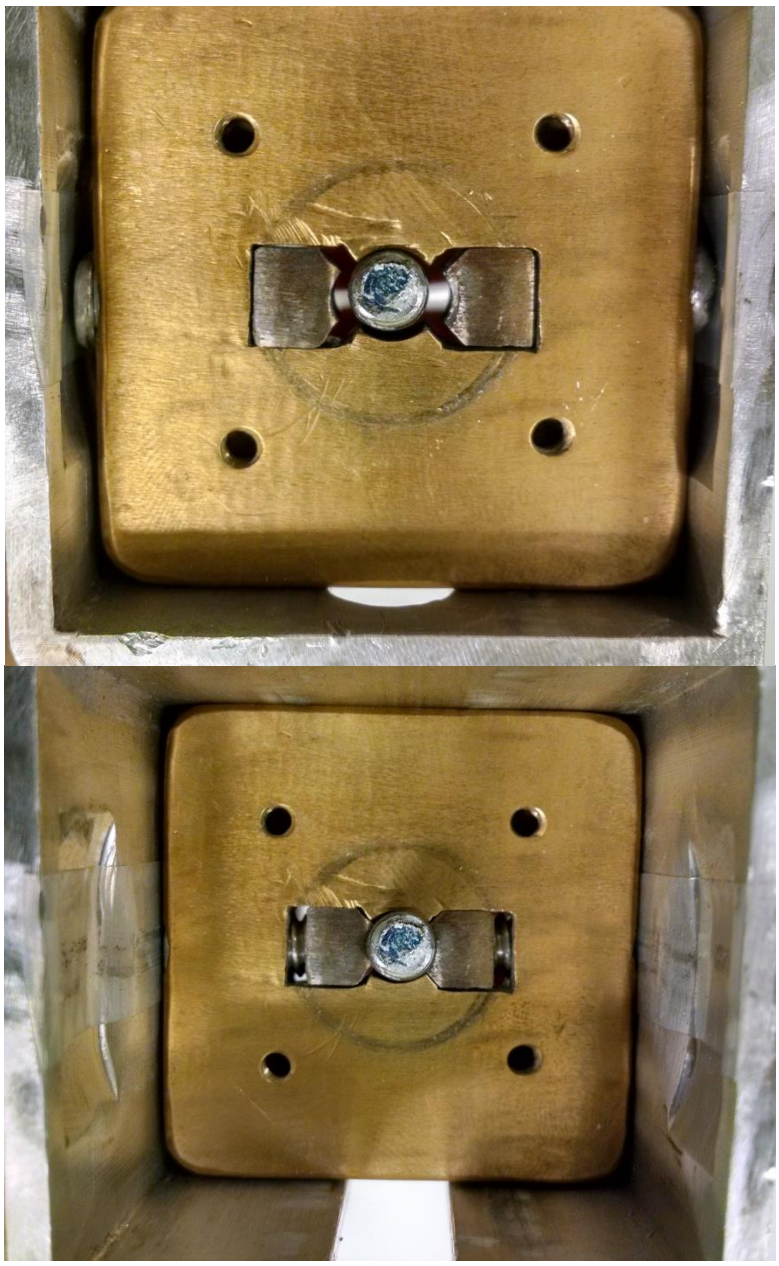

Figure 3.16: Disengaged (top) and engaged (bottom) ESM

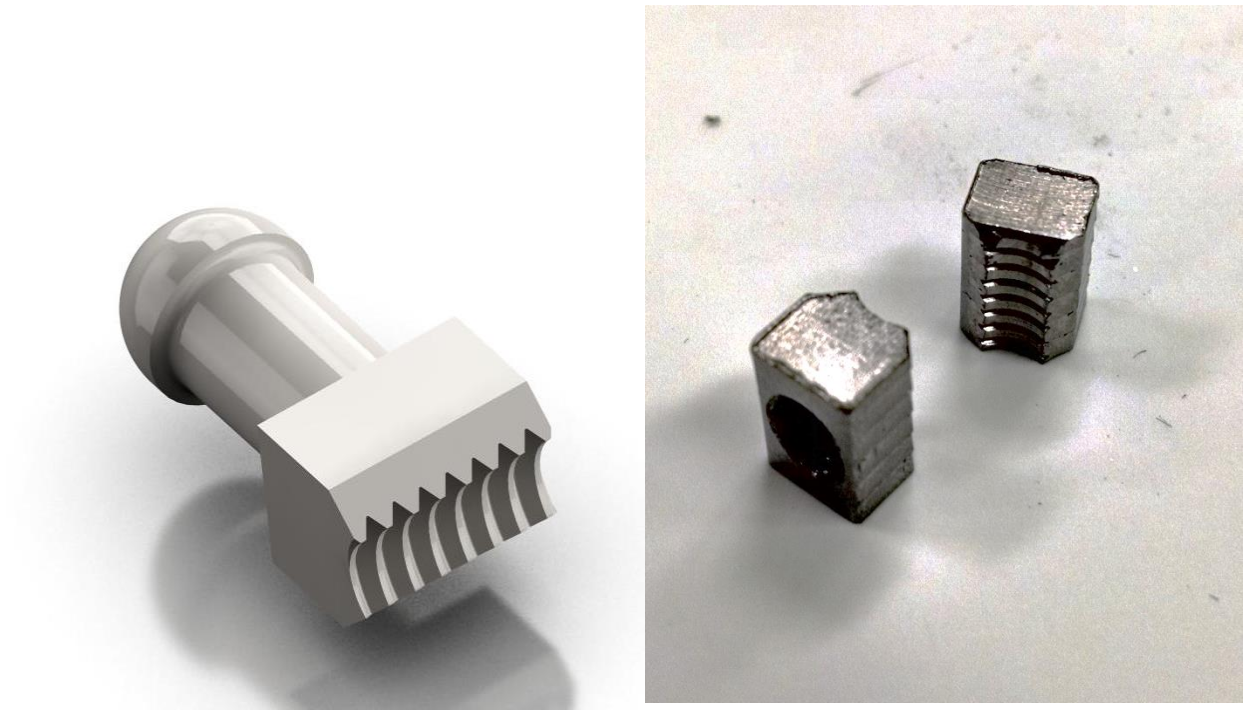

Figure 3.17: CAD rendering of pinch thread insert (left) and interchangeable thread piece (right)

The threaded inserts used to engage the mechanism were made of 4041 Steel to resist the wear of the system and the force of the compressed spring. The remainder of the mechanism is made of brass due to its lower friction coefficient properties. Furthermore, the ESM block's original thickness was 9.5 mm (.375 in) thick. After initial testing, the block would jam inside the shell against the interior walls when the block moved unevenly. This was remedied by attaching another 19 mm (.75 in) block to the first block to stabilize the mechanism. The add-on block had a pocket machined in it to align the main drive spring more effectively as well.

3.5.3 Component 3: Solenoid and Pin

A solenoid is a type of device that uses tightly coiled wire with an electrical input to create armature movement, either rotationally or linearly. For linear solenoids, a push solenoid is one which causes the armature to travel away from the actuator housing when energized. In

contrast, a pull solenoid is one which causes the armature to travel inward towards the actuator housing. For the PAO, a 2 5/8" diameter tubular low profile solenoid was used. This solenoid was chosen because it has enough force to work under maximum conditions for the current PAO design. While this solenoid may be considered bulky for the PAO, the solenoid's power eliminated the concern of having insufficient force in case of PoC redesign. A future prototype would utilize a design optimized for a smaller solenoid. The solenoid used was an 18.0 volt DC solenoid with a Pulse (10%) duty cycle. The 10% duty cycle means that the solenoid is not recommended to operate for more than 10% of a cycle time; for example, the solenoid should not remain energized for more than 6 seconds if used every minute. The maximum time energized should not be longer than 30 seconds. The 10% duty cycle was chosen because it produces considerably more force than similarly sized solenoids with larger duty cycles. Further, the shorter duty cycle was a non-issue since the solenoid is only momentarily energized.

Due to the unique nature of the solenoid's application, the stock pin was unsuitable for the PAO. To overcome this, a custom pin adapter was designed and cut for the PAO (Figure 3.18). The pin attachment was made out of brass rod to reduce friction against the aluminum shell. The pin is designed with a smaller 4.76 mm (.188 in) diameter tip and chamfered edges. The smaller diameter tip allows for the solenoid to catch the housing, but leaves a shoulder to prevent the pin from falling through the shell and beyond the limits of the solenoid. The narrower tip is about 3.18 mm (.125 in) long, this is to match the wall thickness of the shell without interfering with interior mechanisms. Furthermore, it is important to note that the length of the tip that engages with the PAO shell remains less than the stroke length of the solenoid. This was done to ensure the pin is able to retract far enough to release the shell completely.

Figure 3.18: Stock solenoid armature pin next to brass adapter piece

3.5.4 Component 4: Testing Frame

The final PAO design was a tabletop test frame, rather than a device attached to a test subject. A test frame decreases safety concerns in the event of a malfunction, along with several other benefits. It allows for easier analysis as well as part adjustments and design optimizations. This is because of the easy of accessibility and visibility when working on the device. The tabletop testing method also allowed for testing the design without concern of optimizing the design for weight and comfort. Additionally, the tabletop model adds a degree of modularity for reworked components and testing equipment. This is because the frame allows for the subsystems to be removed and modified and easily reinserted back into the PAO. The frame platform provides plenty of space to mount components and testing equipment. Furthermore, the working components for the test frame could generally be compatible with a future orthosis

frame; this means the components will need fewer modification for a wearable prototype. The test frame was assembled from three separate mounts and joined together by one platform. The three individual mounts each contain separate sections of the PAO; the first mounting the electric motor, the second mounting the PAO housing and the third securing the dummy foot (Figure 3.19). The platform secures each individual mount, preventing the mounts from shifting during operation.

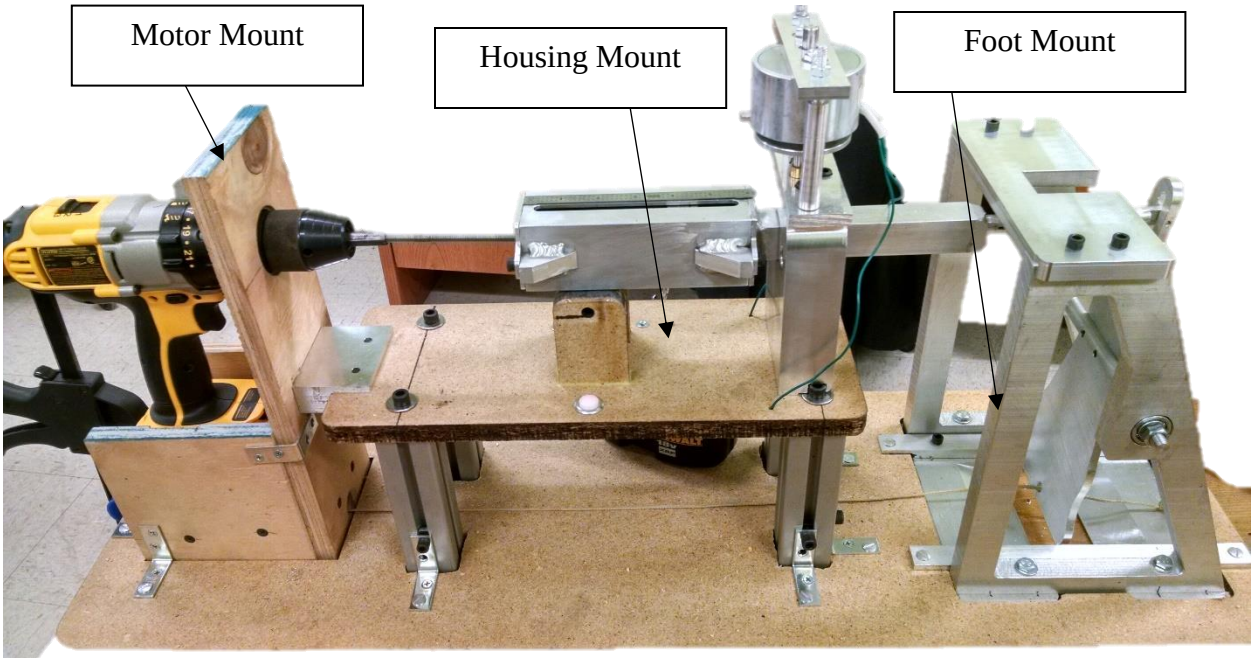

Figure 3.19: The three sections mounted on the testing frame

The electric motor mount was constructed from plywood to secure the electric drill used to power the orthosis. The front of the mount has a hole cut for the drill chuck to be inserted. This allows the drill to support the forces being applied by the operation of the PAO.

The housing mount for the testing frame was fabricated to be much larger than necessary. This was a preemptive step to address possible issue with resetting the PAO, should gravity and

the users gait not be sufficient. The two supports underneath the housing were included for the addition of a rack and pinion mechanism which wound a spring. If it were necessary, the spring would leech some energy during push-off, which would then be used to assist in moving the PAO housing back to its original position. Fortunately, testing showed that these components were unnecessary. The second part of the housing mount is the large aluminum solenoid fixture, which also acts as a guide for the housing shaft. Like the rest of housing mount section, the fixture was designed to anticipate component revisions. This was very beneficial when the original solenoid was swapped for a more powerful version. However, the final mount to be used on the orthosis would be significantly smaller and lighter.

The dummy foot frame, seen in Figure 3.20, was constructed using triangular aluminum supports, connected using three braces. The supports hold bearings for a rod, which acts as an axis for the dummy foot. At the bottom of the foot, a string was attached to the toe area. The string runs the length of the testing platform, with a weight at the opposite end of the string. The purpose of this is to simulate the effect of dorsiflexion during gait to reset the device and to simulate the load required to lift the user's body. The rotational axis of the foot was placed 114 mm (4.5 in) from the heel and 165 mm (6.5 in) from the attachment point of the weight, secured at the ball of the foot.

Figure 3.20: Dummy foot section of the test rig

In addition to securing the three mounting sections, the main platform was used to mount several attachments for testing. The first attachment is a string guide, placed behind the motor mount, pictured in Figure 3.21. The purpose of the guide is mainly to reduce the friction and wear of the string against the testing platform when the system cycles.

A doorbell button was attached to the solenoid's circuit to energize the solenoid. Since the doorbell uses a momentary normally-open switch, it is less likely the solenoid would remain activated for too long, causing it to burn out. An LED light was added to the circuit as a visual indicator of an energized system during video playback analysis. Lastly, an eyebolt was attached on the main platform, underneath the housing mount. The bolt was used to attach a scale to the dummy foot to record the output force of the PAO during initial performance testing. The eye bolt and scale are shown during a test in Figure 3.22. These were both removed during testing for the high-speed video analysis.

Figure 3.21: Guide to align cord and reduce friction

Figure 3.22: The eyebolt used to secure testing equipment with spring scale attached

3.5.5 Component 5: Threaded Rod

Another key feature of the PAO design is the threaded rod, which acts as a transmission for the system. The threaded rod provides a mechanical advantage by using the lead angle of the threads to decrease the necessary torque at the cost of linear movement speed. The lead, the distance between threads, of the threaded rod controls the mechanical advantage, as lead increases, the mechanical advantage decreases (Bhandari, 2007). The power ratio describes the mechanical advantage relationship between input and output force. In this case, the input force is the torque from the motor and the output is the axial force used to compress the main spring.

Since the electric motor's output is rotational, a transmission is needed to transform the rotational motion from the motor into linear motion so that the energy can be stored in the main spring. Using a threaded rod as the transmission has two major advantages; first, the threaded rod can be inexpensively purchased at a local hardware store. The abundance allows for cheaper maintenance for swapping out worn rods. Second, the variety of threaded rods allows for greater adjustability for a larger group of users. For the purposes of the prototype, one foot long ¼"-20 and 3/8"-16 threaded rods were used for testing.

A custom fabricated retaining nut was found to be necessary after initial tests. This was because the standard nut being used to keep the ESM captive was causing jams. The standard nut held the pinch thread inserts in place when they should have been released. The retaining nut was designed with a diameter to extend beyond the threaded pinch inserts to keep normal forces off of the inserts, allowing them to release freely.

3.5.6 Component 6: Ankle Attachment

Another easily overlooked component of the PAO is the connection of the driving mechanism to the ankle mount. While the easiest and most robust method would be to secure a

rigid link between the two components, this method would likely be uncomfortable for a user. A rigid attachment works well when firing the system, but does not relax afterwards. This means a rigid connection will cause the user to be unable to flex their foot freely; all movement will be synchronized with the PAO device. An alternative to the rigid attachment is the use of steel wire attached to the ankle mount and the PAO Shell. This would alleviate the issue of the linkage forcing the toe both up and down by becoming slack when not in tension. However, another anticipated discomfort was considered; the instant jolt from the spring force could be harsh for the user.

The solution was to use an elastic cord to connect the shell to the ankle. The elastic cord connector provides the flexibility to prevent the toe being forced down during the ESM reset. Furthermore, the cord's elasticity allows it to stretch momentarily, reducing the initial jolt that occurs when the system fires. The difficulty with this method is mounting a cord which satisfies the strength and flexibility requirements for the device. Two custom coupling fittings were fabricated that would be clamped onto the ends of the elastic cord, as shown in Figure 3.23. In addition, once the each fitting was clamped onto the cord, set screws were used to hold the cord in place. Lastly, after testing showed signs of wear on the cord, an epoxy was used when inserting the cord into the fitting to aid the fittings in securing the cord. In hindsight, using set screws to hold the cord likely caused more harm than good. The screws tended to cause failures on the rubber cord by cutting into the cord. The elastic cord was replaced with all-nylon Para-cord before final testing due to concerns of wear.

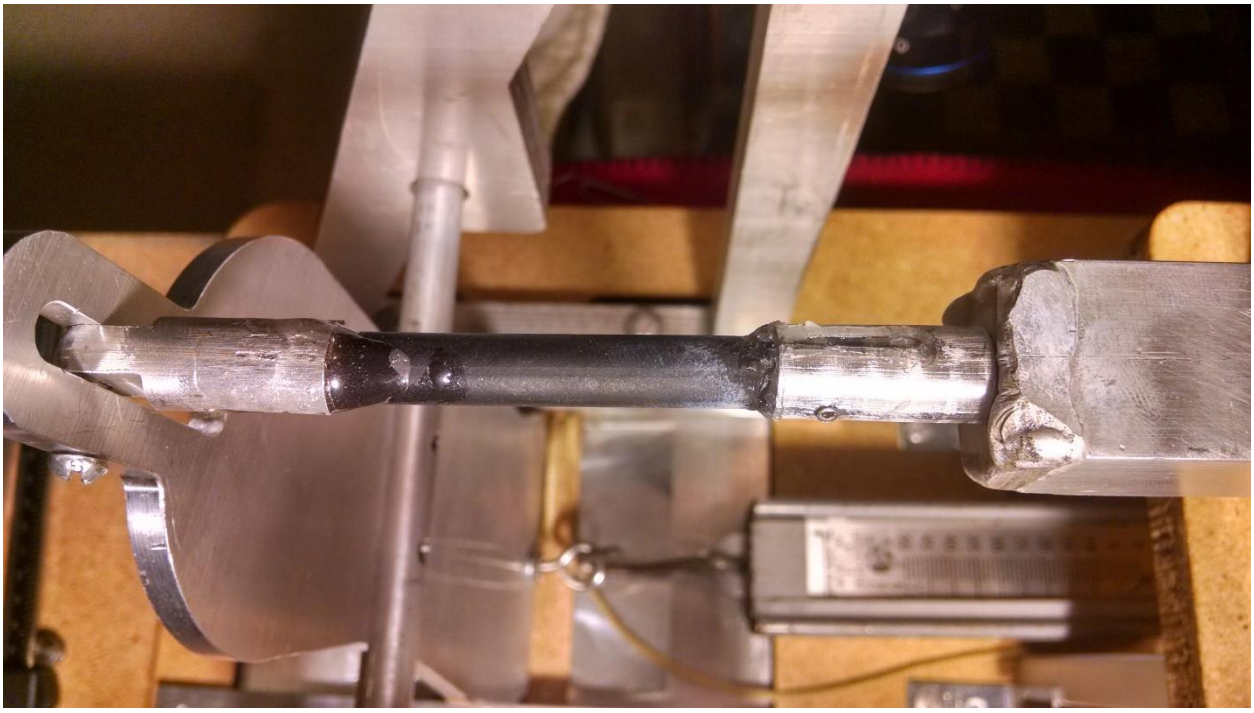

Figure 3.23: Rubber cord linking the PAO with the ankle

The better cord for use in future testing may be one made of Buna-N rubber with a 9.5 mm (.375 in) diameter. The rubber has a 50A durometer rating and an 8.27 MPa (1200 psi) tensile strength; this would mean that with the 9.5 mm (.375 in) cord, the tensile load limit would be approximately 588 N (133 lb_f). This should be plenty of strength to prevent the cord from snapping under normal operational loads with some additional strength for safety. While 50A rubber performed very well, a 40A rubber which offers more flexibility may be needed to promote dampening the jolt during push-off. A revised clamshell style clamp would be necessary to properly secure the cord for longer use.

CHAPTER 4: PERFORMANCE TEST METHODS

Since the powered ankle orthosis was custom fabricated in WCU's facilities, the device was tested in two phases, subsystem testing and complete system testing. The first phase of testing was to ensure there were not any ruinous faults with the design concept. Further, this phase allowed for slight modifications to optimize the PAO design. Once the major issues with components on the substructure level were worked out during the subsystem testing, the completed PAO was evaluated with all subsystems combined in the second phase. During this phase of testing, the recorded data was compared to calculated values for technical specifications. Values tested include output force or spring compression speed. Testing details are described below.

4.1 Subsystem Testing

The first phase of testing was functional testing of each of the PAO components. To complete this, the PAO components were divided into subgroups based on the how they interacted within the system as a whole. For example, the housing, the ESM, spring and threaded rod were partitioned into one group. The housing, the solenoid and wiring were tested as another group. By testing each group individually, the integration of the subgroups into the final design was much easier to troubleshoot.

4.1.1 Motor and Power Transmission

The functional testing for this subsystem required simply driving the threaded rod and ESM block to ensure the system did not jam. This also verified that the drill had enough power to compress the main spring. Lastly, while performing this test, the drill motor's compression

speed was observed to check that it was able to compress the spring in a reasonable amount of time to be considered a viable option.

4.1.2 Energy Storage Subsystem

The Energy storage subsystem is composed of the components used to capture and contain the system rotational energy. These components include the main spring, the ESM, and the larger half of the housing. The goal for testing this subsystem was to show that the mechanism could repetitively and reliably compress a spring to store the desired force and hold that force. To test this, a variety of springs with different spring rates were used. Starting with the weakest first, the ESM block compressed each spring to its rated compressed length. Once the spring force reached approximately 89 Newtons (20 lb_f), the teeth on the pinch thread inserts became too worn to hold more force. Since the concept of the ESM had been proven, it was decided to continue testing with a simple threaded block to compress the spring to help with time and cost constraints. Since this block did not have a quick-release ability, the system was reset by reversing the motor until the block reached the start position.

To address the issue of the worn pinch threads, a few methods were considered. The threads being used were cut from mild steel with the threads tapped/cut into the piece. This method causes the threads to be weaker than standard forged or heat treated threads. To improve the strength of the pinch threads, the parts should be heat treated after being machine cut. Another solution would be the use a stronger thread. A stronger thread could be found by using a wider diameter threaded rod. For example, if a 1/2”-20 thread were to be used as opposed to the 1/4"-20 threads, the pullout strength of the engaged threads would increase by roughly four times.

4.1.3 Energy Release Subsystem

The energy release subsystem is comprised of the smaller half of the housing, the solenoid and the elastic cord connecting to the foot mounting point. Once the storage mechanism was working, the second half of the aluminum housing was added to the device. The energy release subsystem was then tested initially by pulling on the housing to simulate a load. The solenoid was then energized to release the housing and simulate the action of the system pulling the heel up. Initially, the energy release system used a small tubular solenoid from a previous design that had roughly 8.3 N (30 oz) pull at 3.8 mm (.15 in). During this testing it was quickly discovered that the solenoid did not have enough force to overcome the friction caused by the normal force acting against the solenoid pin. To resolve this issue, the solenoid was replace by a larger, low profile clapper solenoid.

Another complication that was addressed during this phase was the solenoid pin's ability to latch the housing in place. The problem came from a 4.8 mm (.188 in) hole on the narrow section of the housing. Once the system's energy was released, the solenoid's pin would not catch the hole quickly enough and would instead bounce over it, like a car tire going over a pothole. The solution was carried out in two parts. The first part was milling a ramp into the hole to allow the pin to begin falling into the hole sooner. The second part was a spring that was added to the solenoid which adds an external force to reset the solenoid pin more quickly.

4.1.4 Testing Frame

The test frame for the powered ankle orthosis was built to test the prototype before it is implemented into a wearable orthosis. The test platform is made up of the "dummy" foot and frame, the drill mount, the PAO Mount and the platform used to secure the mounts in place. The test rig was made mostly of particle board to allow easy implementation of testing equipment.

This worked well for having an adaptable substructure. For example, a force gauge was mounted to the platform to provide rough initial empirical data on the output force of the PAO. However, due to the nature of the forces being applied, the particle board was shown to be too flexible during testing, causing the entire bottom platform to bend. To correct this, both ends were clamped down to the sturdier table underneath. Nonetheless, this gave insight on what types of materials, such as aluminum, need to be used for the mounting points on the wearable orthosis; most plastics are likely not to be suitable for the task.

4.2 Complete System Testing

4.2.1 Testing Configurations

Since the powered ankle orthosis is being designed primarily for rehabilitative purposes, the ability to tune the orthosis for different users is very beneficial. Tuning the output force requires consideration of several system parameters: spring rate, compression rate and foot size.

The results from the testing were recorded using two different strength springs; one with a 95.9 N (21.6 lb_f) load capacity and the other with a 187.3 N (42.1 lb_f) capacity. The spring rates for these springs are 2.12 N/mm (12.1 lb/in) and 4.15 N/mm (23.7 lb/in), respectively. These springs allowed for testing the performance of the PAO at roughly half and quarter capacity. Further, the PAO was also tested using two options for the threaded rod/transmission; a ¼”-20 and 3/8”-16 threaded rod.

Once testing progressed to the high speed video analysis, the tests were conducted solely with the 187.3 N - 4.15 N/mm spring and 3/8”-16 threaded rod. The PAO was attached to the heel 10.8 cm (4.25 in) from the dummy foot fulcrum. The 5 kg (11 lb_m) mass was attached to the ball of the foot, 16.5 cm (6.5 in) from the dummy foot fulcrum. The system was powered by a freshly charged 18v battery.

4.2.2 Complete System Testing Methods

Once the benchtop PAO was completely assembled, the system was tested as a whole. The purpose of this testing was to look for any final system flaws or opportunities for improvement before testing system performance. By testing the PAO's ability to perform reliably, future testing will be done consistently, without requiring modification to the PAO device.

To begin the initial complete system testing of the PAO, the 95.9 N (21.5 lb_f) load capacity 2.16 kg/cm (12.1 lb/in) spring rate spring was used with the 1/4"-20 threaded road. This represents the PAO under quarter load capacity with a threaded rod storing energy more gradually, providing time to watch for component failure. The PAO was tested by compressing the spring by up 63.5 mm (2.5 in) several times before energizing the solenoid to fire the PAO. After ensuring there was no immediate concern, the PAO was cycled three times without manually resetting the device. This means that once the solenoid was released, the drill was reversed until the pin fell back into the PAO shell, and then compressing the spring to cycle the PAO again. After this test was complete, these tests were completed again using the 3/8"-16 threaded rod but with the same spring. Next, the same procedure was ran again using the stiffer 187.3 kg (42.1 lb_f) load capacity and 4.15 N/mm (23.7 lb/in) spring; first with the 1/4"-20 threaded rod followed by the 3/8"-16 threaded rod.

At the conclusion of the final continuous cycle test, the PAO spring was compressed 63.5 mm (2.5 in) and left for over 24 hours. This test was simply to observe if the PAO could hold the force for an extended time. Once these tests were completed without failure, there was confidence that the system would provide consistent results that were not at risk to component failure within the PAO.

4.3 High Speed Video Analysis

The most crucial part of the PAO to be analyzed was the dynamics of the foot at the ball of the foot, where push-off occurs. More specifically, the velocity, acceleration and force throughout the range of motion of the foot while lifting a 5 kg mass (11 lb_m) were desired. With acceleration data, the push-off force and torque data can also be calculated. To determine the velocity and acceleration data, displacement data of the weight attached to the foot was needed. The purpose of the high speed video analysis was to record the displacement of the weight over time.

When performing the tests, the PAO used a 4.15 N/mm (23.7 lb_f/in) main spring, which was compressed from 114.3 mm (4.5 in) to 39.4 mm (1.55 in). The 5 kg (11 lb_m) mass was attached using nylon cord, which was attached to the ball of the dummy foot and run along the bottom of the testing rig. The mass hung from the rig behind the drill where a camera was mounted to observe it. The footage was recorded using a GoPro Hero 4 Black edition. The video was recorded using 720p resolution at 240 frames per second (fps) (GoPro, Inc., 2015). The camera was placed approximately .6 meters (2 ft) from the focal point drawn on the cord above the weight to observe movement. During testing, a digital stopwatch was used alongside the mass to help confirm the time measurement between frames. Further, the LED was placed in the shot to illuminate when the solenoid was energized and indicating the beginning of the test. For the backdrop of the video, a sheet of graph paper with 6.35 mm (.25 in) increments was placed to provide a scale for measurement during video playback.

For the high-speed testing, 14 tests were recorded and analyzed to allow for a good statistical sample. Initially, the test start time began when the LED began to illuminate on the high-speed footage. After performing the displacement calculations and regression, best fit

equations were fit to the data. However, this variation in the delayed start time before movement showed to be a poor representation of the data. Because of this, the analysis began at the frame prior to the mass's first movement.

4.3.1 Measuring Displacement and Time

In order to determine the various dynamic results from the PAO analysis, the high speed footage was processed using GoPro Studio editing software. Each video was trimmed and reduced to 1% play speed to simplify the analysis process. To do this, the video was analyzed frame by frame, noting the difference in displacement after each frame. The displacement was measured during video playback using a .794 mm (1/32 in) scale ruler placed on a 20 inch monitor with a 1680 x 1050 screen resolution. The movement was measured against the .794 mm (1/32 in) ruler and scaled accordingly with the 6.35 mm (.25 in) increments on the graph paper. For example, when the 6.35 mm (.25 in) increment was measured to be equal to 8.64 mm (.34 in) on the monitor, a movement of .794 mm (1/32 in) on the monitor is equal to .584mm (.0230 in) in actual displacement. This method helped to ensure consistency throughout the test, as well as from test to test; accounting for shifting camera positions and the graph paper being shifted during the test by the mass's movement. A picture of the footage being analyzed is shown in Figure 4.1.

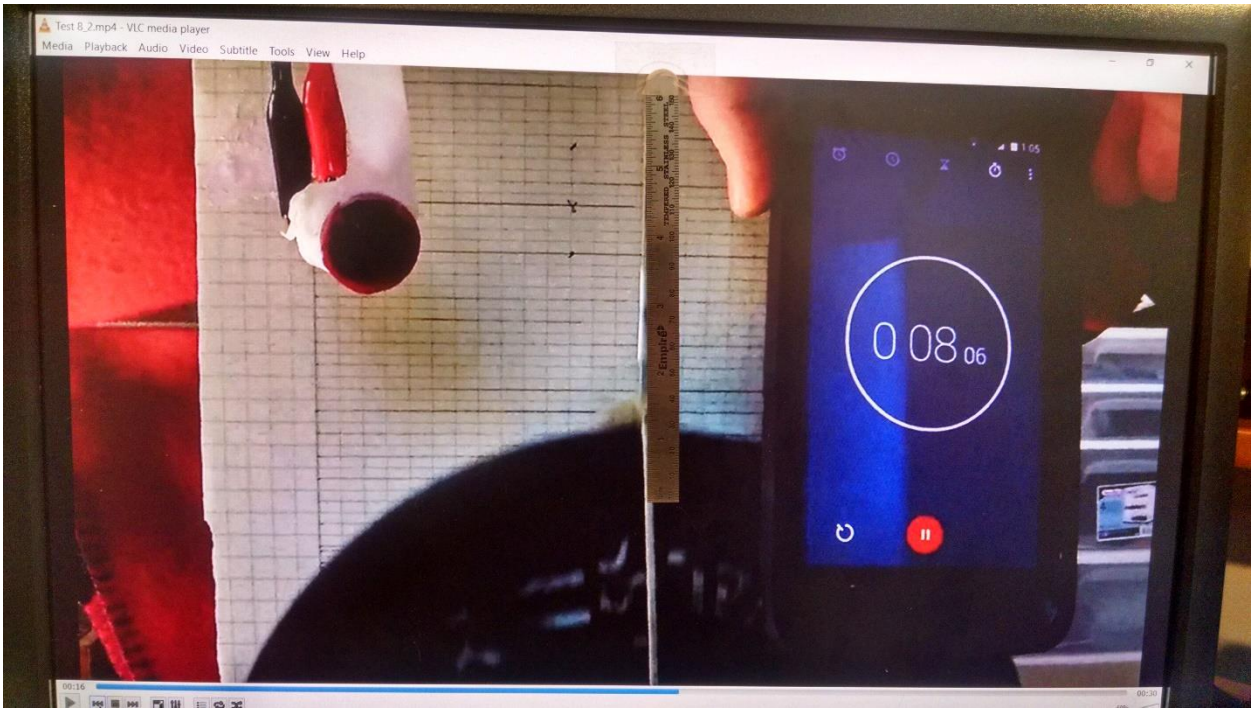

Figure 4.1: Analysis of high speed testing footage

While recording the mass's displacement, it was important to keep a precise measurement of time. Since the camera was set to record at 240 fps, each frame is less than 1/100 of a second, the highest level of precision for common timers. This would mean expensive specialized timing equipment would be required to track time during the test. To avoid this, time was instead tracked using the video frames. With 240 fps, the average time between frames would be about 4.167 milliseconds. Initially, The test started at 0.0 seconds being the first frame with the LED showing light, each frame after was recorded as a 0.004167 (1/240) second progression. This provided roughly 60 data points per test. However, time 0.0 was later changed to the frame before the mass's first movement. The reason for this is due to a large time variation between the LED lighting up and the beginning of mass movement. This is explained in greater detail in chapters 5 and 6. With the displacement over time data recorded, the data was plotted

and a trend line was generated. A statistical regression to calculate the correlation of the data was also ran on the trend line.

4.3.2 Data Analysis Methods

During each test, as each frame progressed, the displacement between frames was recorded on a spreadsheet, as well as total displacement at each frame. Once the test was completed, the total displacement at each frame was plotted over time. A trend line was fit to the data to provide a polynomial equation that describes the plotted data. A statistical polynomial regression was performed on the equation, providing a numerical value to evaluate how well the polynomial equation describes the plotted data. A trend line which perfectly fits the data has a regression value of 1 or -1, where a value of 0 indicates no correlation with the data. If the regression found a poor relationship between the data and the equations, another analysis method would be required. Fortunately, the results from the regression were encouraging, allowing for continued analysis with the generated equations.

4.3.3 Calculating Velocity and Acceleration

After recording the displacement over time empirically, the remaining analysis components were determined mathematically. To find the weight's velocity over time, the generated trend line for the position data is derived to provide an equation for velocity at a given time as well as create a plot for the velocity data. The velocity derivation is shown below.

$$v = \frac{dx}{dt} \tag{9}$$

Continuing with the data analysis, the next step was to again derive the velocity equation, position's second derivative, to calculate the acceleration equation that defines the test data. Again, this equation is used to determine acceleration at a given time and generate a graph

of the mass's acceleration over time. The acceleration data can be used to move forward with calculating the remaining forces of the PAO. The acceleration is found using the equation below.

$$a = \frac{dv}{dt} = \frac{d^2x}{dt^2} \tag{10}$$

4.3.4 Calculating Force and Torque

With the calculation of acceleration, the push-off force overtime could now be calculated using the equation from Newton's second law.

$$F = ma \tag{11}$$

The mass, m, for the equation was the 5 kg (11 lb_m) mass attached to the PAO. The acceleration value, a, used in the equation was found using the method mentioned in section 4.3.2. The point of interest is the maximum force, which occurs at the start; however, a graph of the approximate force overtime can be provide a better understanding of the PAO's movement.

The calculated push-off force data provides the ability to also find the torque at the fulcrum of the ankle. The torque is beneficial in determining the required strength of materials when constructing the orthosis, as it needs to be strong enough to prevent the mount twisting and potentially causing injury to the user.

$$\tau = r \times F \tag{12}$$

Using this equation, torque, τ, is calculated as the product of force, F, and distance between the rotational axis and applied force, r. The force is the previously calculated push-off force, found using the mass and acceleration at a given time. The rotational axis for this test is 6.5 inches, or .165 meters from the weight attachment at the ball of the foot, which is used for "r". This data is used to create a graph of the PAO's torque over time.

4.4 Maximum Force

Once the high speed multiple high tests were complete, the next step was to find maximum output push-off force. This test was saved until the high speed testing was complete due to the possibility of part failure in the PAO. This test was analyzed using a spring scale attached to the ball of the dummy foot and observing the maximum value. This test primarily served to determine how well the device was capable of handling higher spring forces. The test involved compressing a 4.15 kg/cm (23.7 lb/in) spring by 74.9 mm (2.95 in) to full compression and energizing the solenoid to fire the PAO. For this test, only the maximum force was measured, time was not tracked for this test.

CHAPTER 5: RESULTS

Once the functionality testing was completed, testing and recording performance data began. The results from the PAO were found empirically and theoretically. These measurements were tested in order to help understand the feasibility of the PAO design and its capabilities.

The results from these experimental methods are empirical, as opposed to simulated. Simulated results are beneficial to have when working on a design optimization for a few reasons. First, specific variables can easily and quickly be manipulated to find new results. This leads to another benefit or being able to identify patterns created when adjusting testing conditions. However, simulated results can omit important unforeseen factors, such as unanticipated friction among components, flexibility in soft components, or wear on parts. This may lead to inaccuracies in the simulated results when compared to actual results. In the end, a method yielding empirical results was chosen since the results were based off a proof-of-concept design.

5.1 High Speed Results

As mentioned in Chapter 4, the method chosen to determine the performance capabilities of the PAO was the analysis of high frame rate video footage. During the processing of the high-speed footage, the GoPro Studio editing software determined that the actual frame rate of the video was 239.76 fps, as opposed to 240 fps. This meant that the time between frames needed to be adjusted from .004167 seconds to .00417 seconds.

5.1.1 Displacement

The displacement testing yielded results with consistent patterns. Figure 5.1 illustrates the plotted values of the mass's position over time once the solenoid was released. As expected, the plot shows that each of the positional data series follow a relatively consistent 3rd order polynomial fit. Each of the 14 samples had a R^2 value ranging from .9992 to .9998, with the majority being about .9996. These R^2 values indicate a very strong correlation in the data and show that the generated equations are an accurate representation of the data. If this were not the case, deriving these equations to determine the velocity and other characteristics would yield poor and inaccurate results.

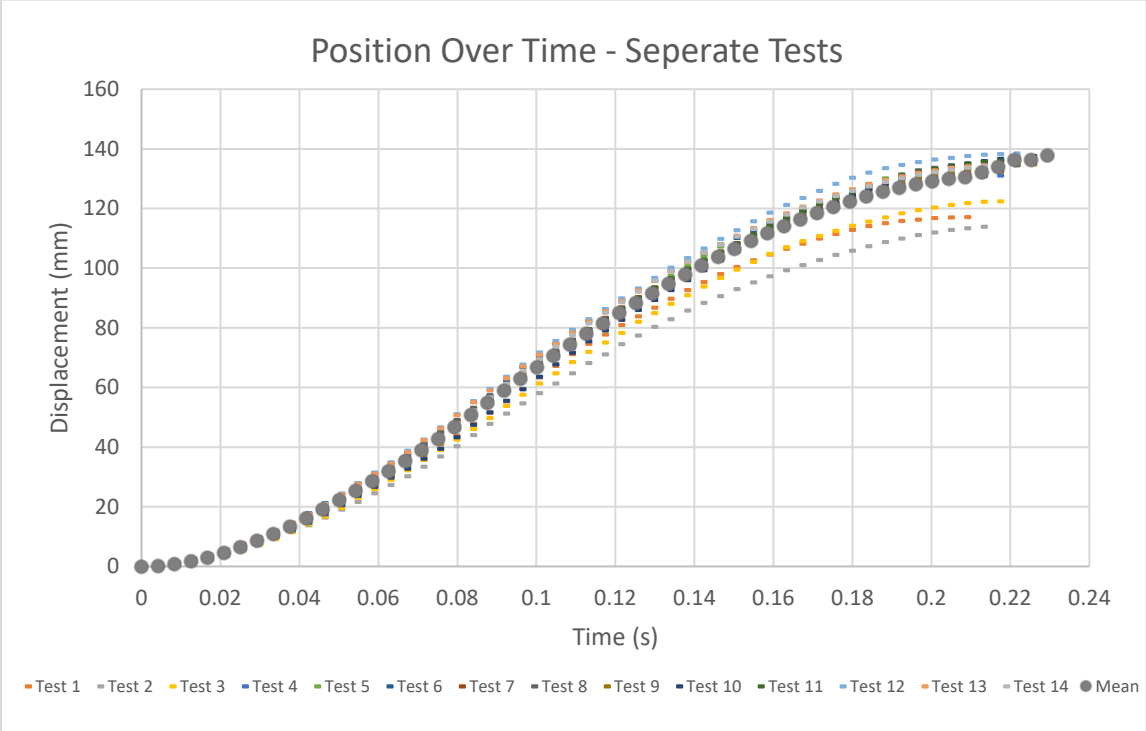

Figure 5.1: Plot of displacement of each of the 14 tests

The difference between the tests was minuscule at the start and increased as each test progressed. Each of the 14 tests is plotted with a short dashed line in varying colors, with the

mean displacement plotted as small grey circles. The time of movement was roughly 22 milliseconds for the most samples, with an average peak of about 131.5 mm. With a few exceptions, the longer tests tended to yield larger displacement. This is not altogether surprising, but worth noting. The data for each of the individual samples can be found in appendix A. Using the same displacement data, another graph was created as shown in Figure 5.2 of the mean displacement data.

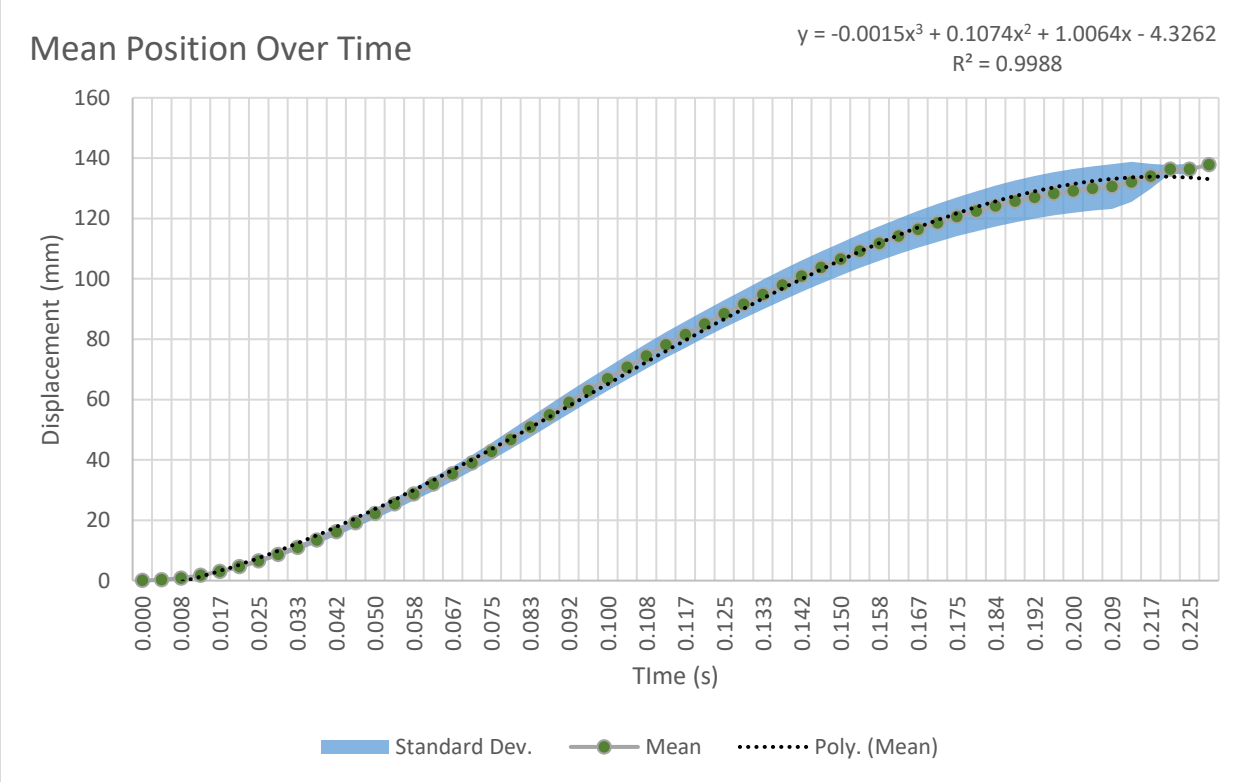

Figure 5.2: Standard Deviation plot of position data

Figure 5.2 is a graph of the mean data shown in a scatter plot with the 3rd polynomial trend line fit to mean data. In the upper right corner of the graph, the R^2 value from the data regression is shown to be .9988. This is less than any of the individual tests, but still indicates a strong correlation. The blue shaded region around the plotted means represents one standard

deviation of data. As the graph indicates, each test started with relative similarities. However, deviations increased as time progressed, until the deviation suddenly decreases near the final three points. This decrease in deviation is caused by less data samples at this time, since these final points only represent the tests with the largest displacement.

The characteristic curve of 3rd order polynomials is easy to explain when considering the mechanical operation of the PAO. When the system is energized, the weight simulating the foot is at rest; meanwhile, the spring's stored energy is released. As the spring decompresses, the weight is propelled upward and continues upward until the springs force is equalized with the weight. The point where the spring should be equalized is at about 74.5 mm (2.93 in) of displacement, the point which the parabolic (or rapid) growth increase changes to decrease, the point of inflection. This pattern is seen at about .11 seconds into the test. After this time, the mass's displacement continues due to its inertia. This indicates that the fastest rate of change occurs just before the spring is fully decompressed. This is a good sign as the continued acceleration of the weight was expected as long as the spring still stores energy. The rate of displacement decreases slowly due to the force of gravity and resistance in the PAO, until it reaches its maximum displacement at 131.5 mm (5.2 in) on average.

5.1.2 Start Delay

Since optimizing cycle time was a point of considerable interest, the delay between system energization and initial weight movement was also examined and analyzed. The reason for this test arose after a delay of movement was noticed in initial testing. The delay time was measured by counting the number of lapsed frames, the same method used while tracking displacement. The results from measuring the delay times are graphed below on Figure 5.3.

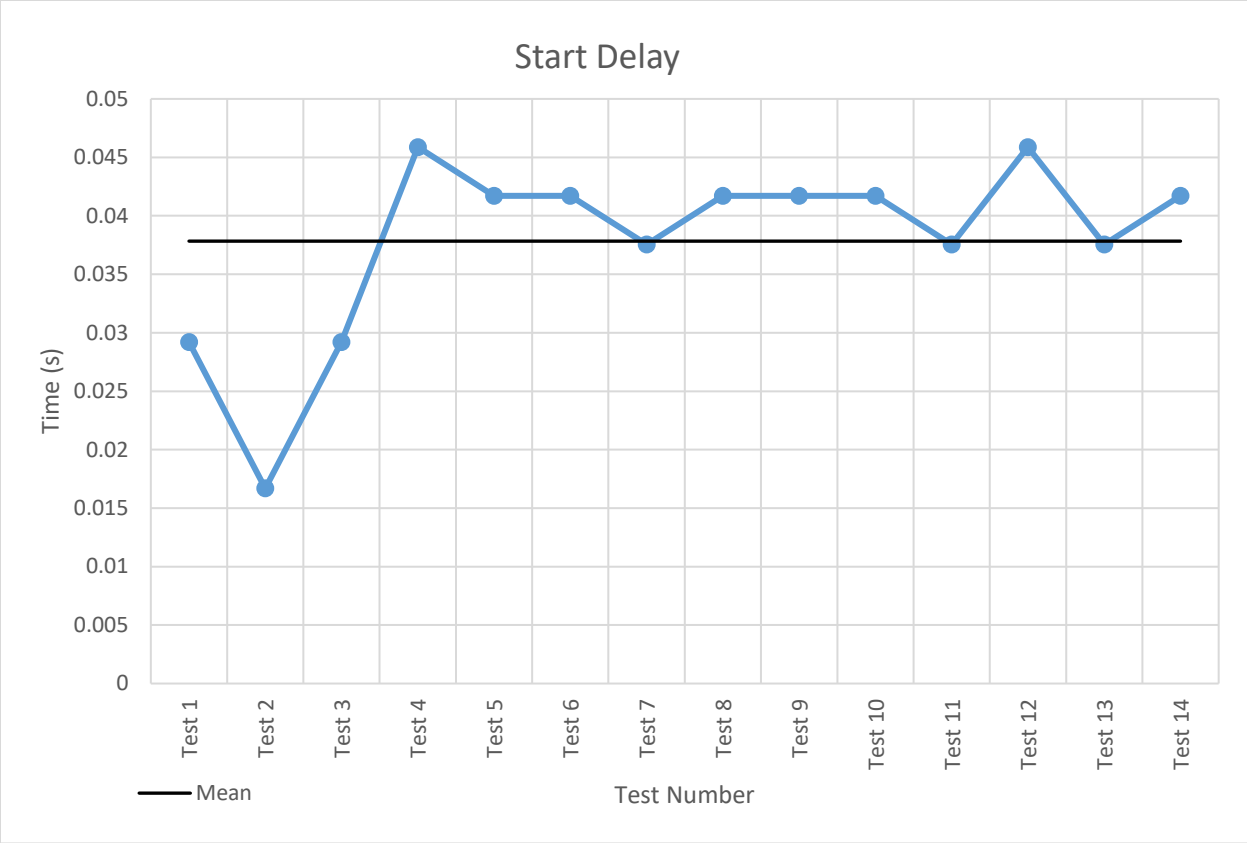

Figure 5.3: Graph showing the start delay from each test

Figure 5.3 shows the start time of each of the 14 tests, varying from .017 seconds to .046 seconds; a range of .029 seconds. The mean delay time was about .038 seconds among the 14 tests on average. However, while looking over the results, a trend was noticed along the first 3 data points. Each of the first 3 tests had a shorter delay time with larger variation then the rest of the data set. Assuming that the first three points were skewed due to learning the setup process, it was decided that these points could be removed from the set. Performing the analysis on the remaining 11 tests shows a much more consistent trend. This new data analysis is shown in Figure 5.4.

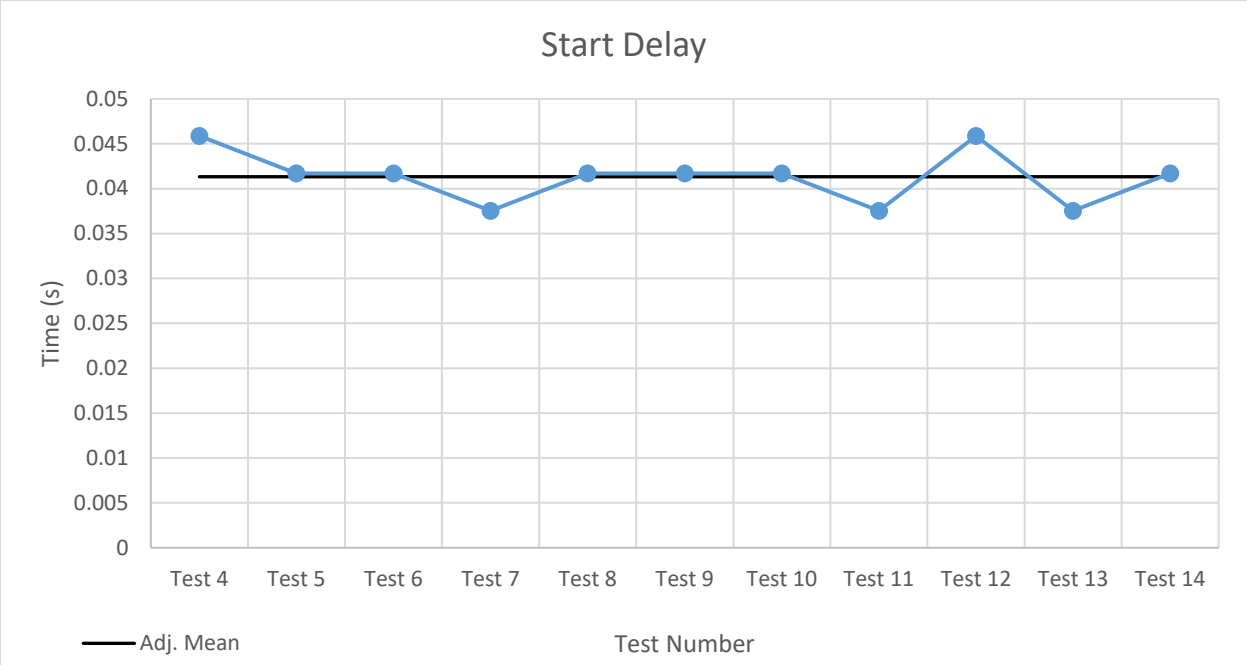

Figure 5.4: Graph of start time delay after first three points were removed

The delay varies from .0375 seconds to .0459 seconds, with a new range of .0084 seconds. The average delay time was about .041 seconds between when the solenoid was energized and weight displacement was observed. Assuming this is a more accurate indication of the delay time for each test, it's much easier to determine a possible causes for the delay with more consistency. Possible causes considered include the time taken for the solenoid pin to retract completely for the PAO shell. Another portion of the delay time occurs from any elasticity or slack in the cord used to attach the PAO to the dummy foot, and further, the dummy foot to the weight. In a fitted prototype, the delay time will be reduced when the cord to the weight is no longer necessary. Ideally, the delay time in a future fitted prototype will be shortened enough to not cause an issue of users needing to anticipate a delay before push-off.

5.1.3 Velocity

Once the positional data was evaluated, the polynomial regression equation was derived for an estimation of the weight's velocity at a specific time. The velocity data provides the answer to a very simple question about the PAO; how fast does it propel the foot? Each of the 14 best fit equations was derived from the respective positional equation to estimate the velocity for each test. The results are plotted on Figure 5.5. Similar to the plot of displacement in Figure 5.1, each of the 14 tests is represented with a small dash. The mean of the data, represented by the circular grey markers, was calculated by averaging each of the 14 individual test's velocity values and fitting a new equation; this line was not generated by calculating the derivative of the previously generated mean displacement equation. The data shows a fairly consistent trend in regard to shape. However, the data range does not share the same pattern of increasing range as the displacement data. Note that each test peaks at about the same time, about .1 seconds into the test. The average velocity at this point is approximately .9 meters per second (3.3 ft/s).

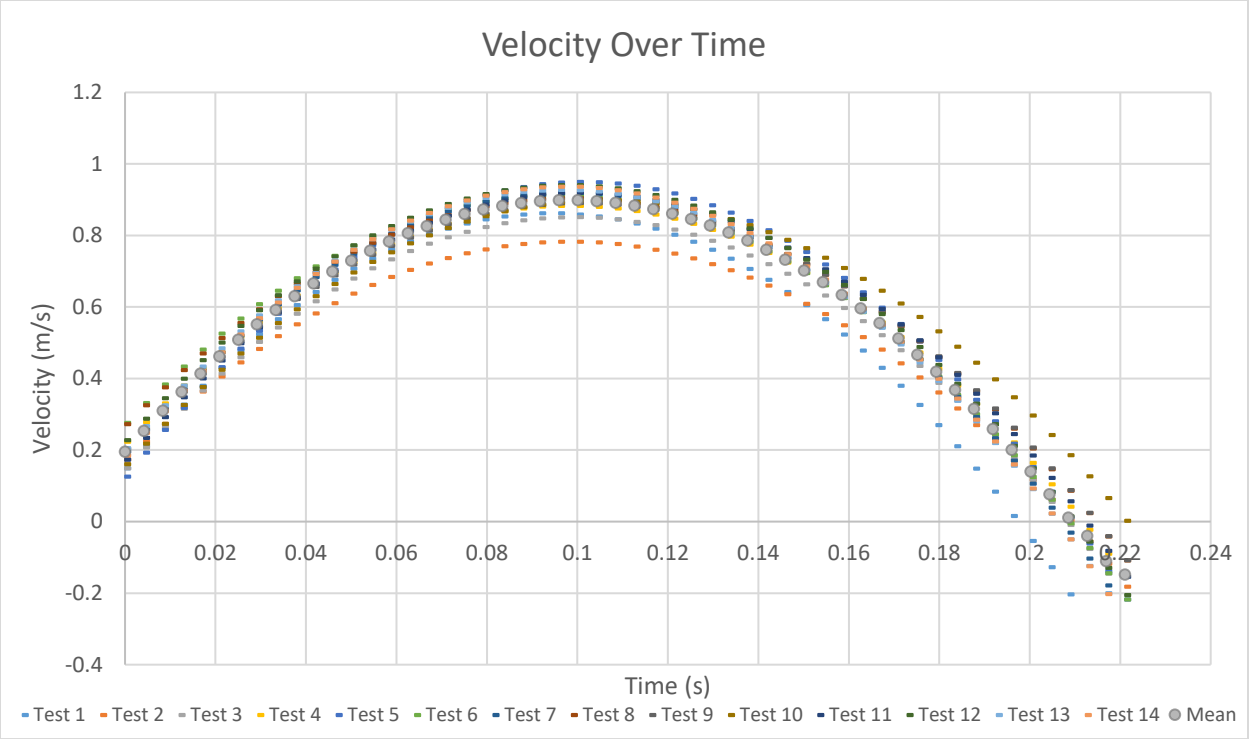

Figure 5.5: Graph of velocity data of each test and mean

Due to the method used to generate the graph, the start point is interpolated as a non-zero value, even though each test started at zero. The value at t=0 should be imagined as the moment that push-off begins. Again, the data was translated into a graph of the average velocity paired with the standard deviation data and regression line. Figure 5.6 is a display of the average velocity data with the shading representing ± 1 standard deviation of the velocity data. Again, a polynomial regression trend line was fit to the curve to determine how well the equation describes the average velocity of the PAO. The R^2 value of .9912 indicates a strong correlation of the data and therefore, a good equation describing the data.

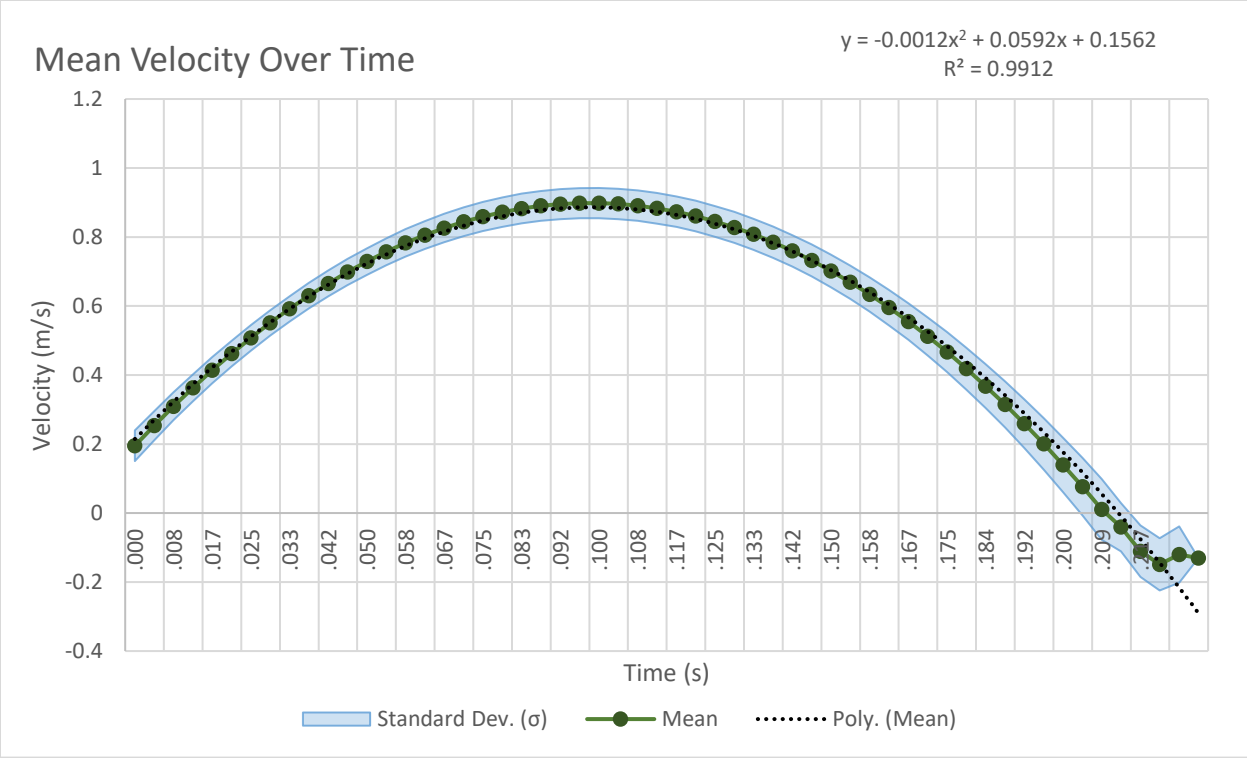

Figure 5.6: Mean and standard deviaition of PAO's velocity

Upon inspection of the data, one can see that the last two data points don't seem to follow the same pattern as the rest of the graph. This is caused by the fact that a majority of the tests being shorter in time. Because of this method, the last point of the graph is only represented by one test; the second to last represented by two tests. An equation better representing the data can be found simply by removing the last two points. This yields a new equation with an R^2 value of .9995, and an R^2 value of .9999 if the last three points are removed. This method may be suggested for representing data if the final points are of no consequence.

The parabolic pattern can, again, be explained when examining the mechanics of the PAO system. While the weight is stationary with zero velocity, the solenoid releases the spring's energy. The mass is lifted upward at an increasing velocity as the spring continues to release the

stored energy. Once the spring's force is equalized with the attached weight, energy is insufficient to increase or maintain the weights velocity. The energy remaining in the spring is enough to offset the force of gravity until the spring is completely decompressed. The weight's velocity then begins to decrease until it reaches peak displacement and after .209 seconds on average, the velocity is zero.

5.1.4 Acceleration

Following the velocity data was the acceleration analysis. For the acceleration data, the velocity equation for each test was again derived for an acceleration equation; the second derivative of the position data. Using the acceleration data, an acceleration graph for each of the 14 tests was plotted. The graphs were then combined into one, along with the average velocity as shown in Figure 5.7.

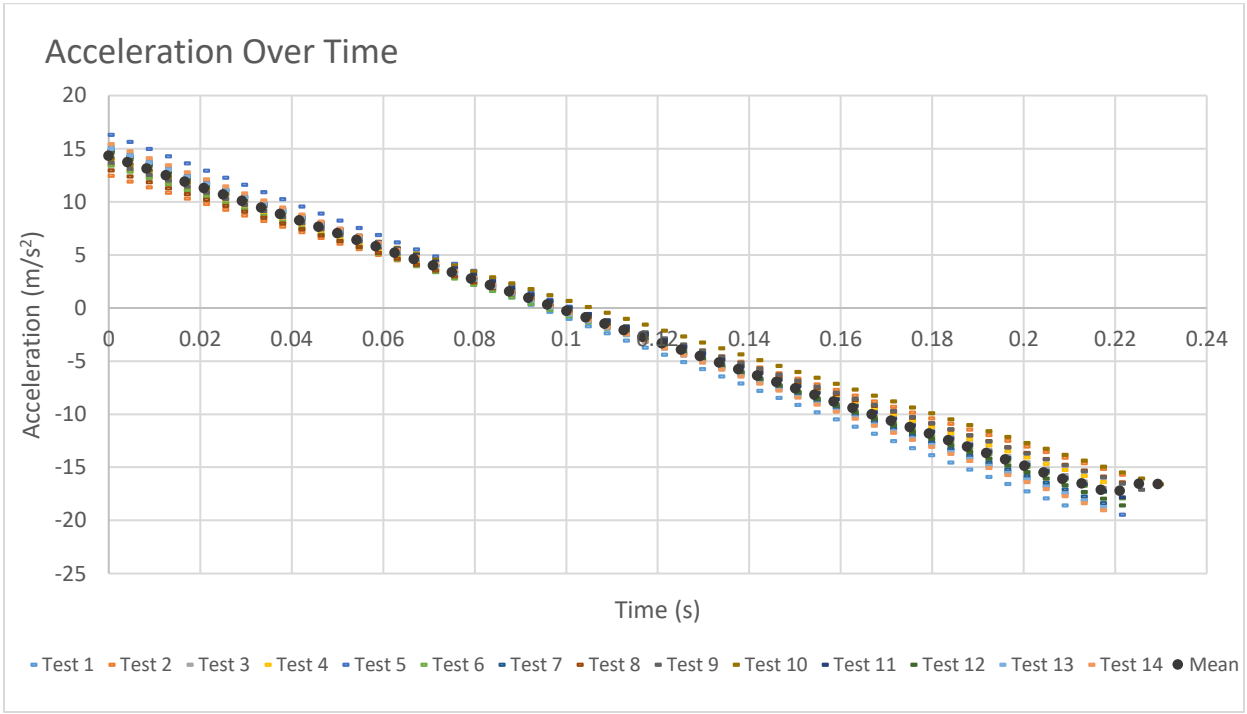

Figure 5.7: Acceleration graph of 14 tests and mean

From this graph, the data shows that each of the tests are accelerating and deaccelerating at slightly varying rates. The test start at their peak acceleration, which averages at 14.3 m/s^2 (46.9 ft/s^2). Being the second derivation of the 3rd order polynomial displacement data, the acceleration can be best represented as a linear pattern. The linear acceleration pattern is usually observed with spring force, as springs are commonly have a constant spring rate. Upon the spring's release, the maximum force is used to thrust ball of the artificial foot downward and the weight upward. Since the spring's force is decreased at a constant (linear) rate, the acceleration decreases at a similar linear rate. This relationship is expected since the equation force, F=ma, can be rewritten as a=F/m. As the spring nears full decompression, the only remaining force is the gravitational constant, which continues to cause deceleration at a constant linear rate.

However, upon closer inspection of Figure 5.7, it was observed that the mass's deceleration was exceeding the gravitational constant of 9.81 m/s^2. This implies that there is another force working against the PAO lifting the mass. One probable cause for the increased deceleration is a large frictional force where the nylon cord hangs from the testing frame. While the PAO is lifting the attached mass, the frictional force works in addition to the gravitational constant to decelerate the mass.

However, the main point of focus is the point where the acceleration rate crosses the x-axis, transitioning from a positive acceleration to negative acceleration; this point corresponds with peak velocity and the length of the spring. The next step was to place this data in one graph with the standard deviation as done for the previous data sets, this is shown in Figure 5.8.

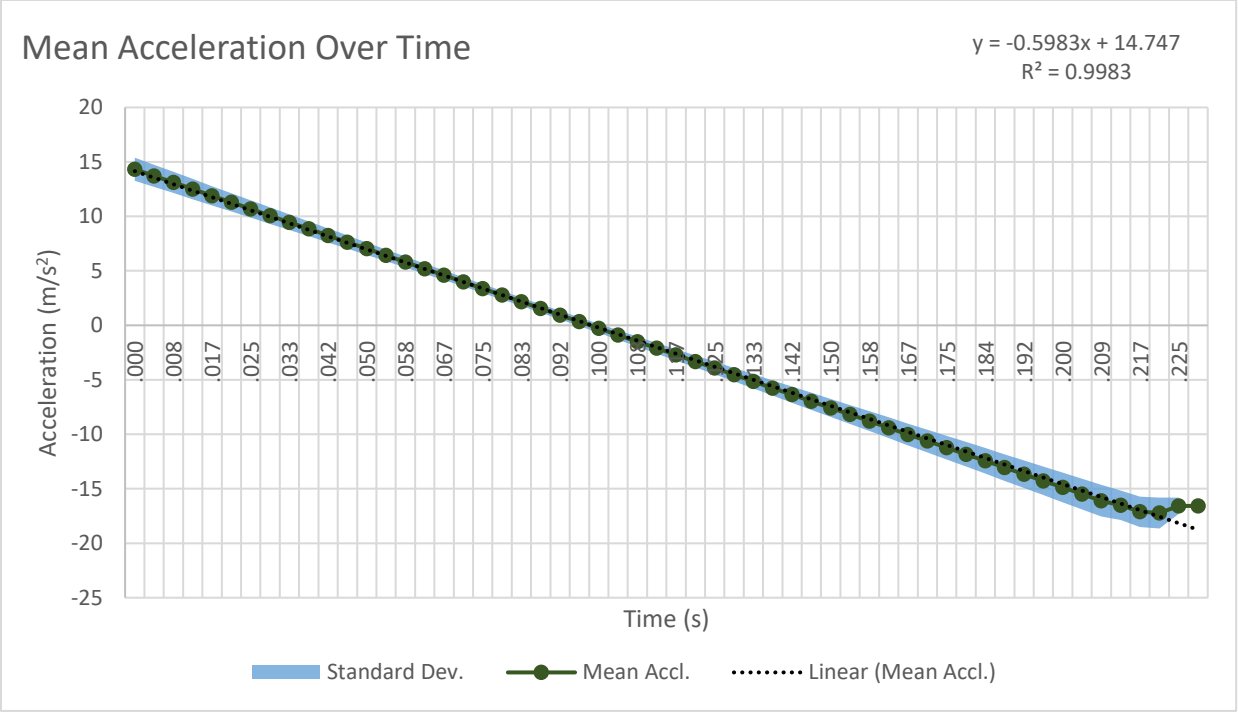

Figure 5.8: Mean and standard deviation of acceleration

From the acceleration graph shown in Figure 5.8, it is easy to see that the standard deviation in the data is proportionally less than the displacement and velocity data. A linear trend line was fit to the mean acceleration data. The R^2 value for the linear trend line was .9983, indicating a strong correlation in the data. Again, the last two points were removed to compare the regression results. With the last two points removed, the new R^2 became .9999, a very strong correlation of the data and an accurate description of the data between the two endpoints.

5.1.5 Push-Off Force

The push-off force is a very valuable part of information to describe the PAO. The push-off force is the primary distinction in configuring the PAO to any specific user. Further, the push-off force provides more information on the stresses being placed on the user by the PAO. The analysis was completed using the same acceleration data from each test. The data was

calculated using the same 5 kg (11 lb_m) mass and the acceleration data from each test. As force was mentioned several times to explain the pattern of acceleration in section 5.1.4, it's easy to guess that the force pattern would follow a similar trend. Since force is the product of mass and acceleration, the constant mass of the attached weight causes a scalable linear decrease in force over time. Because of this, the graph shown in Figure 5.9 follows the same pattern as the acceleration data. For the force data, the graph crosses the x-axis at roughly .17 seconds. This shift in the x-axis is due to accounting for gravity's effect on the mass.

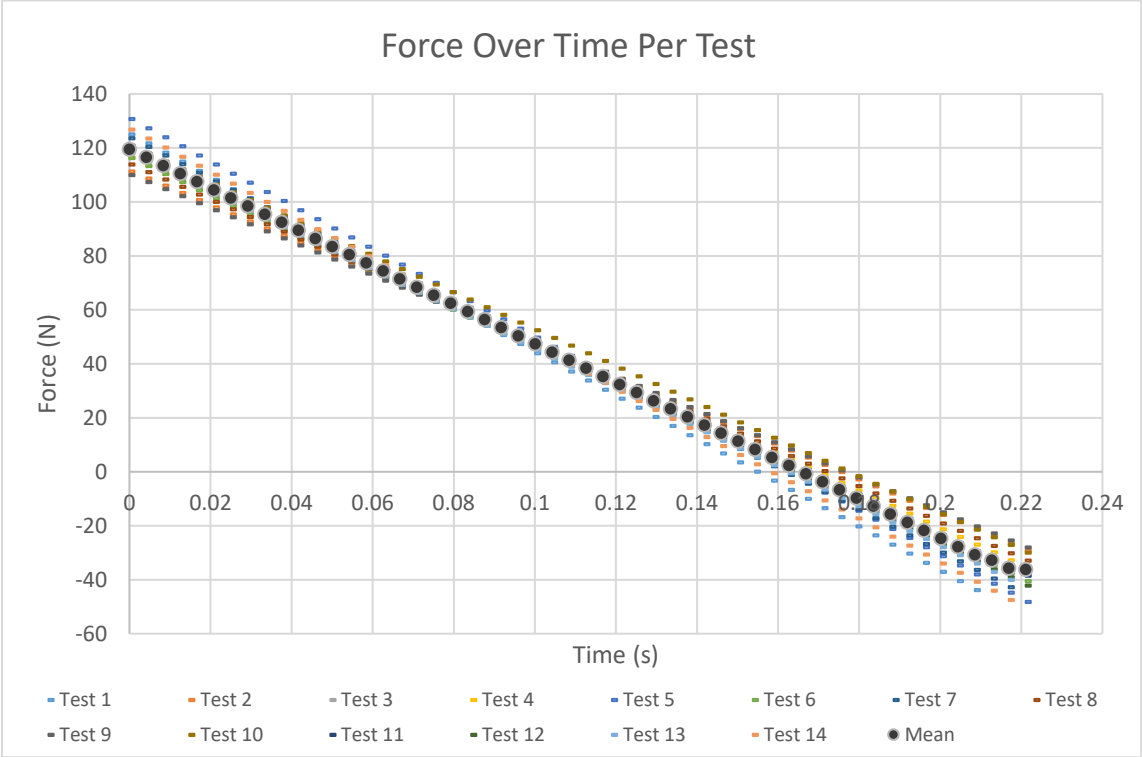

Figure 5.9: Graph of push-off force from each test and average force of all tests.

The resemblance continuous in Figure 5.10, where the mean acceleration is plotted with standard deviation and a linear regression line. As one may expect, the standard deviation of this graph as well as the R^2 value from Figure 5.10 match closely to the acceleration data. The small standard deviation and strong correlation, again, help show a reliable pattern in the data. The

standard deviation of the push-off force is beneficial in determining how consistent the push-off force is from step to step. Too much variability creates difficulty for the user to adjust to the orthosis. As before, when the final two data point are removed, the new R^2 value increases to .9999; a very strong correlation. The peak force occurs at the start of the test at 119.4 N (26.8 lb_f) of force and by .17 seconds, the PAO is no longer producing positive force on the ball of the foot.

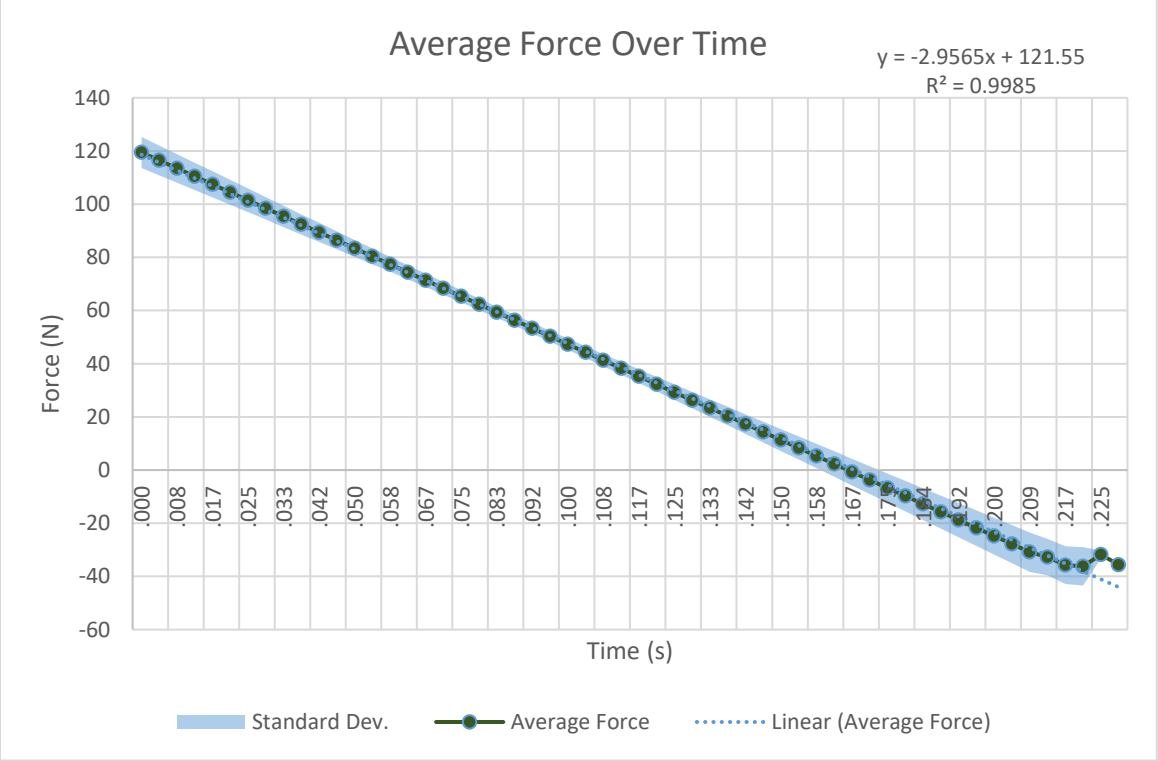

Figure 5.10: Graph of average push-off force and standard deviation of the force data

After noticing the large impact that friction made on the acceleration data, the effect of friction on the recorded force data was also desired.. This was a point of interest to find because the suggested point of friction, where the cord hangs off the testing frame, would be unique to the benchtop test frame. By using a rough friction coefficient value, it was estimated that the

PAO has an output of about 190 N (42.7 lb_f) at the ball of the dummy foot. However, since this value was based largely off of rough estimates, this result was not presented as a result in this research.

5.1.6 Torque

Since the push-off force data has been found, the next step was to estimate the torque at the pivot point of the foot, created by the PAO. The total length from the heel to the ball of the foot measured 273 mm (10.75 in) long and the graph in Figure 5.11 shows and approximate force on the ankle 165 mm (6.5 in) from the ball of the foot for each test.

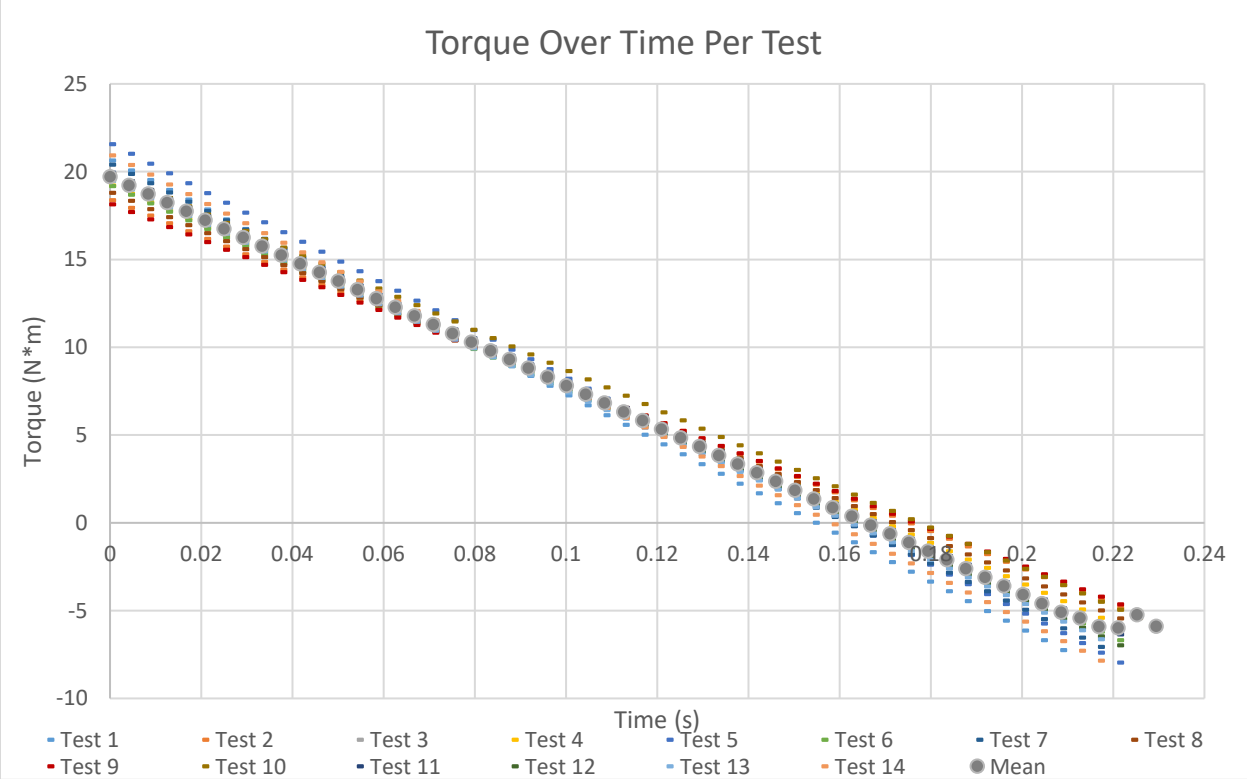

Figure 5.11: Measured PAO torque on ankle from each test, with average torque

Once more, the graph shown in Figure 5.11, appears to follow a similar linear pattern as seen in the acceleration and push-off force data. Since the torque is a product of force and a constant distance between axis and applied force, the relationship is once again linear. The torque data was then taken and used to create another graph plotting average torque and one standard deviation, shown in Figure 5.12 below.

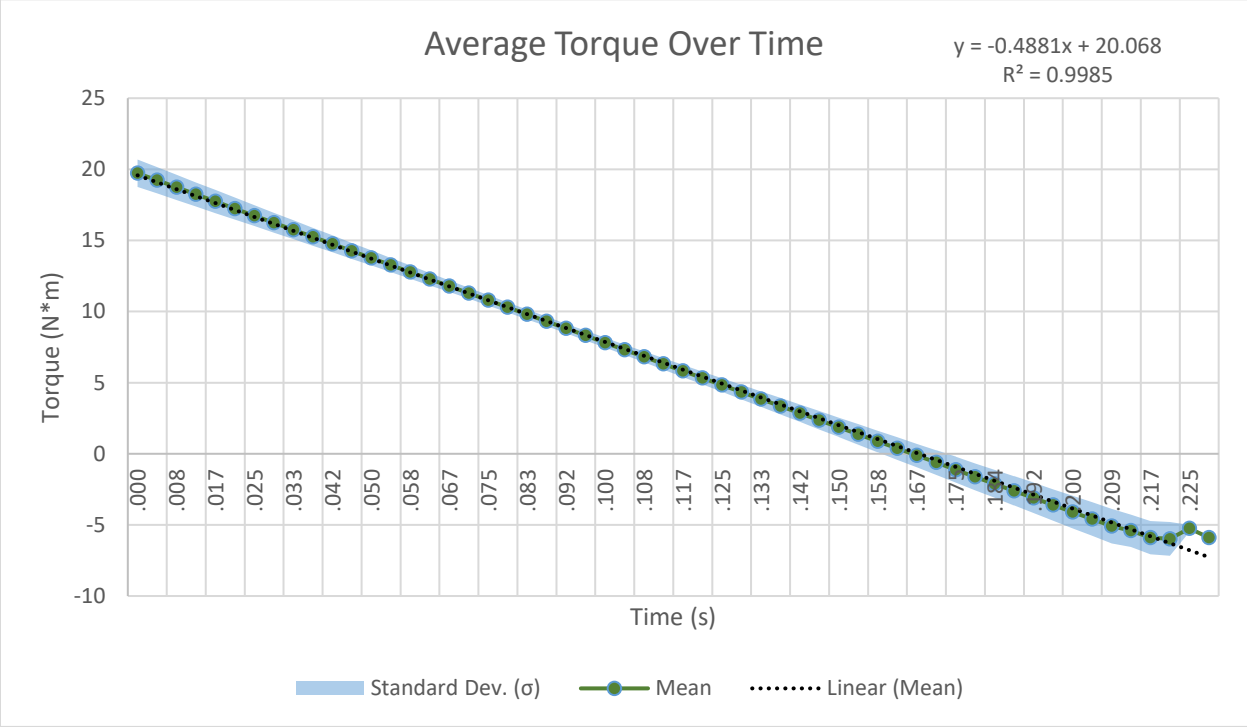

Figure 5.12: Graph of average torque and one standard deviation in the data.

The peak force occurs with the max push-off force at 19.7 N-m (14.5 ft·lb) once the solenoid releases the spring's energy. The torque data serves best as only an approximation of the actual torque placed on the ankle. During the gait process, the angle of force rotates in relation to the foot's angle with the ground. However, the data displayed is most accurate at the initial time of release. This is the same time which yields the highest torque result, and the point

of most concern. When the hypothesized friction between the cord and the frame is accounted for, there is possibly as much as 31 N-m (22.9 ft·lb) of torque at the PAO pivot point. Again, this value is mentioned since it can be interesting, but is not used further in this research.

The torque data was taken another step further to understand the stresses placed on the user by the PAO. A high torque placed on the ankle may cause the push-off event to be uncomfortable, or even dangerous, to the user. Another benefit of the torque data is that the information can be used to determine push-off force from varying foot sizes based on the torque at the foot's fulcrum.

The torque value can be an important value to consider for configuring the device for different users. Since torque is calculated by multiplying force and distance to where the torque is applied, the size of the foot has a direct impact on the amount of necessary force from the system. What this means for the PAO is that a user who weighs more would require more push-off force than a lighter user with the same size foot to propel the weight of their leg. However, this is not the answer in every situation. For two users of the same weight but different foot sizes, the smaller foot would require more torque from the ankle to produce the same push-off force.

5.2 Maximum Output Force

After completing the multiple-high speed tests, the maximum output force of the PAO when the spring was compressed by 74.9 mm (2.95 in) was measured. The solenoid was energized and the spring scale was monitored using the same GoPro 4 camera from the previous high-speed results. From this test, the spring scale measured a push-off force of approximately 191 N (43 lb_f). This would equate to roughly 302 N (68 lb_f) of spring force. However, after analysis of the high-speed testing was complete, it is likely that this measurement may be inaccurate. This is because the maximum force is observed at the initial release of the solenoid,

however, the spring scale measures force through spring displacement in the scale. This means the recorded force is likely less than the actual force.

CHAPTER 6: DISCUSSION

6.1 Development of Powered Ankle Orthosis

To our knowledge, there are no other powered ankle orthoses that use a spring to store the energy generated by an electric motor to assist with gait. This research is the first step in developing this type of PAO device. Since the system will be electric powered, the device can be easily used by any user. The device requires minimal maintenance and does not have some of the potential problems of fluid power, such as leaks.

Overall, the proof-of-concept design of the powered ankle orthosis was successful. The device withstood preliminary testing without breaking down. This ensured reliable results that provided valuable insight on the PAO functionality. The proof-of-concept design allowed for observation of the functionality of an electric motor and spring powered PAO. Because of this, determining which design and analysis methods worked well in testing was achievable. The use of off-the-shelf components for configuring the PAO saved as much as 100 design and machining hours. The saved time was very beneficial during the initial testing and component modification stage of the research.

The preliminary testing also indicated that the square housing and ESM block shape was an effective method of compressing the spring without jamming. The use of a square housing is highly recommended for future PAO designs to function effectively.

The high-speed footage analysis proved to be an effective method for analyzing the PAO movement. The high-speed footage allowed for recording several properties of the PAO at once, using only one device to record data. This saved the time and costs associated with mounting

several types of measurement equipment to the PAO, or running multiple tests with different measurement devices; e.g. separate tests for recording force and displacement.

Before this research and initial testing, powering a PAO with an electric motor seemed impractical. Some users of the device may have found the size of a motor capable of generating enough torque for plantar flexion to be too bulky and uncomfortable, especially a user with abnormal gait. This research shows that powering a PAO using an electric motor is a feasible option. The approach in this research replaces a larger motor required to deliver the output energy over .05 seconds with a much smaller motor that is able to take up to 1 second to generate this same energy.

The initial testing of the PAO helped to identify areas which can be improved in future PAO work. One of these areas is the release of the PAO using a solenoid. While the frictional force holding the solenoid pin can be reduced with different materials, there is still room for design improvement. One consideration was to implement a lever mechanism to add mechanical advantage to the release stage. Reducing the required force would result in a less bulky solenoid and smaller energy draw from the batteries. In addition to reducing the PAO size with a smaller solenoid, The PAO housing and threaded rod transmission can already be reduced by about 5 cm (2 in), possibly more with an improved release mechanism.

Another mechanism that could be improved was the ESM. While the clutch mechanism did not progress past functional testing, it did show potential for being a great method to save time. A clamshell design for the ESM would allow for the use of one piece pinch threads that do not require frequent adjustments. The mechanism could also be improved by adding ball bearings to the pinch thread design to reduce friction against the PAO inner wall. To further

reduce the wear on the pinch thread inserts, an acme threaded rod can be used for stronger threads. Heat treating the threaded inserts to increase hardness may also help to reduce wear.

These improvements will help prepare the PAO for the next stage of research, which may include using the findings from this research to develop a wearable version of the electric motor powered ankle orthosis. This would allow for testing the effects of the PAO on human subjects. Preparing for a wearable PAO would also require automating the system using various control methods. A huge benefit that would occur with this is the precise and consistent release of the PAO's energy. Studies show that this control is an essential feature in success during the rehabilitative process (Sawicki, Domingo, & Ferris, 2006). Most of the system could be controlled using an Arduino microcontroller. There are a large variety of sensors that could be used to track gait and fire the PAO. Some basic sensors include accelerometers, gyroscopic/tilt sensors, strain gages, and footswitches. However, the use of an electromyography to detect electrical muscle signals would be the most advantageous (Gordon, Stephen, & Ferris, 2007).

6.2 Research Limitations and Unexpected Discoveries

While conducting the preliminary tests on the PAO, it was decided to not test the device at the target force of 400 N (90 lb_f) of push-off force. While it will eventually be desirable to determine if the device was capable of withstanding the conditions created at max force, the primary concern was that catastrophic failure may occur before performance testing of the device could be completed. It was more important to understand the performance characteristics under lower loads than to determine if high loads could be achieved. Once all research data is collected from the device, including near-future research, destructive testing may be done on the device to determine points of failure.

While conducting the preliminary tests, it was surprising to observe the intensity in which the PAO pulled up on the heel, even when using the elastic rubber linkage. The push-off motion could be intimidating and uncomfortable to many users. An alternative linkage may be required to reduce this sudden jolt on the heel.

Another result that was not originally considered was the delay time taken to pull the solenoid pin. It may not be known if this delay time is significant until human testing is performed. This delay may cause a user discomfort and even a short delay time could create a moment of anticipation or hesitation for the user. Since the delay time was measured to be consistent, about 40 milliseconds, Controller software may be able to account for the delay.

6.3 Significance of Findings

In total, 14 high-speed video tests were conducted and analyzed in order to understand the dynamics and consistency of the PAO. It was observed that the PAO operates with reasonable consistency. This is an important property of the PAO since it could not be used for rehabilitation if there was large and unpredictable variation in the assistive push-off force for the user.

This research also begins to provide an understanding of the effects that a spring creates on PAO dynamics. The impact of certain spring properties can be tracked through each of the analyzed dynamic characteristics. For example, the relationship between the spring length and the point of inflection could be seen within the displacement data. This relationship can be followed to show the peak velocity is reached as the spring nears complete decompression. With the ability to understand how each spring property effects the dynamics, the PAO can be better configured to perform optimally for each user.

To better understand the PAO's performance, the torque output results can be compared to other powered ankle orthosis technologies. During testing, the PAO had an average peak torque output of about 19.7 N-m (14.5 ft·lb). Similar technologies include the pneumatic muscle ankle-foot orthosis developed at the University of Michigan, capable of producing 70 N-m (51.6 ft·lb) of torque (Shorter, Xia, Hsiao-Wecksler, Durfee, & Kogler, 2013). Also, there is the water/hydraulic powered ankle-foot orthosis developed by the Center for Interdisciplinary Research in Rehabilitation and Social Interaction (CIRRIS), with a peak torque output of 98 N-m (72.3 ft·lb) (Shorter, Xia, Hsiao-Wecksler, Durfee, & Kogler, 2013). While these devices seem to significantly outperform the PAO used in this research, both of the mentioned devices are tethered. When comparing to other portable powered ankle orthosis devices, one of the few remaining devices available for comparison is the pneumatic portable powered ankle-foot orthosis developed at the University of Illinois. This device has a peak plantar flexor torque of 9.2 N-m (6.8 ft·lb) (Kogler, Loth, Durfeee, Hsiao-Wecksler, & Shorter, 2011). Considering this PAO was not tested under maximum load, this research suggests that an electric motor driven PAO is capable of performing alongside of similar current state-of-the-art technology.

CHAPTER 7: CONCLUSIONS

The scope of this research was to design and analyze a proof-of-concept powered ankle orthosis which uses a small electric motor and a spring to generate enough force to assist with plantar flexion. This approach differed from other PAOs because the device did not use fluid power nor was it tethered. This research found that by utilizing the entire time taken to complete the gait cycle, an electric PAO can feasibly use a smaller motor to assist with plantar flexion in the rehabilitation process. The data also begins to provide a foundation for understanding the dynamics of using a spring within a PAO and the effects of some of the spring properties.

The proof-of-concept model that was developed can continue to be used for researching the effects of operating the PAO using different threaded rod, spring or foot configurations. The modular design components and adaptable mounting platforms allow for integration of future testing equipment. Furthermore, based on the results of this research, there is good justification to continue research on an electric PAO utilizing a small motor and spring.

BIBLIOGRAPHY

1, I. T. (2007, August 23). ISO 8549-1:1989, Prosthetics and orthotics -- Vocabulary -- Part 1: General terms for external limb prostheses and external orthoses. United States Of America: American National Standards Institute.

Asselin, P., Knezevic, S., Kornfeld, S., Cirnigliaro, C., Agranova-Breyter, I., Bauman, W., & Spungen, A. M. (2015). Heart rate and oxygen demand of powered exoskeleton-assisted walking in persons with paraplegia. *Journal of Rehabilitation Research & Development 52(2)*, 147-158.

Bhandari, V. B. (2007). *Design of Machine Elements.* New York: McGraw-Hill.

Brault, M. W. (2012). *Americans With Disabilities: 2010.* Washington D.C.: U.S. Census Bureau.

Burris, M. (2016, May). *Stepper Motors vs Servo Motors - Selecting a Motor*. Retrieved from About Tech: http://components.about.com

Compston, A., & Coles, A. (2008). Multiple Sclerosis. *The Lancet; volume 372, issue 9648*, 1502-1517.

Cyberdyne. (2015, November). *What's HAL*. Retrieved from Cyberdyne: www.cyber.jp/english

Dietz, V. (2013). Chapter 12 – Gait disorders. In M. P. Barnes, *Neurological Rehabilitation, Volume 110: Handbook of Clinical Neurology* (pp. 133-143). Amsterdam: Elsevier.

Ferris, D. P., Czerniecki, J. M., & Hannaford, B. (2006). An Ankle-Foot Orthosis Powered by Artificial Pneumatic Muscles. *HSS Journal*, 189-197.

General Electric. (1969). *Hardiman I Prototype Project: Hardiman Arm Test.* Schenectady, NY: General Electric Company.

GoPro, Inc. (2015). GoPro Hero 4: Black. *User Manual*, 27.

Gordon, K. E., & Ferris, D. P. (2007). Learning to walk with a robotic ankle exoskeleton. *J Biomech*, 40(12):2636-44.

Gordon, K. E., Stephen, C. M., & Ferris, D. P. (2007). Locomotor adaptation to a powered ankle-foot orthosis depends on control method. *Journal of NeuroEngineering and Rehabilitation*.

Kazerooni, H. (2009). *HULC*. Retrieved from Berkeley Robotics & Human Engineering Laboratory: http://bleex.me.berkeley.edu/research/exoskeleton/hulc/

Keizai, T. (2013, November 25). *CYBERDYNE Inc. — The robot suit obtains certification in Europe.* Retrieved from Discuss Japan: http://www.japanpolicyforum.jp

Kogler, G. F., Loth, E., Durfeee, W. K., Hsiao-Wecksler, E. T., & Shorter, K. A. (2011). A portable powered ankle-foot orthosis for rehabilitation. *Journal of Rehabilitation Research & Development*, 459-472.

Krebs, H. I., Dipietro, L., & Levy-Tzedek, S. (2008). A Paradigm Shift for Rehabilitation Robotics. *IEEE Engineering in Medicine & Biology Magazine*, 61-70.

Kreighbaum, E., & Barthels, K. M. (1990). *Biomechanics: A Qualitative Approach for Studying Human Movement; 3rd Ed.* New York: Macmillan Publishing Company.

Kuo, A. D., Donelan, J. M., & Ruina, A. (2005). Energetic consequences of walking like an inverted pendulum: step-to-step transitions. *Exercise & Sport Sciences Reviews*, 88-97.

Magnetic Sensor Sytems. (2005). *Low Profile Clapper Solenoid, S-16-264.*

Ministry of Internal Affairs and Communication. (2014). *Chapter 2 Population and Households.* Toyko: Statistics Bureau.

National Stroke Association. (2016, May). *What is stroke?* Retrieved from National Stroke Association: Stoke.org

Nuruzzaman, D. M., & Chawdhury, M. A. (2012). Effect of Load and Sliding Velocity on Friction Coefficient of Aluminum Sliding Different Pin Materials. *American Journal of Materials Science*, 26-31.

Oberg, E., Jones, F. D., Horton, H. L., & Ryffel, H. H. (2008). *Machinery's Handbook, Twenty-Eigth Edition.* New York: Industrial Press.

Rose, J., & Gamble, J. G. (1994). Human Walking. Baltimore, MD: Williams and Wilkins.

Sawicki, G. S., Domingo, A., & Ferris, D. P. (2006). The effects of powered ankle-foot orthoses on joint kinematics and muscle activation during walking in individuals with incomplete spinal cord injury. *Journal of NeuroEngineering and Rehabilitation*.

Sawicki, G. S., Lewis, C. L., & Ferris, D. P. (2009). It Pays to Have a Spring in Your Step. *Exercise and Sport Sciences Reviews*, 130-138.

Shorter, K. A., Xia, J., Hsiao-Wecksler, E. T., Durfee, W. K., & Kogler, G. F. (2013). Technologies for Powered Ankle-Foot Orthotic Systems: Possibilites and Challenges. *Mechatronics (Volume:18, Issue 1)*, 337-347.

Stansbury, L. G., Lalliss, S. J., Branstetter, J. G., Bagg, M. R., & Holcomb, J. B. (2008). Amputations in U.S. military personnel in the current conflicts in Afghanistan and Iraq. *J Orthop Trauma*, 43-46.

The Muscular Dystrophy Association. (2016, May 1). *About Neuromuscular Diseases*. Retrieved from MDA: mda.org

U.S. National Library of Medicine. (2016, May). *Muscular Dystrophy*. Retrieved from MedlinePlus: nlm.nih.gov/medlineplus/musculardystrophy

Vahid-Araghi, O., & Golnaraghi, F. (2011). *Friction-Induced Vibration in Lead Screw Drives.* New York: Springer-Verlag.

von Schroeder, H. P., Coutts, R. D., Lyden, P. D., Billings Jr., E., & Nickel, V. (1995). Gait parameters following stroke: A practical assessment. *Journal of Rehabilitation Research & Development*, 25.

Winter, D. A. (2009). *Biomechanic and Motor Control of Human Movement.* Hoboken: John Wiley & Sons.

Yan, T., Cempini, M., Oddo, C. M., & Vitiello, N. (2014). Review of assistive strategies in powered lower-limb orthoses and exoskeletons. *Robotics and Autonomous Systems*, 120-136.

APPENDIX A: HIGH SPEED TESTING DATA

Test 1		5	kg Mass		5	Delayed Frames
Time (s)	Displacement (in)	Displacement (mm)	Velocity (m/s)	Acceleration (m/s^2)	Force (N)	Torque (N*m)
0	0	0	0.149579	15.196892	125.034	20.64318951
0.004	0.00422	0.11	0.211554	14.521298	121.656	20.08548659
0.008	0.01370	0.35	0.270711	13.845704	118.279	19.52778367
0.013	0.06166	1.57	0.327051	13.170110	114.901	18.97008074
0.017	0.10962	2.78	0.380572	12.494516	111.523	18.41237782
0.021	0.15758	4.00	0.431276	11.818922	108.145	17.8546749
0.025	0.22472	5.71	0.479162	11.143328	104.767	17.29697198
0.0292	0.31116	7.90	0.524230	10.467734	101.389	16.73926905
0.033	0.40718	10.34	0.566480	9.792139	98.0107	16.18156613
0.038	0.51259	13.02	0.605913	9.116545	94.6327	15.62386321
0.04171	0.61799	15.70	0.642527	8.440951	91.2548	15.06616029
0.04588	0.73320	18.62	0.676324	7.765357	87.8768	14.50845736
0.05005	0.83861	21.30	0.707303	7.089763	84.4988	13.95075444
0.05422	0.94401	23.98	0.735465	6.414169	81.1208	13.39305152
0.05839	1.05922	26.90	0.760808	5.738575	77.7429	12.83534859
0.063	1.19361	30.32	0.783334	5.062981	74.3649	12.27764567
0.06673	1.32800	33.73	0.803042	4.387387	70.9869	11.71994275
0.0709	1.47199	37.39	0.819932	3.711793	67.609	11.16223983
0.07508	1.61597	41.05	0.834005	3.036199	64.231	10.6045369
0.07925	1.73118	43.97	0.845259	2.360604	60.853	10.04683398
0.08342	1.88475	47.87	0.853696	1.685010	57.4751	9.489131059
0.08759	2.02874	51.53	0.859315	1.009416	54.0971	8.931428136
0.09176	2.18231	55.43	0.862116	0.333822	50.7191	8.373725214
0.09593	2.34569	59.58	0.862100	-0.341772	47.3411	7.816022291
0.1001	2.49927	63.48	0.859265	-1.017366	43.9632	7.258319368
0.10427	2.65284	67.38	0.853613	-1.692960	40.5852	6.700616446
0.10844	2.80642	71.28	0.845143	-2.368554	37.2072	6.142913523
0.11261	2.94081	74.70	0.833855	-3.044148	33.8293	5.585210601
0.11678	3.06561	77.87	0.819750	-3.719742	30.4513	5.027507678
0.12095	3.19041	81.04	0.802827	-4.395336	27.0733	4.469804755
0.12513	3.30562	83.96	0.783085	-5.070931	23.6953	3.912101833
0.1293	3.42083	86.89	0.760526	-5.746525	20.3174	3.35439891
0.13347	3.53604	89.82	0.735150	-6.422119	16.9394	2.796695988
0.13764	3.65124	92.74	0.706955	-7.097713	13.5614	2.238993065
0.14181	3.75665	95.42	0.675943	-7.773307	10.1835	1.681290142
0.14598	3.86205	98.10	0.642113	-8.448901	6.80549	1.12358722
0.15015	3.95797	100.53	0.605465	-9.124495	3.42752	0.565884297
0.15432	4.04430	102.73	0.565999	-9.800089	0.04955	0.008181375
0.15849	4.12104	104.67	0.523716	-10.475683	-3.32842	-0.549521548
0.16266	4.19777	106.62	0.478615	-11.151277	-6.70639	-1.107224471
0.16683	4.26491	108.33	0.430695	-11.826871	-10.0844	-1.664927393
0.171	4.33206	110.03	0.379959	-12.502466	-13.4623	-2.222630316
0.17518	4.38961	111.50	0.326404	-13.178060	-16.8403	-2.780333238
0.17935	4.44716	112.96	0.270032	-13.853654	-20.2183	-3.338036161
0.18352	4.49512	114.18	0.210841	-14.529248	-23.5962	-3.895739084
0.18769	4.53349	115.15	0.148833	-15.204842	-26.9742	-4.453442006
0.19186	4.56226	115.88	0.084007	-15.880436	-30.3522	-5.011144929
0.19603	4.58145	116.37	0.016364	-16.556030	-33.7302	-5.568847852
0.2002	4.60063	116.86	-0.054098	-17.231624	-37.1081	-6.126550774
0.20437	4.61022	117.10	-0.127377	-17.907218	-40.4861	-6.684253697
0.20854	4.61507	117.22	-0.203474	-18.582812	-43.8641	-7.241956619

Test 2		5	kg Mass		2	Delayed Frames
Time (s)	Displacement (in)	Displacement (mm)	Velocity (m/s)	Acceleration (m/s^2)	Force (N)	Torque (N*m)
0	0	0	0.1740005	12.450153	111.301	18.3758
0.00417	0.0113	0.29	0.2248217	11.919633	108.648	17.9378
0.00834	0.0396	1.01	0.2734302	11.389113	105.996	17.4999
0.01251	0.0849	2.16	0.3198260	10.858593	103.343	17.0619
0.01668	0.1189	3.02	0.3640091	10.328073	100.69	16.6240
0.02085	0.1755	4.46	0.4059794	9.797553	98.0378	16.1860
0.02503	0.2321	5.90	0.4457371	9.267034	95.3852	15.7481
0.0292	0.3001	7.62	0.4832820	8.736514	92.7326	15.3101
0.03337	0.3793	9.64	0.5186142	8.205994	90.08	14.8722
0.03754	0.4586	11.65	0.5517337	7.675474	87.4274	14.4343
0.04171	0.5492	13.95	0.5826405	7.144954	84.7748	13.9963
0.04588	0.6511	16.54	0.6113346	6.614434	82.1222	13.5584
0.05005	0.7530	19.13	0.6378160	6.083914	79.4696	13.1204
0.05422	0.8549	21.71	0.6620847	5.553395	76.817	12.6825
0.05839	0.9681	24.59	0.6841406	5.022875	74.1644	12.2445
0.06256	1.0814	27.47	0.7039838	4.492355	71.5118	11.8066
0.06673	1.1946	30.34	0.7216144	3.961835	68.8592	11.3686
0.0709	1.3192	33.51	0.7370322	3.431315	66.2066	10.9307
0.07508	1.4551	36.96	0.7502373	2.900795	63.554	10.4928
0.07925	1.5909	40.41	0.7612297	2.370275	60.9014	10.0548
0.08342	1.7381	44.15	0.7700094	1.839755	58.2488	9.6169
0.08759	1.8853	47.89	0.7765763	1.309236	55.5962	9.1789
0.09176	2.0212	51.34	0.7809306	0.778716	52.9436	8.7410
0.09593	2.1570	54.79	0.7830721	0.248196	50.291	8.3030
0.1001	2.2929	58.24	0.7830009	-0.282324	47.6384	7.8651
0.10427	2.4175	61.40	0.7807171	-0.812844	44.9858	7.4272
0.10844	2.5533	64.85	0.7762205	-1.343364	42.3332	6.9892
0.11261	2.6892	68.31	0.7695112	-1.873884	39.6806	6.5513
0.11678	2.8025	71.18	0.7605891	-2.404403	37.028	6.1133
0.12095	2.9383	74.63	0.7494544	-2.934923	34.3754	5.6754
0.12513	3.0516	77.51	0.7361070	-3.465443	31.7228	5.2374
0.1293	3.1649	80.39	0.7205468	-3.995963	29.0702	4.7995
0.13347	3.2667	82.98	0.7027739	-4.526483	26.4176	4.3615
0.13764	3.3800	85.85	0.6827883	-5.057003	23.765	3.9236
0.14181	3.4819	88.44	0.6605901	-5.587523	21.1124	3.4857
0.14598	3.5725	90.74	0.6361791	-6.118043	18.4598	3.0477
0.15015	3.6630	93.04	0.6095553	-6.648562	15.8072	2.6098
0.15432	3.7536	95.34	0.5807189	-7.179082	13.1546	2.1718
0.15849	3.8329	97.36	0.5496698	-7.709602	10.502	1.7339
0.16266	3.9122	99.37	0.5164079	-8.240122	7.84939	1.2959
0.16683	3.9801	101.10	0.4809333	-8.770642	5.19679	0.8580
0.171	4.0481	102.82	0.4432461	-9.301162	2.54419	0.4200
0.17518	4.1161	104.55	0.4033461	-9.831682	-0.10841	-0.0179
0.17935	4.1727	105.99	0.3612334	-10.362201	-2.76101	-0.4558
0.18352	4.2293	107.42	0.3169080	-10.892721	-5.41361	-0.8938
0.18769	4.2859	108.86	0.2703698	-11.423241	-8.06621	-1.3317
0.19186	4.3312	110.01	0.2216190	-11.953761	-10.7188	-1.7697
0.19603	4.3764	111.16	0.1706554	-12.484281	-13.3714	-2.2076
0.2002	4.4104	112.03	0.1174792	-13.014801	-16.024	-2.6456
0.20437	4.4444	112.89	0.0620902	-13.545321	-18.6766	-3.0835
0.20854	4.4671	113.46	0.0044885	-14.075841	-21.3292	-3.5215
0.21271	4.4898	114.04	-0.0553259	-14.606360	-23.9818	-3.9594
0.21688	4.5011	114.33	-0.1173530	-15.136880	-26.6344	-4.3973
0.22105	4.5067	114.47	-0.1815928	-15.667400	-29.287	-4.8353

Test 3		5	kg Mass		5	Delayed Frames
Time (s)	Displacement (in)	Displacement (mm)	Velocity (m/s)	Acceleration (m/s^2)	Force (N)	Torque (N*m)
0	0	0	0.14960570	14.19058160	120.0029	19.81248011
0.00417	0.005652174	0.143565217	0.20754513	13.59253206	117.0127	19.31879021
0.00834	0.016956522	0.430695652	0.26299018	12.99448251	114.0224	18.82510031
0.01251	0.050942029	1.293927536	0.31594088	12.39643297	111.0322	18.33141041
0.01668	0.084927536	2.15715942	0.36639720	11.79838342	108.0419	17.83772051
0.021	0.141521739	3.594652174	0.41435916	11.20033388	105.0517	17.34403062
0.0250	0.209492754	5.321115942	0.45982675	10.60228433	102.0614	16.85034072
0.029	0.288768116	7.334710145	0.50279997	10.00423479	99.07117	16.35665082
0.033	0.368043478	9.348304348	0.54327882	9.40618524	96.08093	15.86296092
0.03754	0.458623188	11.64902899	0.58126331	8.80813570	93.09068	15.36927102
0.04171	0.560507246	14.23688406	0.61675343	8.21008615	90.10043	14.87558112
0.04588	0.662391304	16.82473913	0.64974918	7.61203661	87.11018	14.38189122
0.05005	0.775652174	19.70156522	0.68025056	7.01398707	84.11994	13.88820132
0.05422	0.911521739	23.15265217	0.70825758	6.41593752	81.12969	13.39451142
0.05839	1.024782609	26.02947826	0.73377023	5.81788798	78.13944	12.90082152
0.06256	1.149347826	29.19343478	0.75678851	5.21983843	75.14919	12.40713163
0.06673	1.273913043	32.3573913	0.77731242	4.62178889	72.15894	11.91344173
0.0709	1.409782609	35.80847826	0.79534197	4.02373934	69.1687	11.41975183
0.07508	1.545652174	39.25956522	0.81087715	3.42568980	66.17845	10.92606193
0.07925	1.681521739	42.71065217	0.82391796	2.82764025	63.1882	10.43237203
0.08342	1.817391304	46.16173913	0.83446440	2.22959071	60.19795	9.93868213
0.08759	1.964565217	49.89995652	0.84251648	1.63154116	57.20771	9.444992231
0.09176	2.123115942	53.92714493	0.84807419	1.03349162	54.21746	8.951302332
0.09593	2.270289855	57.66536232	0.85113753	0.43544208	51.22721	8.457612433
0.1001	2.417463768	61.40357971	0.85170651	-0.16260747	48.23696	7.963922534
0.10427	2.553333333	64.85466667	0.84978111	-0.76065701	45.24671	7.470232635
0.10844	2.700507246	68.59288406	0.84536135	-1.35870656	42.25647	6.976542736
0.11261	2.836376812	72.04397101	0.83844723	-1.95675610	39.26622	6.482852837
0.11678	2.960942029	75.20792754	0.82903873	-2.55480565	36.27597	5.989162938
0.12095	3.085507246	78.37188406	0.81713587	-3.15285519	33.28572	5.495473039
0.12513	3.232681159	82.11010145	0.80273864	-3.75090474	30.29548	5.00178314
0.1293	3.345942029	84.98692754	0.78584704	-4.34895428	27.30523	4.508093241
0.13347	3.470507246	88.15088406	0.76646107	-4.94700383	24.31498	4.014403342
0.13764	3.583768116	91.02771014	0.74458074	-5.54505337	21.32473	3.520713443
0.14181	3.697028986	93.90453623	0.72020604	-6.14310291	18.33449	3.027023544
0.14598	3.810289855	96.78136232	0.69333697	-6.74115246	15.34424	2.533333645
0.15015	3.923550725	99.65818841	0.66397354	-7.33920200	12.35399	2.039643746
0.15432	4.025434783	102.2460435	0.63211573	-7.93725155	9.363742	1.545953847
0.15849	4.127318841	104.8338986	0.59776356	-8.53530109	6.373495	1.052263948
0.16266	4.217898551	107.1346232	0.56091703	-9.13335064	3.383247	0.558574049
0.16683	4.297173913	109.1482174	0.52157612	-9.73140018	0.392999	0.06488415
0.171	4.365144928	110.8746812	0.47974085	-10.32944973	-2.59725	-0.428805749
0.17518	4.433115942	112.6011449	0.43541121	-10.92749927	-5.5875	-0.922495648
0.17935	4.501086957	114.3276087	0.38858720	-11.52554882	-8.57774	-1.416185547
0.18352	4.557681159	115.7651014	0.33926883	-12.12359836	-11.568	-1.909875446
0.18769	4.608405797	117.0535072	0.28745608	-12.72164790	-14.5582	-2.403565345
0.19186	4.665	118.491	0.23314897	-13.31969745	-17.5485	-2.897255244
0.19603	4.708478261	119.5953478	0.17634750	-13.91774699	-20.5387	-3.390945143
0.2002	4.742463768	120.4585797	0.11705165	-14.51579654	-23.529	-3.884635042
0.20437	4.776449275	121.3218116	0.05526144	-15.11384608	-26.5192	-4.378324941
0.20854	4.799130435	121.897913	-0.00902314	-15.71189563	-29.5095	-4.87201484
0.21271	4.816086957	122.3286087	-0.07580209	-16.30994517	-32.4997	-5.365704739
0.21688	4.82173913	122.4721739	-0.14507540	-16.90799472	-35.49	-5.859394638

Test 4		5	kg Mass		9	Delayed Frames
Time (s)	Displacement (in)	Displacement (mm)	Velocity (m/s)	Acceleration (m/s^2)	Force (N)	Torque (N*m)
0	0	0	0.22345050	13.4757	116.428	19.22230886
0.00417	0.02	0.508	0.27845871	12.9019	113.559	18.74865951
0.00834	0.06	1.524	0.33107382	12.3281	110.691	18.27501015
0.01251	0.11	2.794	0.38129580	11.7543	107.822	17.80136079
0.01668	0.16	4.064	0.42912468	11.1806	104.953	17.32771143
0.02085	0.2225	5.6515	0.47456044	10.6068	102.084	16.85406207
0.02503	0.285	7.239	0.51760310	10.0330	99.2151	16.38041272
0.0292	0.37875	9.62025	0.55825263	9.4592	96.3462	15.90676336
0.03337	0.4725	12.0015	0.59650906	8.8855	93.4774	15.433114
0.03754	0.5525	14.0335	0.63237237	8.3117	90.6085	14.95946464
0.04171	0.6625	16.8275	0.66584257	7.7379	87.7396	14.48581528
0.04588	0.7875	20.0025	0.69691966	7.1642	84.8708	14.01216593
0.05005	0.9125	23.1775	0.72560364	6.5904	82.0019	13.53851657
0.05422	1.0375	26.3525	0.75189450	6.0166	79.1331	13.06486721
0.05839	1.1675	29.6545	0.77579225	5.4428	76.2642	12.59121785
0.06256	1.2975	32.9565	0.79729688	4.8691	73.3953	12.1175685
0.06673	1.4375	36.5125	0.81640841	4.2953	70.5265	11.64391914
0.0709	1.5775	40.0685	0.83312682	3.7215	67.6576	11.17026978
0.07508	1.7075	43.3705	0.84745212	3.1477	64.7887	10.69662042
0.07925	1.8575	47.1805	0.85938431	2.5740	61.9199	10.22297106
0.08342	2.0325	51.6255	0.86892338	2.0002	59.051	9.749321707
0.08759	2.1925	55.6895	0.87606934	1.4264	56.1821	9.275672349
0.09176	2.3375	59.3725	0.88082219	0.8527	53.3133	8.802022991
0.09593	2.4875	63.1825	0.88318192	0.2789	50.4444	8.328373633
0.1001	2.6175	66.4845	0.88314855	-0.2949	47.5756	7.854724275
0.10427	2.7525	69.9135	0.88072206	-0.8687	44.7067	7.381074917
0.10844	2.8925	73.4695	0.87590245	-1.4424	41.8378	6.90742556
0.11261	3.0375	77.1525	0.86868974	-2.0162	38.969	6.433776202
0.11678	3.1725	80.5815	0.85908391	-2.5900	36.1001	5.960126844
0.12095	3.3225	84.3915	0.84708497	-3.1638	33.2312	5.486477486
0.12513	3.4525	87.6935	0.83269292	-3.7375	30.3624	5.012828128
0.1293	3.5775	90.8685	0.81590775	-4.3113	27.4935	4.539178771
0.13347	3.7025	94.0435	0.79672947	-4.8851	24.6246	4.065529413
0.13764	3.8225	97.0915	0.77515808	-5.4588	21.7558	3.591880055
0.14181	3.9425	100.1395	0.75119358	-6.0326	18.8869	3.118230697
0.14598	4.0625	103.1875	0.72483596	-6.6064	16.0181	2.644581339
0.15015	4.1575	105.6005	0.69608523	-7.1802	13.1492	2.170931981
0.15432	4.2675	108.3945	0.66494139	-7.7539	10.2803	1.697282624
0.15849	4.3725	111.0615	0.63140444	-8.3277	7.41147	1.223633266
0.16266	4.4775	113.7285	0.59547437	-8.9015	4.5426	0.749983908
0.16683	4.5775	116.2685	0.55715119	-9.4753	1.67374	0.27633455
0.171	4.6725	118.6815	0.51643490	-10.0490	-1.1951	-0.197314808
0.17518	4.76625	121.06275	0.47332549	-10.6228	-4.064	-0.670964165
0.17935	4.83625	122.84075	0.42782298	-11.1966	-6.9328	-1.144613523
0.18352	4.90625	124.61875	0.37992735	-11.7703	-9.8017	-1.618262881
0.18769	4.96875	126.20625	0.32963860	-12.3441	-12.671	-2.091912239
0.19186	5.01875	127.47625	0.27695675	-12.9179	-15.539	-2.565561597
0.19603	5.05875	128.49225	0.22188178	-13.4917	-18.408	-3.039210955
0.2002	5.08875	129.25425	0.16441370	-14.0654	-21.277	-3.512860312
0.20437	5.11875	130.01625	0.10455250	-14.6392	-24.146	-3.98650967
0.20854	5.13875	130.52425	0.04229820	-15.2130	-27.015	-4.460159028
0.21271	5.15375	130.90525	-0.02234922	-15.7868	-29.884	-4.933808386
0.21688	5.16375	131.15925	-0.08938975	-16.3605	-32.753	-5.407457744

Test 5		5	kg Mass		8	Delayed Frames
Time (s)	Displacement (in)	Displacement (mm)	Velocity (m/s)	Acceleration (m/s^2)	Force (N)	Torque (N*m)
0	0	0	0.12639210	16.330247	130.701	21.57877357
0.004	0.005571429	0.141514286	0.19309527	15.655257	127.326	21.02157006
0.008	0.016714286	0.424542857	0.25698317	14.980268	123.951	20.46436656
0.013	0.050214286	1.275442857	0.31805580	14.305279	120.576	19.90716305
0.017	0.094857143	2.409371429	0.37631316	13.630290	117.201	19.34995955
0.0209	0.150642857	3.826328571	0.43175525	12.955301	113.827	18.79275604
0.025	0.228785714	5.811157143	0.48438207	12.280312	110.452	18.23555254
0.029	0.306928571	7.795985714	0.53419362	11.605323	107.077	17.67834903
0.03337	0.396214286	10.06384286	0.58118990	10.930334	103.702	17.12114552
0.03754	0.481928571	12.24098571	0.62537091	10.255345	100.327	16.56394202
0.04171	0.582357143	14.79187143	0.66673666	9.580356	96.9518	16.00673851
0.04588	0.694	17.6276	0.70528713	8.905366	93.5768	15.44953501
0.05005	0.816785714	20.74635714	0.74102233	8.230377	90.2019	14.8923315
0.05422	0.939571429	23.86511429	0.77394226	7.555388	86.8269	14.335128
0.05839	1.0735	27.2669	0.80404692	6.880399	83.452	13.77792449
0.06256	1.196285714	30.38565714	0.83133631	6.205410	80.0771	13.22072099
0.06673	1.341357143	34.07047143	0.85581044	5.530421	76.7021	12.66351748
0.0709	1.497714286	38.04194286	0.87746929	4.855432	73.3272	12.10631398
0.07508	1.654071429	42.01341429	0.89631287	4.180443	69.9522	11.54911047
0.07925	1.810428571	45.98488571	0.91234118	3.505454	66.5773	10.99190696
0.08342	1.966785714	49.95635714	0.92555423	2.830465	63.2023	10.43470346
0.08759	2.134214286	54.20904286	0.93595200	2.155475	59.8274	9.877499954
0.09176	2.301642857	58.46172857	0.94353450	1.480486	56.4524	9.320296449
0.09593	2.480214286	62.99744286	0.94830173	0.805497	53.0775	8.763092943
0.1001	2.6365	66.9671	0.95025370	0.130508	49.7025	8.205889438
0.10427	2.792785714	70.93675714	0.94939039	-0.544481	46.3276	7.648685932
0.10844	2.949071429	74.90641429	0.94571181	-1.219470	42.9526	7.091482427
0.11261	3.105357143	78.87607143	0.93921797	-1.894459	39.5777	6.534278921
0.11678	3.250428571	82.56088571	0.92990885	-2.569448	36.2028	5.977075416
0.12095	3.3955	86.2457	0.91778446	-3.244437	32.8278	5.419871911
0.12513	3.5455	90.0557	0.90284481	-3.919427	29.4529	4.862668405
0.1293	3.690571429	93.74051429	0.88508988	-4.594416	26.0779	4.3054649
0.13347	3.835642857	97.42532857	0.86451969	-5.269405	22.703	3.748261394
0.13764	3.969571429	100.8271143	0.84113422	-5.944394	19.328	3.191057889
0.14181	4.1035	104.2289	0.81493348	-6.619383	15.9531	2.633854383
0.14598	4.226285714	107.3476571	0.78591748	-7.294372	12.5781	2.076650878
0.15015	4.349071429	110.4664143	0.75408620	-7.969361	9.20319	1.519447373
0.15432	4.460714286	113.3021429	0.71943966	-8.644350	5.82825	0.962243867
0.15849	4.55	115.57	0.68197784	-9.319339	2.4533	0.405040362
0.16266	4.639285714	117.8378571	0.64170076	-9.994328	-0.9216	-0.152163144
0.16683	4.728571429	120.1057143	0.59860840	-10.669318	-4.2966	-0.709366649
0.171	4.817857143	122.3735714	0.55270078	-11.344307	-7.6715	-1.266570155
0.17518	4.896	124.3584	0.50397788	-12.019296	-11.046	-1.82377366
0.17935	4.974142857	126.3432286	0.45243972	-12.694285	-14.421	-2.380977166
0.18352	5.052285714	128.3280571	0.39808628	-13.369274	-17.796	-2.938180671
0.18769	5.124857143	130.1713714	0.34091758	-14.044263	-21.171	-3.495384176
0.19186	5.180642857	131.5883286	0.28093361	-14.719252	-24.546	-4.052587682
0.19603	5.225285714	132.7222571	0.21813436	-15.394241	-27.921	-4.609791187
0.2002	5.258785714	133.5731571	0.15251985	-16.069230	-31.296	-5.166994693
0.20437	5.292285714	134.4240571	0.08409006	-16.744220	-34.671	-5.724198198
0.20854	5.325785714	135.2749571	0.01284501	-17.419209	-38.046	-6.281401704
0.21271	5.348142857	135.8428286	-0.06121531	-18.094198	-41.421	-6.838605209
0.21688	5.364857143	136.2673714	-0.13809091	-18.769187	-44.796	-7.395808714
0.22105	5.370428571	136.4088857	-0.21778177	-19.444176	-48.171	-7.95301222

Test 6		5	kg Mass		8	Delayed Frames
Time (s)	Displacement (in)	Displacement (mm)	Velocity (m/s)	Acceleration (m/s^2)	Force (N)	Torque (N*m)
0	0	0	0.27675240	13.429454	116.197	19.18416928
0.004	0.0210	0.53340	0.33153163	12.838283	113.241	18.6961575
0.008	0.0528	1.34144	0.38384518	12.247112	110.286	18.20814572
0.013	0.0969	2.46158	0.43369306	11.655941	107.33	17.72013394
0.017	0.1516	3.85108	0.48107525	11.064769	104.374	17.23212216
0.0209	0.2172	5.51796	0.52599177	10.473598	101.418	16.74411038
0.025	0.2939	7.46487	0.56844260	9.882427	98.4621	16.2560986
0.029	0.3810	9.67848	0.60842776	9.291256	95.5063	15.76808682
0.03337	0.4682	11.89209	0.64594724	8.700085	92.5504	15.28007504
0.03754	0.5774	14.66577	0.68100104	8.108914	89.5946	14.79206327
0.04171	0.7086	17.99952	0.71358917	7.517743	86.6387	14.30405149
0.04588	0.8399	21.33327	0.74371161	6.926571	83.6829	13.81603971
0.05005	0.9606	24.40032	0.77136837	6.335400	80.727	13.32802793
0.05422	1.1024	28.00077	0.79655946	5.744229	77.7711	12.84001615
0.05839	1.2336	31.33452	0.81928487	5.153058	74.8153	12.35200437
0.06256	1.3649	34.66827	0.83954459	4.561887	71.8594	11.86399259
0.06673	1.4961	38.00202	0.85733864	3.970716	68.9036	11.37598081
0.0709	1.6274	41.33577	0.87266701	3.379545	65.9477	10.88796903
0.07508	1.7807	45.22959	0.88552971	2.788373	62.9919	10.39995725
0.07925	1.9340	49.12341	0.89592672	2.197202	60.036	9.911945475
0.08342	2.0873	53.01723	0.90385805	1.606031	57.0802	9.423933695
0.08759	2.2626	57.47112	0.90932371	1.014860	54.1243	8.935921916
0.09176	2.4595	62.47174	0.91232368	0.423689	51.1684	8.447910137
0.09593	2.6349	66.92563	0.91285798	-0.167482	48.2126	7.959898358
0.1001	2.7661	70.25938	0.91092660	-0.758653	45.2567	7.471886579
0.10427	2.9415	74.71327	0.90652954	-1.349825	42.3009	6.9838748
0.10844	3.0948	78.60709	0.89966680	-1.940996	39.345	6.495863021
0.11261	3.2481	82.50091	0.89033839	-2.532167	36.3892	6.007851242
0.11678	3.3793	85.83466	0.87854429	-3.123338	33.4333	5.519839463
0.12095	3.5106	89.16841	0.86428452	-3.714509	30.4775	5.031827684
0.12513	3.6418	92.50216	0.84755906	-4.305680	27.5216	4.543815905
0.1293	3.7731	95.83591	0.82836793	-4.896851	24.5657	4.055804126
0.13347	3.9043	99.16966	0.80671112	-5.488023	21.6099	3.567792347
0.13764	4.0356	102.50341	0.78258863	-6.079194	18.654	3.079780567
0.14181	4.1448	105.27709	0.75600046	-6.670365	15.6982	2.591768788
0.14598	4.2540	108.05077	0.72694661	-7.261536	12.7423	2.103757009
0.15015	4.3411	110.26438	0.69542709	-7.852707	9.78646	1.61574523
0.15432	4.4398	112.77136	0.66144188	-8.443878	6.83061	1.127733451
0.15849	4.5270	114.98497	0.62499100	-9.035049	3.87475	0.639721672
0.16266	4.6089	117.06523	0.58607444	-9.626221	0.9189	0.151709893
0.16683	4.6960	119.27884	0.54469219	-10.217392	-2.037	-0.336301886
0.171	4.7832	121.49245	0.50084427	-10.808563	-4.9928	-0.824313665
0.17518	4.8598	123.43936	0.45453068	-11.399734	-7.9487	-1.312325444
0.17935	4.9254	125.10624	0.40575140	-11.990905	-10.905	-1.800337223
0.18352	4.9911	126.77311	0.35450644	-12.582076	-13.86	-2.288349002
0.18769	5.0567	128.43999	0.30079581	-13.173247	-16.816	-2.776360782
0.19186	5.1114	129.82950	0.24461949	-13.764419	-19.772	-3.264372561
0.19603	5.1544	130.92297	0.18597750	-14.355590	-22.728	-3.75238434
0.2002	5.1943	131.93643	0.12486983	-14.946761	-25.684	-4.240396119
0.20437	5.2327	132.90988	0.06129648	-15.537932	-28.64	-4.728407898
0.20854	5.2547	133.46995	-0.00474255	-16.129103	-31.596	-5.216419677
0.21271	5.2768	134.03002	-0.07324726	-16.720274	-34.551	-5.704431456
0.21688	5.2873	134.29672	-0.14421765	-17.311445	-37.507	-6.192443235
0.22105	5.2978	134.56342	-0.21765371	-17.902617	-40.463	-6.680455014

Test 7		5	kg Mass		7	Delayed Frames
Time (s)	Displacement (in)	Displacement (mm)	Velocity (m/s)	Acceleration (m/s^2)	Force (N)	Torque (N*m)
0	0	0	0.19554830	14.908768	123.594	20.40534282
0.004	0.0092	0.23	0.25639631	14.269070	120.395	19.87727197
0.008	0.0322	0.82	0.31457624	13.629371	117.197	19.34920113
0.0125	0.0667	1.69	0.37008810	12.989673	113.998	18.82113028
0.017	0.1126	2.86	0.42293187	12.349975	110.8	18.29305943
0.021	0.1758	4.47	0.47310757	11.710277	107.601	17.76498859
0.025	0.2563	6.51	0.52061520	11.070579	104.403	17.23691774
0.0292	0.3367	8.55	0.56545474	10.430881	101.204	16.7088469
0.0334	0.4286	10.89	0.60762621	9.791182	98.0059	16.18077605
0.0375	0.5205	13.22	0.64712961	9.151484	94.8074	15.6527052
0.0417	0.6354	16.14	0.68396492	8.511786	91.6089	15.12463436
0.0459	0.7618	19.35	0.71813216	7.872088	88.4104	14.59656351
0.0501	0.8882	22.56	0.74963132	7.232390	85.2119	14.06849267
0.0542	1.0032	25.48	0.77846240	6.592691	82.0135	13.54042182
0.0584	1.1296	28.69	0.80462541	5.952993	78.815	13.01235097
0.0626	1.2674	32.19	0.82812034	5.313295	75.6165	12.48428013
0.0667	1.4053	35.69	0.84894719	4.673597	72.418	11.95620928
0.0709	1.5546	39.49	0.86710597	4.033899	69.2195	11.42813844
0.0751	1.7040	43.28	0.88259666	3.394201	66.021	10.90006759
0.0792	1.8649	47.37	0.89541928	2.754502	62.8225	10.37199674
0.0834	2.0257	51.45	0.90557383	2.114804	59.624	9.843925897
0.0876	2.1924	55.69	0.91306029	1.475106	56.4255	9.315855051
0.0918	2.3532	59.77	0.91787868	0.835408	53.227	8.787784205
0.0959	2.5141	63.86	0.92002899	0.195710	50.0285	8.259713359
0.1001	2.6865	68.24	0.91951123	-0.443988	46.8301	7.731642513
0.1043	2.8358	72.03	0.91632539	-1.083687	43.6316	7.203571667
0.1084	2.9851	75.82	0.91047147	-1.723385	40.4331	6.675500821
0.1126	3.1345	79.62	0.90194947	-2.363083	37.2346	6.147429975
0.1168	3.2838	83.41	0.89075940	-3.002781	34.0361	5.619359128
0.121	3.4217	86.91	0.87690125	-3.642479	30.8376	5.091288282
0.1251	3.5596	90.41	0.86037502	-4.282178	27.6391	4.563217436
0.1293	3.6860	93.62	0.84118071	-4.921876	24.4406	4.03514659
0.1335	3.8009	96.54	0.81931833	-5.561574	21.2421	3.507075744
0.1376	3.9273	99.75	0.79478787	-6.201272	18.0436	2.979004898
0.1418	4.0422	102.67	0.76758933	-6.840970	14.8451	2.450934052
0.146	4.1571	105.59	0.73772272	-7.480668	11.6467	1.922863206
0.1502	4.2605	108.22	0.70518803	-8.120367	8.44817	1.39479236
0.1543	4.3639	110.84	0.66998526	-8.760065	5.24968	0.866721514
0.1585	4.4673	113.47	0.63211442	-9.399763	2.05119	0.338650668
0.1627	4.5661	115.98	0.59157549	-10.039461	-1.14731	-0.189420178
0.1668	4.6523	118.17	0.54836849	-10.679159	-4.3458	-0.717491025
0.171	4.7327	120.21	0.50249342	-11.318858	-7.54429	-1.245561871
0.1752	4.8132	122.25	0.45395026	-11.958556	-10.7428	-1.773632717
0.1793	4.8821	124.01	0.40273903	-12.598254	-13.9413	-2.301703563
0.1835	4.9511	125.76	0.34885972	-13.237952	-17.1398	-2.829774409
0.1877	5.0085	127.22	0.29231234	-13.877650	-20.3383	-3.357845255
0.1919	5.0545	128.38	0.23309687	-14.517348	-23.5367	-3.885916101
0.196	5.1004	129.55	0.17121334	-15.157047	-26.7352	-4.413986947
0.2002	5.1349	130.43	0.10666172	-15.796745	-29.9337	-4.942057793
0.2044	5.1694	131.30	0.03944202	-16.436443	-33.1322	-5.470128639
0.2085	5.1924	131.89	-0.03044575	-17.076141	-36.3307	-5.998199485
0.2127	5.2096	132.32	-0.10300160	-17.715839	-39.5292	-6.526270331
0.2169	5.2188	132.56	-0.17822552	-18.355537	-42.7277	-7.054341178

Test 8		5	kg Mass		8	Delayed Frames
Time (s)	Displacement (in)	Displacement (mm)	Velocity (m/s)	Acceleration (m/s^2)	Force (N)	Torque (N*m)
0	0	0	0.2725570	12.958650	113.8433	18.79552058
0.004	0.0057	0.145249267	0.3254501	12.404647	111.0732	18.33819089
0.008	0.0287	0.728108504	0.3760325	11.850644	108.3032	17.88086121
0.013	0.0688	1.746715543	0.4243043	11.296640	105.5332	17.42353153
0.017	0.1146	2.910571848	0.4702654	10.742637	102.7632	16.96620185
0.0209	0.1834	4.65728739	0.5139159	10.188634	99.99317	16.50887217
0.025	0.2636	6.694501466	0.5552557	9.634631	97.22315	16.05154249
0.029	0.3438	8.731715543	0.5942849	9.080627	94.45314	15.5942128
0.0334	0.4354	11.05942815	0.6310033	8.526624	91.68312	15.13688312
0.0375	0.5385	13.6776393	0.6654112	7.972621	88.9131	14.67955344
0.0417	0.6531	16.58821114	0.6975084	7.418618	86.14309	14.22222376
0.0459	0.7791	19.78928152	0.7272949	6.864614	83.37307	13.76489408
0.0501	0.9051	22.99035191	0.7547707	6.310611	80.60306	13.3075644
0.0542	1.0426	26.48192082	0.7799359	5.756608	77.83304	12.85023472
0.0584	1.1801	29.97348974	0.8027905	5.202605	75.06302	12.39290503
0.0626	1.3175	33.46505865	0.8233344	4.648601	72.29301	11.93557535
0.0667	1.4664	37.2471261	0.8415676	4.094598	69.52299	11.47824567
0.0709	1.6153	41.02919355	0.8574902	3.540595	66.75297	11.02091599
0.0751	1.7757	45.1036217	0.8711021	2.986592	63.98296	10.56358631
0.0792	1.9361	49.17804985	0.8824034	2.432588	61.21294	10.10625663
0.0834	2.0966	53.25247801	0.8913940	1.878585	58.44293	9.648926946
0.0876	2.2570	57.32690616	0.8980739	1.324582	55.67291	9.191597265
0.0918	2.4117	61.25608504	0.9024432	0.770579	52.90289	8.734267584
0.0959	2.5606	65.03815249	0.9045018	0.216575	50.13288	8.276937902
0.1001	2.7095	68.82021994	0.9042498	-0.337428	47.36286	7.819608221
0.1043	2.8584	72.60228739	0.9016871	-0.891431	44.59284	7.362278539
0.1084	2.9958	76.0938563	0.8968138	-1.445434	41.82283	6.904948858
0.1126	3.1333	79.58542522	0.8896298	-1.999438	39.05281	6.447619176
0.1168	3.2707	83.07699413	0.8801351	-2.553441	36.2828	5.990289495
0.121	3.4082	86.56856305	0.8683298	-3.107444	33.51278	5.532959814
0.1251	3.5457	90.06013196	0.8542138	-3.661447	30.74276	5.075630132
0.1293	3.6717	93.26120235	0.8377872	-4.215451	27.97275	4.618300451
0.1335	3.7977	96.46227273	0.8190499	-4.769454	25.20273	4.160970769
0.1376	3.9238	99.66334311	0.7980020	-5.323457	22.43271	3.703641088
0.1418	4.0383	102.573915	0.7746433	-5.877460	19.6627	3.246311406
0.146	4.1529	105.4844868	0.7489741	-6.431464	16.89268	2.788981725
0.1502	4.2675	108.3950587	0.7209942	-6.985467	14.12267	2.331652044
0.1543	4.3821	111.3056305	0.6907036	-7.539470	11.35265	1.874322362
0.1585	4.4852	113.9238416	0.6581024	-8.093473	8.582633	1.416992681
0.1627	4.5883	116.5420528	0.6231905	-8.647477	5.812617	0.959662999
0.1668	4.6913	119.1602639	0.5859679	-9.201480	3.0426	0.502333318
0.171	4.7830	121.4879765	0.5464347	-9.755483	0.272584	0.045003636
0.1752	4.8746	123.8156891	0.5045908	-10.309486	-2.49743	-0.412326045
0.1793	4.9548	125.8529032	0.4604363	-10.863490	-5.26745	-0.869655726
0.1835	5.0350	127.8901173	0.4139711	-11.417493	-8.03746	-1.326985408
0.1877	5.1038	129.6368328	0.3651953	-11.971496	-10.8075	-1.784315089
0.1919	5.1726	131.3835484	0.3141088	-12.525499	-13.5775	-2.241644771
0.196	5.2298	132.8379032	0.2607117	-13.079503	-16.3475	-2.698974452
0.2002	5.2642	133.711261	0.2050039	-13.633506	-19.1175	-3.156304134
0.2044	5.2986	134.5846188	0.1469854	-14.187509	-21.8875	-3.613633815
0.2085	5.3216	135.167478	0.0866563	-14.741512	-24.6576	-4.070963496
0.2127	5.3445	135.7503372	0.0240165	-15.295516	-27.4276	-4.528293178
0.2169	5.3617	136.186085	-0.0409340	-15.849519	-30.1976	-4.985622859
0.2211	5.3674	136.3313343	-0.1081951	-16.403522	-32.9676	-5.442952541

Test 9		5	kg Mass		8	Delayed Frames
Time (s)	Displacement (in)	Displacement (mm)	Velocity (m/s)	Acceleration (m/s^2)	Force (N)	Torque (N*m)
0	0	0	0.28987890	12.17179020	109.909	18.14596781
0.004	0.005873494	0.149186747	0.33955955	11.65107499	107.3054	17.7161174
0.008	0.023493976	0.596746988	0.38706838	11.13035977	104.7018	17.28626699
0.013	0.052936747	1.344593373	0.43240539	10.60964456	102.0982	16.85641659
0.017	0.1	2.54	0.47557059	10.08892935	99.49465	16.42656618
0.0209	0.17063253	4.334066265	0.51656396	9.56821414	96.89107	15.99671577
0.025	0.253012048	6.426506024	0.55538552	9.04749892	94.28749	15.56686536
0.029	0.335391566	8.518945783	0.59203526	8.52678371	91.68392	15.13701495
0.0334	0.429518072	10.90975904	0.62651318	8.00606850	89.08034	14.70716455
0.0375	0.523644578	13.30057229	0.65881928	7.48535329	86.47677	14.27731414
0.0417	0.629518072	15.98975904	0.68895356	6.96463807	83.87319	13.84746373
0.0459	0.747213855	18.97923193	0.71691603	6.44392286	81.26961	13.41761332
0.0501	0.876656627	22.26707831	0.74270667	5.92320765	78.66604	12.98776291
0.0542	1.006099398	25.5549247	0.76632550	5.40249243	76.06246	12.5579125
0.0584	1.135542169	28.84277108	0.78777251	4.88177722	73.45889	12.1280621
0.0626	1.276731928	32.42899096	0.80704770	4.36106201	70.85531	11.69821169
0.0667	1.417921687	36.01521084	0.82415107	3.84034680	68.25173	11.26836128
0.0709	1.570858434	39.89980422	0.83908263	3.31963158	65.64816	10.83851087
0.0751	1.73561747	44.08468373	0.85184236	2.79891637	63.04458	10.40866046
0.0792	1.900376506	48.26956325	0.86243028	2.27820116	60.44101	9.978810056
0.0834	2.065135542	52.45444277	0.87084637	1.75748595	57.83743	9.548959648
0.0876	2.218072289	56.33903614	0.87709065	1.23677073	55.23385	9.11910924
0.0918	2.371009036	60.22362952	0.88116311	0.71605552	52.63028	8.689258832
0.0959	2.523945783	64.10822289	0.88306376	0.19534031	50.0267	8.259408424
0.1001	2.67688253	67.99281627	0.88279258	-0.32537491	47.42313	7.829558016
0.1043	2.818072289	71.57903614	0.88034958	-0.84609012	44.81955	7.399707608
0.1084	2.959262048	75.16525602	0.87573477	-1.36680533	42.21597	6.9698572
0.1126	3.100451807	78.7514759	0.86894814	-1.88752054	39.6124	6.540006792
0.1168	3.229894578	82.03932229	0.85998969	-2.40823576	37.00882	6.110156383
0.121	3.359337349	85.32716867	0.84885942	-2.92895097	34.40525	5.680305975
0.1251	3.477033133	88.31664157	0.83555733	-3.44966618	31.80167	5.250455567
0.1293	3.594728916	91.30611446	0.82008342	-3.97038139	29.19809	4.820605159
0.1335	3.724171687	94.59396084	0.80243770	-4.49109661	26.59452	4.390754751
0.1376	3.84186747	97.58343373	0.78262015	-5.01181182	23.99094	3.960904343
0.1418	3.959563253	100.5729066	0.76063079	-5.53252703	21.38736	3.531053935
0.146	4.071310241	103.4112801	0.73646961	-6.05324224	18.78379	3.101203527
0.1502	4.183057229	106.2496536	0.71013661	-6.57395746	16.18021	2.671353119
0.1543	4.288930723	108.9388404	0.68163180	-7.09467267	13.57664	2.241502711
0.1585	4.394804217	111.6280271	0.65095516	-7.61538788	10.97306	1.811652303
0.1627	4.500677711	114.3172139	0.61810671	-8.13610310	8.369485	1.381801894
0.1668	4.594804217	116.7080271	0.58308643	-8.65681831	5.765908	0.951951486
0.171	4.688930723	119.0988404	0.54589434	-9.17753352	3.162332	0.522101078
0.1752	4.771310241	121.1912801	0.50653043	-9.69824873	0.558756	0.09225067
0.1793	4.853689759	123.2837199	0.46499470	-10.21896395	-2.04482	-0.337599738
0.1835	4.924021084	125.0701355	0.42128715	-10.73967916	-4.6484	-0.767450146
0.1877	4.99435241	126.8565512	0.37540779	-11.26039437	-7.25197	-1.197300554
0.1919	5.064683735	128.6429669	0.32735660	-11.78110958	-9.85555	-1.627150962
0.196	5.123493976	130.136747	0.27713360	-12.30182480	-12.4591	-2.05700137
0.2002	5.170557229	131.3321536	0.22473878	-12.82254001	-15.0627	-2.486851778
0.2044	5.211746988	132.3783735	0.17017214	-13.34325522	-17.6663	-2.916702187
0.2085	5.241189759	133.1262199	0.11343368	-13.86397044	-20.2699	-3.346552595
0.2127	5.264759036	133.7248795	0.05452340	-14.38468565	-22.8734	-3.776403003
0.2169	5.288328313	134.3235392	-0.00655869	-14.90540086	-25.477	-4.206253411
0.2211	5.305948795	134.7710994	-0.06981261	-15.42611607	-28.0806	-4.636103819
0.2252	5.311822289	134.9202861	-0.13523834	-15.94683129	-30.6842	-5.065954227

Test 10		5	kg Mass		8	Delayed Frames
Time (s)	Displacement (in)	Displacement (mm)	Velocity (m/s)	Acceleration (m/s^2)	Force (N)	Torque (N*m)
0	0	0	0.1540540	14.3107490	120.6037	19.9116783
0.0042	0.005446927	0.138351955	0.2125567	13.7424441	117.7622	19.44254263
0.0083	0.018575419	0.471815642	0.2686890	13.1741393	114.9207	18.97340696
0.0125	0.051326816	1.303701117	0.3224510	12.6058344	112.0792	18.50427129
0.0167	0.094972067	2.412290503	0.3738428	12.0375295	109.2376	18.03513562
0.0209	0.16047486	4.076061453	0.4228642	11.4692247	106.3961	17.56599995
0.025	0.236871508	6.016536313	0.4695153	10.9009198	103.5546	17.09686428
0.0292	0.313268156	7.957011173	0.5137961	10.3326149	100.7131	16.62772861
0.0334	0.400558659	10.17418994	0.5557066	9.7643100	97.87155	16.15859294
0.0375	0.487849162	12.39136872	0.5952468	9.1960052	95.03003	15.68945727
0.0417	0.58603352	14.8852514	0.6324167	8.6277003	92.1885	15.2203216
0.0459	0.695181564	17.65761173	0.6672163	8.0593954	89.34698	14.75118593
0.0501	0.815223464	20.70667598	0.6996456	7.4910906	86.50545	14.28205026
0.0542	0.935265363	23.75574022	0.7297045	6.9227857	83.66393	13.81291459
0.0584	1.055307263	26.80480447	0.7573932	6.3544808	80.8224	13.34377892
0.0626	1.175349162	29.85386872	0.7827116	5.7861760	77.98088	12.87464325
0.0667	1.295391061	32.90293296	0.8056596	5.2178711	75.13936	12.40550758
0.0709	1.426326816	36.22870112	0.8262373	4.6495662	72.29783	11.93637191
0.0751	1.55726257	39.55446927	0.8444448	4.0812613	69.45631	11.46723624
0.0792	1.710055866	43.43541899	0.8602819	3.5129565	66.61478	10.99810057
0.0834	1.873743017	47.59307263	0.8737487	2.9446516	63.77326	10.5289649
0.0876	2.037430168	51.75072626	0.8848452	2.3763467	60.93173	10.05982923
0.0918	2.190223464	55.63167598	0.8935714	1.8080419	58.09021	9.590693558
0.0959	2.34301676	59.5126257	0.8999273	1.2397370	55.24868	9.121557888
0.1001	2.506703911	63.67027933	0.9039129	0.6714321	52.40716	8.652422218
0.1043	2.670391061	67.82793296	0.9055282	0.1031273	49.56564	8.183286548
0.1084	2.823184358	71.70888268	0.9047732	-0.4651776	46.72411	7.714150877
0.1126	2.975977654	75.5898324	0.9016478	-1.0334825	43.88259	7.245015207
0.1168	3.117807263	79.19230447	0.8961522	-1.6017874	41.04106	6.775879537
0.121	3.259636872	82.79477654	0.8882862	-2.1700922	38.19954	6.306743867
0.1251	3.390572626	86.12054469	0.8780500	-2.7383971	35.35801	5.837608197
0.1293	3.52150838	89.44631285	0.8654434	-3.3067020	32.51649	5.368472527
0.1335	3.652444134	92.77208101	0.8504666	-3.8750068	29.67497	4.899336857
0.1376	3.783379888	96.09784916	0.8331194	-4.4433117	26.83344	4.430201187
0.1418	3.914315642	99.42361732	0.8134019	-5.0116166	23.99192	3.961065517
0.146	4.045251397	102.7493855	0.7913141	-5.5799214	21.15039	3.491929847
0.1502	4.165293296	105.7984497	0.7668560	-6.1482263	18.30887	3.022794177
0.1543	4.285335196	108.847514	0.7400276	-6.7165312	15.46734	2.553658507
0.1585	4.39448324	111.6198743	0.7108289	-7.2848361	12.62582	2.084522837
0.1627	4.503631285	114.3922346	0.6792599	-7.8531409	9.784295	1.615387166
0.1668	4.61277933	117.164595	0.6453205	-8.4214458	6.942771	1.146251496
0.171	4.710963687	119.6584777	0.6090109	-8.9897507	4.101247	0.677115826
0.1752	4.809148045	122.1523603	0.5703310	-9.5580555	1.259722	0.207980156
0.1793	4.896438547	124.3695391	0.5292807	-10.1263604	-1.5818	-0.261155514
0.1835	4.98372905	126.5867179	0.4858601	-10.6946653	-4.42333	-0.730291184
0.1877	5.060125698	128.5271927	0.4400693	-11.2629701	-7.26485	-1.199426854
0.1919	5.125349162	130.1838687	0.3919081	-11.8312750	-10.1064	-1.668562524
0.196	5.190572626	131.8405447	0.3413766	-12.3995799	-12.9479	-2.137698194
0.2002	5.245111732	133.225838	0.2884748	-12.9678848	-15.7894	-2.606833864
0.2044	5.288756983	134.3344274	0.2332028	-13.5361896	-18.6309	-3.075969534
0.2085	5.32150838	135.1663128	0.1755604	-14.1044945	-21.4725	-3.545105204
0.2127	5.354259777	135.9981983	0.1155476	-14.6727994	-24.314	-4.014240874
0.2169	5.381494413	136.6899581	0.0531646	-15.2411042	-27.1555	-4.483376545
0.2211	5.403317039	137.2442528	-0.0115887	-15.8094091	-29.997	-4.952512215
0.2252	5.419657821	137.6593087	-0.0787123	-16.3777140	-32.8386	-5.421647885
0.2294	5.425104749	137.7976606	-0.1482063	-16.9460188	-35.6801	-5.890783555

Test 11		5	kg Mass		7	Delayed Frames
Time (s)	Displacement (in)	Displacement (mm)	Velocity (m/s)	Acceleration (m/s^2)	Force (N)	Torque (N*m)
0	0	0	0.20345140	14.36042620	120.8521	19.95268683
0.004	0.005820896	0.147850746	0.26209239	13.75910325	117.8455	19.45629473
0.008	0.029179104	0.741149254	0.31822537	13.15778030	114.8389	18.95990264
0.013	0.064179104	1.630149254	0.37185032	12.55645736	111.8323	18.46351055
0.017	0.110820896	2.814850746	0.42296725	11.95513441	108.8257	17.96711845
0.0209	0.180820896	4.592850746	0.47157617	11.35381146	105.8191	17.47072636
0.025	0.262462687	6.666552239	0.51767706	10.75248851	102.8124	16.97433427
0.029	0.355746269	9.035955224	0.56126993	10.15116556	99.80583	16.47794217
0.0334	0.449029851	11.40535821	0.60235478	9.54984262	96.79921	15.98155008
0.0375	0.553955224	14.07046269	0.64093162	8.94851967	93.7926	15.48515799
0.0417	0.658880597	16.73556716	0.67700043	8.34719672	90.78598	14.98876589
0.0459	0.775522388	19.69826866	0.71056122	7.74587377	87.77937	14.4923738
0.0501	0.90380597	22.95667164	0.74161399	7.14455082	84.77275	13.99598171
0.0542	1.020447761	25.91937313	0.77015874	6.54322788	81.76614	13.49958961
0.0584	1.137089552	28.88207463	0.79619547	5.94190493	78.75952	13.00319752
0.0626	1.253731343	31.84477612	0.81972418	5.34058198	75.75291	12.50680543
0.0667	1.382014925	35.1031791	0.84074487	4.73925903	72.7463	12.01041333
0.0709	1.521940299	38.65728358	0.85925754	4.13793608	69.73968	11.51402124
0.0751	1.673507463	42.50708955	0.87526219	3.53661314	66.73307	11.01762914
0.0792	1.836791045	46.65449254	0.88875881	2.93529019	63.72645	10.52123705
0.0834	2.000074627	50.80189552	0.89974742	2.33396724	60.71984	10.02484496
0.0876	2.163358209	54.94929851	0.90822801	1.73264429	57.71322	9.528452864
0.0918	2.338283582	59.39240299	0.91420058	1.13132135	54.70661	9.03206077
0.0959	2.501567164	63.53980597	0.91766513	0.52999840	51.69999	8.535668677
0.1001	2.664850746	67.68720896	0.91862165	-0.07132455	48.69338	8.039276583
0.1043	2.828134328	71.83461194	0.91707016	-0.67264750	45.68676	7.54288449
0.1084	2.979701493	75.68441791	0.91301065	-1.27397045	42.68015	7.046492396
0.1126	3.131268657	79.53422388	0.90644311	-1.87529339	39.67353	6.550100303
0.1168	3.27119403	83.08832836	0.89736756	-2.47661634	36.66692	6.053708209
0.121	3.411119403	86.64243284	0.88578398	-3.07793929	33.6603	5.557316116
0.1251	3.551044776	90.19653731	0.87169239	-3.67926224	30.65369	5.060924022
0.1293	3.679328358	93.4549403	0.85509277	-4.28058519	27.64707	4.564531929
0.1335	3.80761194	96.71334328	0.83598514	-4.88190813	24.64046	4.068139835
0.1376	3.935895522	99.97174627	0.81436948	-5.48323108	21.63384	3.571747742
0.1418	4.052537313	102.9344478	0.79024581	-6.08455403	18.62723	3.075355648
0.146	4.157462687	105.5995522	0.76361411	-6.68587698	15.62062	2.578963555
0.1502	4.274104478	108.5622537	0.73447439	-7.28719993	12.614	2.082571461
0.1543	4.390746269	111.5249552	0.70282666	-7.88852287	9.607386	1.586179367
0.1585	4.495671642	114.1900597	0.66867090	-8.48984582	6.600771	1.089787274
0.1627	4.600597015	116.8551642	0.63200712	-9.09116877	3.594156	0.59339518
0.1668	4.693880597	119.2245672	0.59283532	-9.69249172	0.587541	0.097003087
0.171	4.787164179	121.5939701	0.55115551	-10.29381467	-2.41907	-0.399389007
0.1752	4.86880597	123.6676716	0.50696767	-10.89513761	-5.42569	-0.8957811
0.1793	4.950447761	125.7413731	0.46027181	-11.49646056	-8.4323	-1.392173194
0.1835	5.020149254	127.511791	0.41106793	-12.09778351	-11.4389	-1.888565287
0.1877	5.089850746	129.282209	0.35935603	-12.69910646	-14.4455	-2.384957381
0.1919	5.148134328	130.7626119	0.30513611	-13.30042941	-17.4521	-2.881349474
0.196	5.20641791	132.2430149	0.24840817	-13.90175235	-20.4588	-3.377741568
0.2002	5.253059701	133.4277164	0.18917221	-14.50307530	-23.4654	-3.874133661
0.2044	5.288059701	134.3167164	0.12742823	-15.10439825	-26.472	-4.370525755
0.2085	5.317238806	135.0578657	0.06317623	-15.70572120	-29.4786	-4.866917848
0.2127	5.340559701	135.6502164	-0.00358379	-16.30704415	-32.4852	-5.363309942
0.2169	5.358022388	136.0937687	-0.07285183	-16.90836709	-35.4918	-5.859702036
0.2211	5.363843284	136.2416194	-0.14462790	-17.50969004	-38.4985	-6.356094129

Test 12		5	kg Mass		9	Delayed Frames
Time (s)	Displacement (in)	Displacement (mm)	Velocity (m/s)	Acceleration (m/s^2)	Force (N)	Torque (N*m)
0	0	0	0.27032850	14.00945460	119.0973	19.66295977
0.004	0.008014706	0.203573529	0.32749052	13.40087641	116.0544	19.16057848
0.008	0.036764706	0.933823529	0.38211426	12.79229822	113.0115	18.65819718
0.013	0.07125	1.80975	0.43419971	12.18372004	109.9686	18.15581589
0.017	0.117205882	2.977029412	0.48374689	11.57514185	106.9257	17.65343459
0.0209	0.186176471	4.728882353	0.53075578	10.96656366	103.8828	17.1510533
0.025	0.266617647	6.772088235	0.57522640	10.35798547	100.8399	16.64867201
0.029	0.358529412	9.106647059	0.61715873	9.74940728	97.79704	16.14629071
0.0334	0.461911765	11.73255882	0.65655279	9.14082909	94.75415	15.64390942
0.0375	0.576838235	14.65169118	0.69340856	8.53225091	91.71125	15.14152812
0.0417	0.703235294	17.86217647	0.72772605	7.92367272	88.66836	14.63914683
0.0459	0.829632353	21.07266176	0.75950526	7.31509453	85.62547	14.13676553
0.0501	0.9675	24.5745	0.78874619	6.70651634	82.58258	13.63438424
0.0542	1.105367647	28.07633824	0.81544884	6.09793815	79.53969	13.13200295
0.0584	1.243235294	31.57817647	0.83961321	5.48935997	76.4968	12.62962165
0.0626	1.381102941	35.08001471	0.86123930	4.88078178	73.45391	12.12724036
0.0667	1.530441176	38.87320588	0.88032710	4.27220359	70.41102	11.62485906
0.0709	1.679779412	42.66639706	0.89687663	3.66362540	67.36813	11.12247777
0.0751	1.840661765	46.75280882	0.91088788	3.05504721	64.32524	10.62009647
0.0792	2.013014706	51.13057353	0.92236084	2.44646902	61.28235	10.11771518
0.0834	2.185367647	55.50833824	0.93129553	1.83789084	58.23945	9.615333885
0.0876	2.34625	59.59475	0.93769193	1.22931265	55.19656	9.112952591
0.0918	2.507132353	63.68116176	0.94155005	0.62073446	52.15367	8.610571297
0.0959	2.668014706	67.76757353	0.94286990	0.01215627	49.11078	8.108190002
0.1001	2.828897059	71.85398529	0.94165146	-0.59642192	46.06789	7.605808708
0.1043	2.978235294	75.64717647	0.93789474	-1.20500010	43.025	7.103427414
0.1084	3.127573529	79.44036765	0.93159974	-1.81357829	39.98211	6.601046119
0.1126	3.265441176	82.94220588	0.92276646	-2.42215648	36.93922	6.098664825
0.1168	3.403308824	86.44404412	0.91139490	-3.03073467	33.89633	5.596283531
0.121	3.541176471	89.94588235	0.89748505	-3.63931286	30.85344	5.093902236
0.1251	3.673308824	93.30204412	0.88103693	-4.24789105	27.81054	4.591520942
0.1293	3.811176471	96.80388235	0.86205053	-4.85646923	24.76765	4.089139647
0.1335	3.949044118	100.3057206	0.84052584	-5.46504742	21.72476	3.586758353
0.1376	4.075441176	103.5162059	0.81646288	-6.07362561	18.68187	3.084377059
0.1418	4.201838235	106.7266912	0.78986163	-6.68220380	15.63898	2.581995764
0.146	4.328235294	109.9371765	0.76072210	-7.29078199	12.59609	2.07961447
0.1502	4.443161765	112.8563088	0.72904430	-7.89936017	9.553199	1.577233176
0.1543	4.558088235	115.7754412	0.69482821	-8.50793836	6.510308	1.074851881
0.1585	4.673014706	118.6945735	0.65807384	-9.11651655	3.467417	0.572470587
0.1627	4.776397059	121.3204853	0.61878119	-9.72509474	0.424526	0.070089293
0.1668	4.868308824	123.6550441	0.57695026	-10.33367293	-2.61836	-0.432292002
0.171	4.960220588	125.9896029	0.53258105	-10.94225112	-5.66126	-0.934673296
0.1752	5.052132353	128.3241618	0.48567356	-11.55082930	-8.70415	-1.43705459
0.1793	5.132573529	130.3673676	0.43622779	-12.15940749	-11.747	-1.939435885
0.1835	5.201544118	132.1192206	0.38424373	-12.76798568	-14.7899	-2.441817179
0.1877	5.258970588	133.5778529	0.32972140	-13.37656387	-17.8328	-2.944198473
0.1919	5.304926471	134.7451324	0.27266078	-13.98514206	-20.8757	-3.446579768
0.196	5.339411765	135.6210588	0.21306189	-14.59372024	-23.9186	-3.948961062
0.2002	5.373897059	136.4969853	0.15092471	-15.20229843	-26.9615	-4.451342356
0.2044	5.396911765	137.0815588	0.08624926	-15.81087662	-30.0044	-4.953723651
0.2085	5.419926471	137.6661324	0.01903552	-16.41945481	-33.0473	-5.456104945
0.2127	5.437132353	138.1031618	-0.05071650	-17.02803300	-36.0902	-5.95848624
0.2169	5.448602941	138.3945147	-0.12300680	-17.63661119	-39.1331	-6.460867534
0.2211	5.454338235	138.5401912	-0.19783538	-18.24518937	-42.1759	-6.963248828

Test 13		5	kg Mass		7	Delayed Frames
Time (s)	Displacement (in)	Displacement (mm)	Velocity (m/s)	Acceleration (m/s^2)	Force (N)	Torque (N*m)
0	0	0	0.27020840	13.78616080	117.9808	19.47863074
0.004	0.011304348	0.287130435	0.32644038	13.17819755	114.941	18.97675708
0.008	0.039637681	1.006797101	0.38013664	12.57023430	111.9012	18.47488342
0.013	0.084927536	2.15715942	0.43129719	11.96227106	108.8614	17.97300976
0.017	0.152862319	3.882702899	0.47992202	11.35430781	105.8215	17.47113609
0.0209	0.232137681	5.896297101	0.52601113	10.74634456	102.7817	16.96926243
0.025	0.311413043	7.909891304	0.56956453	10.13838131	99.74191	16.46738877
0.029	0.390688406	9.923485507	0.61058222	9.53041806	96.70209	15.96551511
0.0334	0.481268116	12.22421014	0.64906418	8.92245481	93.66227	15.46364145
0.0375	0.583152174	14.81206522	0.68501043	8.31449157	90.62246	14.96176779
0.0417	0.696413043	17.6888913	0.71842097	7.70652832	87.58264	14.45989413
0.0459	0.820978261	20.85284783	0.74929579	7.09856507	84.54283	13.95802046
0.0501	0.956847826	24.30393478	0.77763489	6.49060182	81.50301	13.4561468
0.0542	1.092717391	27.75502174	0.80343828	5.88263857	78.46319	12.95427314
0.0584	1.228586957	31.2061087	0.82670595	5.27467532	75.42338	12.45239948
0.0626	1.364456522	34.65719565	0.84743791	4.66671208	72.38356	11.95052582
0.0667	1.511630435	38.39541304	0.86563415	4.05874883	69.34374	11.44865216
0.0709	1.670181159	42.42260145	0.88129467	3.45078558	66.30393	10.9467785
0.0751	1.828731884	46.44978986	0.89441948	2.84282233	63.26411	10.44490483
0.0792	1.998586957	50.7641087	0.90500857	2.23485908	60.2243	9.943031173
0.0834	2.168442029	55.07842754	0.91306195	1.62689584	57.18448	9.441157512
0.0876	2.326992754	59.10561594	0.91857961	1.01893259	54.14466	8.93928385
0.0918	2.485543478	63.13280435	0.92156155	0.41096934	51.10485	8.437410189
0.0959	2.644094203	67.15999275	0.92200778	-0.19699391	48.06503	7.935536528
0.1001	2.79692029	71.04177536	0.91991829	-0.80495716	45.02521	7.433662866
0.1043	2.944094203	74.77999275	0.91529309	-1.41292041	41.9854	6.931789205
0.1084	3.091268116	78.51821014	0.90813217	-2.02088365	38.94558	6.429915543
0.1126	3.238442029	82.25642754	0.89843553	-2.62884690	35.90577	5.928041882
0.1168	3.374311594	85.70751449	0.88620318	-3.23681015	32.86595	5.42616822
0.121	3.510181159	89.15860145	0.87143512	-3.84477340	29.82613	4.924294559
0.1251	3.646050725	92.60968841	0.85413133	-4.45273665	26.78632	4.422420898
0.1293	3.770615942	95.77364493	0.83429183	-5.06069990	23.7465	3.920547236
0.1335	3.895181159	98.93760145	0.81191662	-5.66866314	20.70668	3.418673575
0.1376	4.019746377	102.101558	0.78700569	-6.27662639	17.66687	2.916799913
0.1418	4.144311594	105.2655145	0.75955904	-6.88458964	14.62705	2.414926252
0.146	4.257572464	108.1423406	0.72957668	-7.49255289	11.58724	1.91305259
0.1502	4.370833333	111.0191667	0.69705860	-8.10051614	8.547419	1.411178929
0.1543	4.472717391	113.6070217	0.66200481	-8.70847939	5.507603	0.909305268
0.1585	4.574601449	116.1948768	0.62441530	-9.31644263	2.467787	0.407431606
0.1627	4.665181159	118.4956014	0.58429007	-9.92440588	-0.57203	-0.094442055
0.1668	4.75576087	120.7963261	0.54162913	-10.53236913	-3.61185	-0.596315717
0.171	4.835036232	122.8099203	0.49643247	-11.14033238	-6.65166	-1.098189378
0.1752	4.914311594	124.8235145	0.44870009	-11.74829563	-9.69148	-1.60006304
0.1793	4.981992754	126.5426159	0.39843200	-12.35625887	-12.7313	-2.101936701
0.1835	5.049673913	128.2617174	0.34562820	-12.96422212	-15.7711	-2.603810362
0.1877	5.106268116	129.6992101	0.29028868	-13.57218537	-18.8109	-3.105684024
0.1919	5.151557971	130.8495725	0.23241344	-14.18014862	-21.8507	-3.607557685
0.196	5.196847826	131.9999348	0.17200249	-14.78811187	-24.8906	-4.109431347
0.2002	5.230833333	132.8631667	0.10905582	-15.39607512	-27.9304	-4.611305008
0.2044	5.264818841	133.7263986	0.04357343	-16.00403836	-30.9702	-5.11317867
0.2085	5.2875	134.3025	-0.02444467	-16.61200161	-34.01	-5.615052331
0.2127	5.298804348	134.5896304	-0.09499849	-17.21996486	-37.0498	-6.116925992
0.2169	5.304456522	134.7331957	-0.16808802	-17.82792811	-40.0896	-6.618799654

Test 14		5	kg Mass		8	Delayed Frames
Time (s)	Displacement (in)	Displacement (mm)	Velocity (m/s)	Acceleration (m/s^2)	Force (N)	Torque (N*m)
0	0	0	0.18984060	15.55551220	126.8276	20.93923032
0.004	0.005820896	0.147850746	0.25332220	14.88518279	123.4759	20.38587339
0.008	0.029179104	0.741149254	0.31400796	14.21485338	120.1243	19.83251646
0.013	0.064179104	1.630149254	0.37189788	13.54452396	116.7726	19.27915953
0.017	0.110820896	2.814850746	0.42699197	12.87419455	113.421	18.7258026
0.0209	0.174925373	4.443104478	0.47929023	12.20386514	110.0693	18.17244567
0.025	0.256567164	6.51680597	0.52879265	11.53353573	106.7177	17.61908874
0.029	0.349850746	8.886208955	0.57549924	10.86320632	103.366	17.06573181
0.0334	0.443134328	11.25561194	0.61940999	10.19287690	100.0144	16.51237488
0.0375	0.548059701	13.92071642	0.66052490	9.52254749	96.66274	15.95901796
0.0417	0.652985075	16.5858209	0.69884398	8.85221808	93.31109	15.40566103
0.0459	0.769626866	19.54852239	0.73436723	8.18188867	89.95944	14.8523041
0.0501	0.886268657	22.51122388	0.76709464	7.51155926	86.6078	14.29894717
0.0542	1.014552239	25.76962687	0.79702622	6.84122985	83.25615	13.74559024
0.0584	1.142835821	29.02802985	0.82416196	6.17090043	79.9045	13.19223331
0.0626	1.271119403	32.28643284	0.84850186	5.50057102	76.55286	12.63887638
0.0667	1.411044776	35.84053731	0.87004593	4.83024161	73.20121	12.08551945
0.0709	1.56261194	39.69034328	0.88879417	4.15991220	69.84956	11.53216252
0.0751	1.725895522	43.83774627	0.90474657	3.48958279	66.49791	10.97880559
0.0792	1.889179104	47.98514925	0.91790313	2.81925337	63.14627	10.42544866
0.0834	2.064104478	52.42825373	0.92826386	2.14892396	59.79462	9.87209173
0.0876	2.239029851	56.87135821	0.93582876	1.47859455	56.44297	9.318734801
0.0918	2.413955224	61.31446269	0.94059782	0.80826514	53.09133	8.765377871
0.0959	2.577238806	65.46186567	0.94257104	0.13793573	49.73968	8.212020942
0.1001	2.740522388	69.60926866	0.94174843	-0.53239369	46.38803	7.658664012
0.1043	2.90380597	73.75667164	0.93812999	-1.20272310	43.03638	7.105307083
0.1084	3.06119403	77.75432836	0.93171571	-1.87305251	39.68474	6.551950153
0.1126	3.212761194	81.60413433	0.92250559	-2.54338192	36.33309	5.998593224
0.1168	3.352686567	85.15823881	0.91049964	-3.21371133	32.98144	5.445236294
0.121	3.49261194	88.71234328	0.89569786	-3.88404075	29.6298	4.891879365
0.1251	3.632537313	92.26644776	0.87810024	-4.55437016	26.27815	4.338522435
0.1293	3.772462687	95.82055224	0.85770678	-5.22469957	22.9265	3.785165506
0.1335	3.900746269	99.07895522	0.83451749	-5.89502898	19.57486	3.231808576
0.1376	4.029029851	102.3373582	0.80853237	-6.56535839	16.22321	2.678451647
0.1418	4.145671642	105.3000597	0.77975141	-7.23568781	12.87156	2.125094717
0.146	4.250597015	107.9651642	0.74817461	-7.90601722	9.519914	1.571737787
0.1502	4.355522388	110.6302687	0.71380198	-8.57634663	6.168267	1.018380858
0.1543	4.460447761	113.2953731	0.67663351	-9.24667604	2.81662	0.465023928
0.1585	4.553731343	115.6647761	0.63666921	-9.91700545	-0.53503	-0.088333001
0.1627	4.647014925	118.0341791	0.59390908	-10.58733486	-3.88667	-0.641689931
0.1668	4.740298507	120.4035821	0.54835311	-11.25766428	-7.23832	-1.19504686
0.171	4.821940299	122.4772836	0.50000130	-11.92799369	-10.59	-1.74840379
0.1752	4.891940299	124.2552836	0.44885366	-12.59832310	-13.9416	-2.301760719
0.1793	4.961940299	126.0332836	0.39491018	-13.26865251	-17.2933	-2.855117649
0.1835	5.020223881	127.5136866	0.33817087	-13.93898192	-20.6449	-3.408474578
0.1877	5.078507463	128.9940896	0.27863573	-14.60931134	-23.9966	-3.961831508
0.1919	5.125149254	130.178791	0.21630474	-15.27964075	-27.3482	-4.515188437
0.196	5.171791045	131.3634925	0.15117793	-15.94997016	-30.6999	-5.068545367
0.2002	5.206791045	132.2524925	0.08325528	-16.62029957	-34.0515	-5.621902296
0.2044	5.241791045	133.1414925	0.01253679	-17.29062898	-37.4031	-6.175259226
0.2085	5.265149254	133.734791	-0.06097753	-17.96095840	-40.7548	-6.728616156
0.2127	5.288507463	134.3280896	-0.13728769	-18.63128781	-44.1064	-7.281973085
0.2169	5.300149254	134.623791	-0.21639368	-19.30161722	-47.4581	-7.835330015